Drill Stem Testing
Operations and Data Interpretation

Thesis submitted in partial fulfillment of the requirements for the Degree of

Bachelor of Technology
(Applied Petroleum Engineering)

By

Kamal Pant (RO40205027)
Varun Jhaldiyal (R010205057)

Under the guidance of

Dr. Sant Kumar
Shri. Rajeshwar Mahajan

University of Petroleum & Energy Studies
College of Engineering

UNIVERSITY OF PETROLEUM & ENERGY STUDIES
(ISO 9001:2000 Certified)

Certificate

This is to certify that the work contained in this thesis titled **"Drill Stem Testing-Operations and Data Interpretation"** has been carried out by Kamal Pant and Varun Jhaldiyal under my/our supervision and has not been submitted elsewhere for a degree.

Sant Kumar
10.5.09

Dr. Sant Kumar
Former Director IMD,
Former GM (Res)
Former Professor ISM
Visiting Professor UPES

Rajeshwar Mahajan
11.05.09

Shri. Rajeshwar Mahajan
Assistant Professor
College Of Engineering
UPES

Corporate Office:
Hydrocarbons Education & Research Society
3rd Floor, PHD House,
4/2 Siri Institutional Area
August Kranti Marg, New Delhi - 110 016 India
Ph.: +91-11-41730151-53 Fax : +91-11-41730154

Main Campus:
Energy Acres,
PO Bidholi Via Prem Nagar,
Dehradun - 248 007 (Uttarakhand), India
Ph.: +91-135-2102690-91, 2694201/ 203/ 208
Fax: +91-135-2694204

Regional Centre (NCR) :
SCO. 9-12, Sector-14,
Gurgaon 122 007
(Haryana), India.
Ph: +91-124-4540 300
Fax: +91-124-4540 330

Regional Centre (Rajahmundry):
GIET, NH 5, Velugubanda,
Rajahmundry - 533 294,
East Godavari Dist., (Andhra Pradesh), India
Tel: +91-883-2484811/ 855
Fax: +91-883-2484822

Acknowledgement

We take the first opportunity to thank College of Engineering, University of Petroleum and Energy Studies for providing the facilities of which we have taken maximum utilization during this project.

We thank Dr. Sant Kumar and Shri. Rajeshwar Mahajan for their approval for the initiation of this project. They have been a tremendous influence during the course of this project with various inputs and suggestions.

And finally we thank Mr. Prabhat Saxena of Weatherford and Mr. Kavish Grover of RIL (E&P) and many others who have helped us during this tenure.

Synopsis

DST tool comprises of an arrangement of packers and valves placed on the end of the drill pipe. This arrangement can be used to isolate a zone of interest and to let it produce into the drill pipe. The sample is analyzed for PVT parameters. In the DST set-up, it is possible to have a sequence of flow periods followed by shut-in periods. The downhole pressure gauges on the DST device record pressures during the flow and shut-in periods.

The major purpose of DST pressure transient analysis is to determine the ability of the formation to produce the reservoir fluids. A properly designed, executed, and analyzed well test usually can provide information about formation permeability, extent of well bore damage and reservoir pressure.

The analysis restricts itself to interpretation of well data obtained from a drill stem tester for a gas well. The pressure v/s time data with respect to pressure build-up test is obtained from the downhole gauges. The flow-rate v/s time data is obtained from the separator. The other parameters to be input are well radius, payzone thickness and PVT parameters.

TABLE OF CONTENTS

LIST OF FIGURES

LIST OF TABLES

Chapter 1

Well Testing-Objectives and Types Of Tests

1.1 Introduction

Tests on oil and gas wells are performed at various stages of drilling, completion and production.The test objectives at each stage range from simple identification of produced fluids and determination of reservoir deliverability to the characterisation of complex reservoir features. Most well tests can be grouped either as productivity testing or as descriptive/reservoir testing.

- Productivity well tests are conducted to;
  - Identify produced fluids and determine their respective volume ratios.
  - Measure reservoir pressure and temperature.
  - Obtain samples suitable for PVT analysis.
  - Determine well deliverability.
  - Evaluate completion efficiency.
  - Characterise well damage.
  - Evaluate workover or stimulation treatment.
- Descriptive tests seek to;
  - Evaluate reservoir parameters.
  - Characterise reservoir heterogenities.
  - Assess reservoir extent and geometry.
  - Determine hydraulic communication between wells.

Whatever the objectives, well test data are essential for the analysis and improvement of reservoir performance and for reliable predictions. These, in turn are vital to optimising reservoir development and efficient management of the asset. Well testing technology is evolving rapidly.

Integration with data from other reservoir related disciplines, constant evolution of interactive software for transient analysis, improvements in downhole sensors and better control of the downhole environment have all dramatically increased the importance and capabilities of well testing.

1.1.1 Productivity Well Testing

Productivity well testing, the simplest form of testing, provides identification of productive fluids, the collection of representative samples and determination of reservoir deliverability. Formation fluid samples are used for PVT analysis, which reveals how hydrocarbon phases coexist at different pressures and temperatures. PVT analysis also provides fluid physical properties required for well test analysis and fluid flow simulation. Reservoir deliverability is a key concern for commercial exploitation. Estimating a reservoir's productivity requires relating flow rates to drawdown pressures. This can be achieved by flowing the well at several flow rates (different choke sizes) and measuring the stabilised bottomhole pressure and temperature prior to changing the choke.

The plot of flow data verses drawdown pressure is known as the inflow performance relationship (IPR). For monophasic oil conditions, the IPR is a straight line whose intersection with the vertical axis yields the static reservoir pressure. The inverse of the slope represents the productivity index of the well. The IPR is governed by properties of the rock-fluid system and near wellbore conditions.

Examples of IPR curves for low and high productivity are shown in Figure 1-2. The steeper line corresponds to poor productivity, which could be caused either by poor formation flow properties (low mobility-thickness product) or by damage caused while drilling or completing the well (high skin factor).

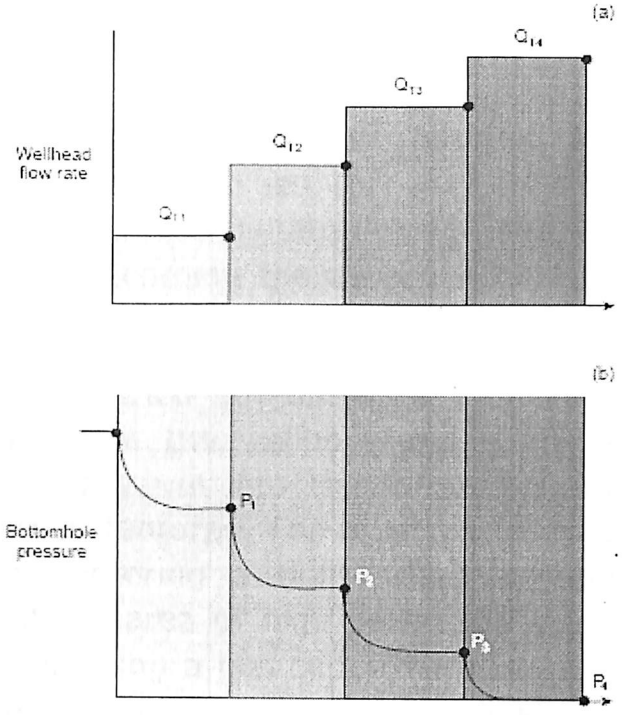

Fig.1-1 Relations between flow rates and drawdown pressures used for estimating reservoir productivity. A stepped production schedule during a productivity test (a) is achieved by flowing the well at several flow rates.Associated (stabilized) bottomhole pressure (b) is measured before changing the choke.

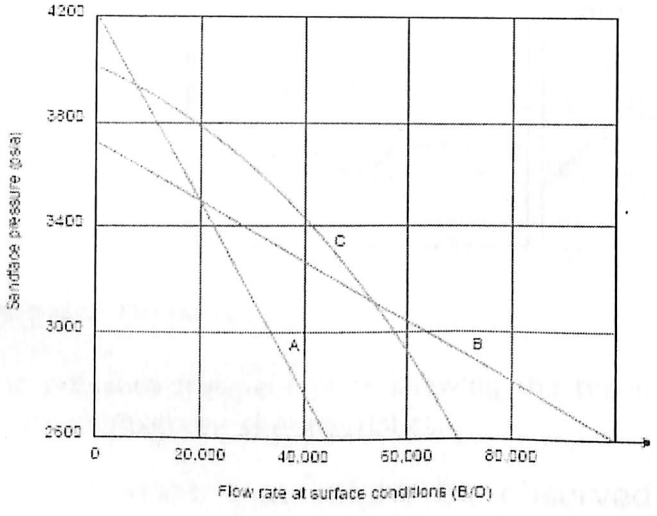

Fig.1-2 Typical inflow performance curves showing low (a) and high (b) productivity. For gas wells, IPR curves exhibit certain curvature (C) due to extra inertial and turbulent flow effects in the vicinity of the wellbore and changes of gas properties with with pressure. Oil wells flowing below the bubblepoint also display similar curvature, but these are due to changes in relative permeability created by variations in saturation distributions.

1.1.2 Descriptive Well Testing

Estimation of the formation's flow capacity, characterisation of wellbore damage and evaluation of a workover or stimulation treatment all require a transient test because a stabilised test is unable to provide unique values for mobility-thickness and skin. Transient tests are performed by introducing abrupt changes in surface production rates and recording the associated changes in bottomhole pressure.

Production changes, carried out during a transient well test, induce pressure disturbances in the wellbore and surrounding rock. These pressure disturbances travel into the formation and are affected in various ways by rock features. For example, a pressure disturbance will have difficulty entering a tight reservoir zone, but will pass unhindered through an area of high permeability. It may diminish or even vanish upon entering a gas cap. Therefore, a record of wellbore pressure response over time produces a curve whose shape is defined by the reservoir's unique characteristics. Unlocking the information contained in pressure transient curves is the fundamental objective of well test interpretation.

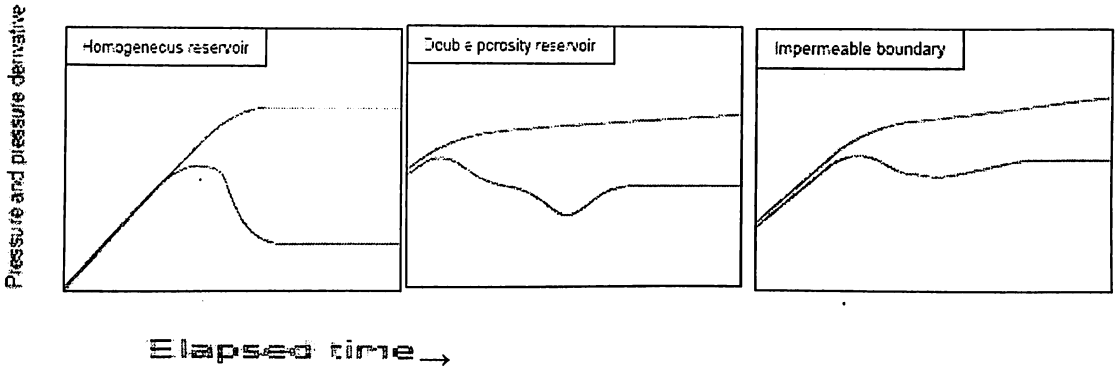

Fig.1-3 Characteristic pressure transient plots showing the types of responses that might occur due to various reservoir characteristics.

Typical pressure responses that might be observed with different formation characteristics are shown in Figure 1-3. Each plot consists of two curves presented as log-log graphs. The top curve represents the pressure changes associated with an abrupt production rate perturbation, and the bottom curve (termed the derivative curve) indicates the rate of pressure change with respect to time (refer to section 5). Its sensitivity to transient features resulting from well and

reservoir geometries (which are virtually too subtle to recognise in the pressure change response) makes the derivative curve the single most effective interpretation tool. However, it is always viewed together with the pressure change curve to quantify skin effects that are not recognised in the derivative response alone.

Pressure transient curve analysis probably provides more information about reservoir characteristics than any other technique. Horizontal and vertical permeability, well damage, fracture length, storativity ratio and interporosity flow coefficient are just a few of the characteristics that can be determined. In addition pressure transient curves can indicate the reservoir's extent and boundary details. The shape of the curve, however, is also affected by the reservoir's production history. Each change in production rate generates a new pressure transient that passes into the reservoir and merges with previous pressure effects. The observed pressures at the wellbore will be a result of the superposition of all these pressure changes.

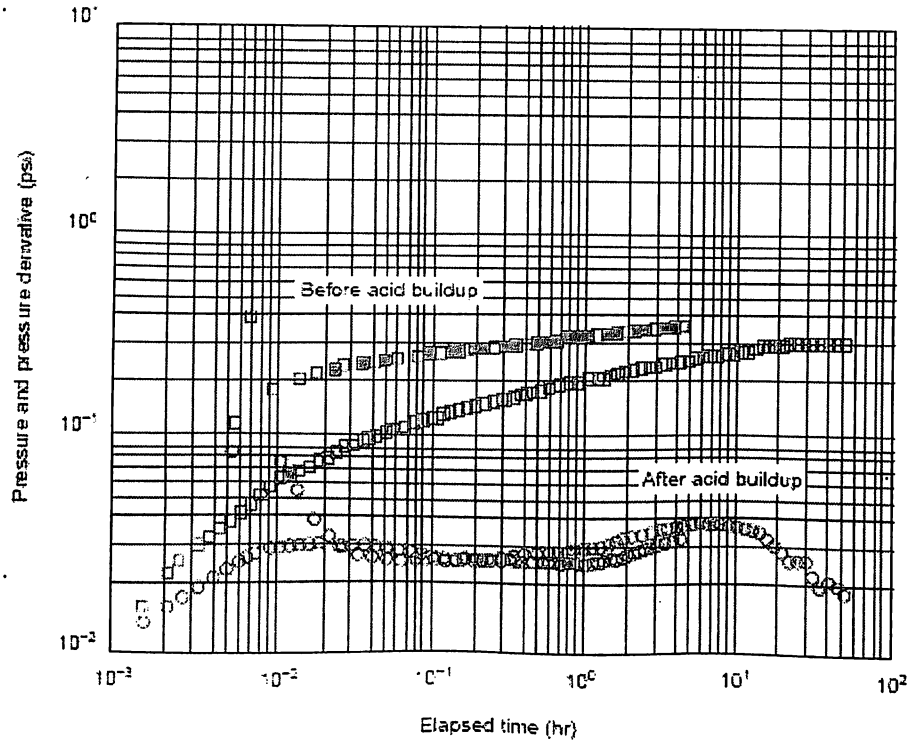

Fig. 1-4 Derivative curves showing features of outer boundary effects. The effects of damage removal are clearly seen in the after-treatment pressure response curve.

Different types of well tests can be achieved by altering production rates. Whereas a build-up test is performed by closing a valve (shut-in) on a producing well, a drawdown test is performed by putting a well into production. Other well tests, such as multi-rate, isochronal and injection well falloff are also possible.

Mathematical models are used to simulate the reservoir's response to production rate changes. The observed and simulated reservoir response can then be compared during well test interpretation to verify the accuracy of the model. By altering model parameters such as permeability or the distance from the well to a fault, a good match can be reached between the real and modelled data. The model parameters are then regarded as a good representation of those of the actual reservoir. Today's computer generated models provide much greater flexibility and improve the accuracy of the match between real and simulated data. It is now possible to compare an almost unlimited number of reservoir models with the observed data.

1.2 Test Design

Design and implementation of a well testing program can no longer be conducted under standard or traditional rule-of-thumb guidelines. Increasingly sophisticated reservoir development and management practises, stringent safety requirements, environmental concerns and a greater need for cost efficiency require that the entire testing sequence, from program design to data evaluation, be conducted intelligently. Proper test design, correct handling of surface effluents, high performance gauges, flexible downhole tools and perforating systems, wellsite validation and comprehensive interpretation are keys to successful well testing.

The importance of clearly defined objectives and careful planning cannot be overstated. Design of a well test includes development of a dynamic measurement sequence and selection of hardware that can acquire data at the wellsite in a cost effective manner. Test design is best accomplished in a software environment where interpreted openhole logs, production optimisation analysis, well perforation and

completion design and reservoir test interpretation modules are all simultaneously available to the analyst.

The first step in test design involves dividing the reservoir into vertical zones using openhole logs and geological data. The types of well or reservoir data that should be collected during the test are then specified. The data to be collected drive the type of well test to be run. (See Figure 1-5).

Once the type of test is determined, the sequence changes in surface flow rate that should occur during the test are calculated. The changes in flowrate and their duration should be realistic and practical so they generate the expected interpretation patterns in the test data. This is best achieved by selecting an appropriate reservoir model and simulating the entire test sequence in advance. Test sequence simulation allows the range of possible pressure and flow rate measurements to be explored. Simulation also helps isolate the types of sensors capable of measuring the expected ranges. Diagnostic plots of simulated data should be examined to determine when essential features will appear, such as the end of wellbore storage effects, the duration of infinite acting radial flow and the start of total system response in fissured systems. The plots can also help anticipate the emergence of external boundary effects, including sealed or partially sealed faults and constant pressure boundaries.

The next step is to generate sensitivity plots to determine the effects of reservoir parameters on the duration of different flow regimes.

Selecting the instrumentation and equipment for data acquisition is the final step of the test design process. Surface and downhole equipment should be versatile to allow for safe and flexible operations. Key factors to consider include;

- Controlling the downhole environment to minimise wellbore storage.
- Using combined perforating and testing techniques to minimise rig time.
- Choosing reliable downhole recorders to ensure that the expected data will be retrieved when pulling the tools out of hole.
- Running ultra-high precision gauges when test objectives call for detailed reservoir description.

- Selecting surface equipment to safely handle expected rates and pressures.
- Environmentally sound disposal of produced fluids.

Whatever the choice, it is important to ensure that all data is acquired with the utmost precision. To do this a good understanding of the available hardware options is necessary along with its prospective impact, if any, on the data quality.

Summary of current test types

Test type	Measurement condition: Flowing	Shut-in	Pulse	Slug	Distinguishing characteristics	Design consideration
Closed-chamber test	+	▪		▪	Downhole shut-in	Chamber and cushion lengths; valve open/shut sequence
Constant-pressure flow test	▪			▪	Requires transient flow rate measurement	Flow rate sensitivity
Drillstem test	+	▪			Downhole shut-in; open- or cased hole	Flowing and shut-in sequence/ duration
Formation test	▪	▪			Test conducted on borehole wall; formation fluid sampling	Tool module sizing/selection; pressure sensitivity
Horizontal well test	▪	▪			Testing hardware usually located in vertical part of hole	Minimize wellbore storage effects; requires long-duration test
Impulse test	▪	▪			Transients initiated by short-rate impulse	Trade-off between impulse duration and pressure sensitivity
Multilayer transient test	▪	▪			Multirate test; pressure and rate measured at several depths	Flow rate/pressure sensitivity; test sequence; measurement depths
Multiwell interference test	▪	▪	+		Transient induced in active well, measured in observation well	Test duration; pressure sensitivity, gauge resolution
Pumped-well test		▪			Downhole pressure measured or computed from liquid level soundings	Downhole pressure sensor versus surface acoustic device
Stabilized-flow test	▪				Includes isochronal, flow-after-flow, inflow performance, production logs, etc.	Time to reach stabilization Definition of stabilization
Step-rate test	▪				Flow test to determine injection well parting pressure	Flowing pressure range must include parting pressure
Testing while perforating	▪	▪		▪	Testing hardware and perforating guns on the same string	Underbalance determination
Transient rate and pressure test	▪	▪			Downhole measurement of pressure, flow rate, temperature and (usually) density	Flow rate/pressure sensitivity
Vertical interference test	+	▪	+		Transient induced at one depth and measured at another	Test duration; pressure sensitivity

+ = Under certain conditions
▪ = Yes, commonly

Fig. 1-5 Summary of Current Test Types

Chapter 2

Basics Of Well Testing

2.1 Basic Assumptions

2.1.1 Darcy's Law

In Henri Darcy's original experiment in 1856, as shown below, the equation for fluid flow through a porous medium was established:

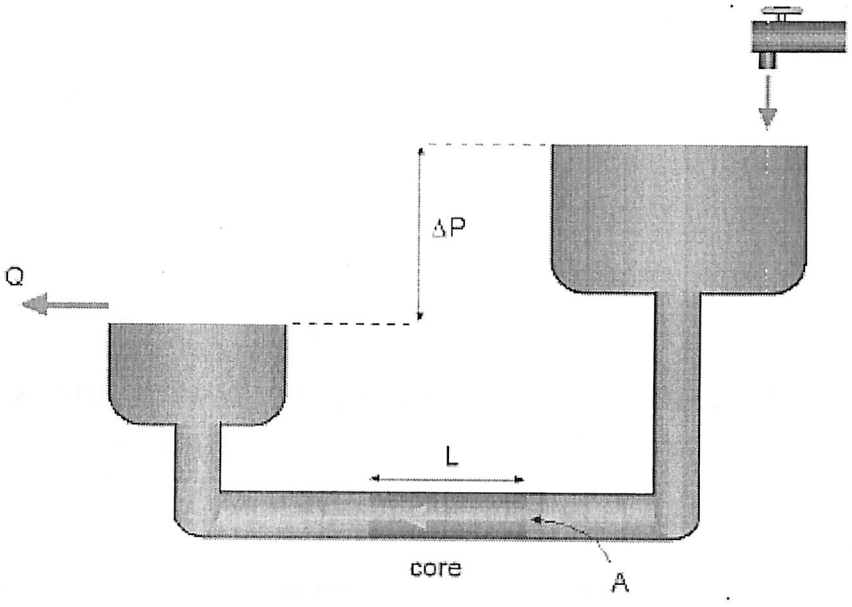

Fig. 2.1 Darcy's Law

$$Q = A\frac{k}{\mu}\frac{\Delta p}{L}$$

where: q = flowrate A = flow area k = permeability

L = length μ= viscosity Δp = pressure drop

Darcy's Law is the most fundamental law used in well testing, and in differential form it relates the flow rate (**q**) across a surface to the pressure gradient ($\partial \mathbf{p}/\partial \mathbf{x}$) across its section.

For linear flow:

$$-\frac{\partial p}{\partial x} = \frac{q\mu}{kA}$$

If we consider the flow across a cylindrical section of an isotropic medium (assumed by most of the models used in well testing), and considering the flow rate to be positive in the direction of the well (production):

$$r\frac{\partial p}{\partial r} = \frac{q\mu}{2\pi kh}$$

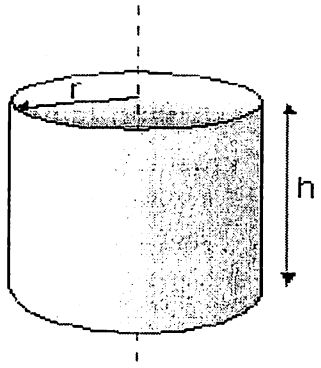

Fig. 2.2 Radial form of Darcy's Law

Darcy's Law states that the pressure drop between 2 points, close enough to consider all parameters to be constant, will be:

- proportional to the flowrate density (q/A)
- proportional to the fluid viscosity (μ)
- inversely proportional to the reservoir permeability (k).

The value of the overall constant depends upon the units.

2.1.2 The Diffusivity Equation

Fluid flow in porous media is governed by the diffusivity equation. To derive it in its simplest form, various assumptions and simplifications have to be made:

- the reservoir is homogeneous; constant properties throughout.
- fluid flow is horizontal only, in a zone of constant thickness.
- the fluid is monophasic and slightly compressible.
- pressure gradients are small, and Darcy's Law applies.

The diffusivity equation can be derived by combining the law of conservation of mass, Darcy's law and an equation of state. For radial flow:

$$\frac{\partial p}{\partial t} = \frac{k}{\phi \mu C_t}\left[\frac{\partial}{\partial r}\left(\frac{\partial p}{\partial r}\right) + \frac{1}{r}\left(\frac{\partial p}{\partial r}\right)\right]$$

This equation can only be solved in Laplace space, and with certain boundary conditions, as will be seen in the next section.

2.1.3 Infinite-Acting Radial Flow

Fluid flows towards the wellbore equally from all directions – the pressure drop expands radially.

The upper and lower bed boundaries are parallel and clearly defined, the reservoir rock between them is homogeneous, and the wellbore is perpendicular to the bed boundaries:

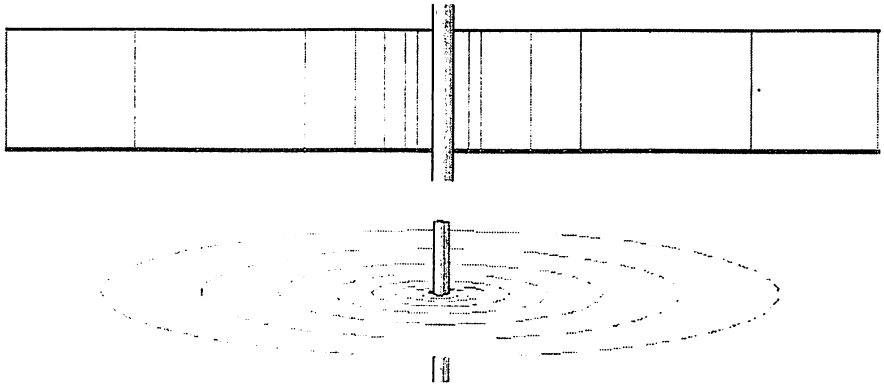

Fig. 2.3 Infinite-Acting Radial Flow (IARF)

The initial radial flow (IARF) regime is called infinite-acting because until the first boundary is reached, the flow pattern and corresponding pressure drop at the wellbore are exactly as would be obtained if the reservoir were truly infinite.

2.2 WTI Essentials

The pressure response during a transient well test is a function of both the well and reservoir characteristics and the flowrate history. In interpretation terms, the actual pressure and time are unimportant, with analysis performed in terms of pressure change Δp versus elapsed time, Δt:

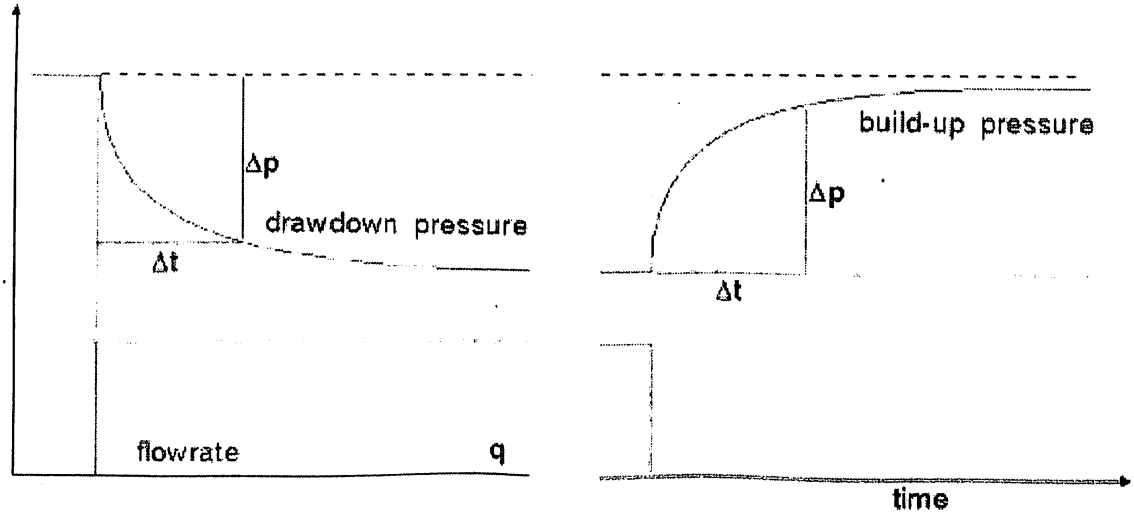

Fig 2.4 WTI Essentials

The change in pressure with respect to time is similar for drawdowns and build-ups, but one is not quite a mirror-image of the other, as will be seen in section 5.4. Although, in principle, either a drawdown or a build-up will reveal the reservoir characteristics, the build-up response is 'cleaner' than the drawdown data, which can be adversely affected by even a slight instability in the flow rate. The linear or Cartesian plot of pressure versus time, as shown above, is of limited value in well testing, but does have specialized uses, as will be seen later. Well test interpretation is predominantly carried out using semi-log and log-log techniques.

2.2.1 Wellbore Storage

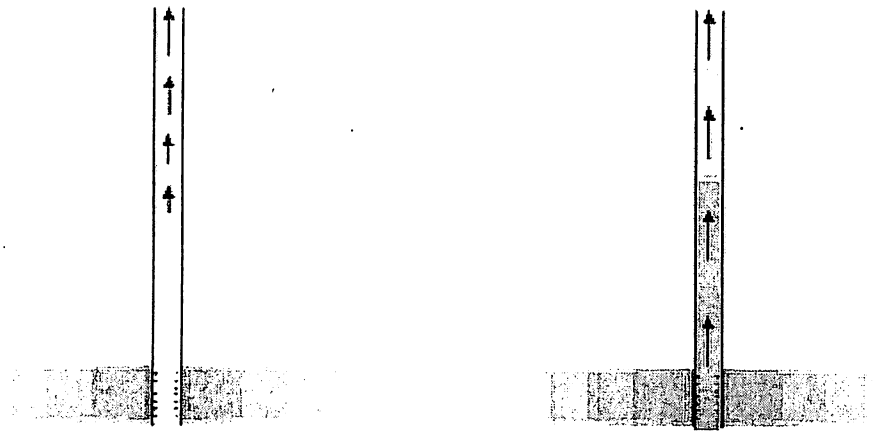

Fig 2.5 Wellbore Storage

Wellbore storage prevents the sandface flowrate from instantaneously following the surface flowrate. Initially, flow at surface is due only to decompression of fluid in the wellbore. Eventually, decompression effects become negligible and the downhole flowrate approaches the surface rate:

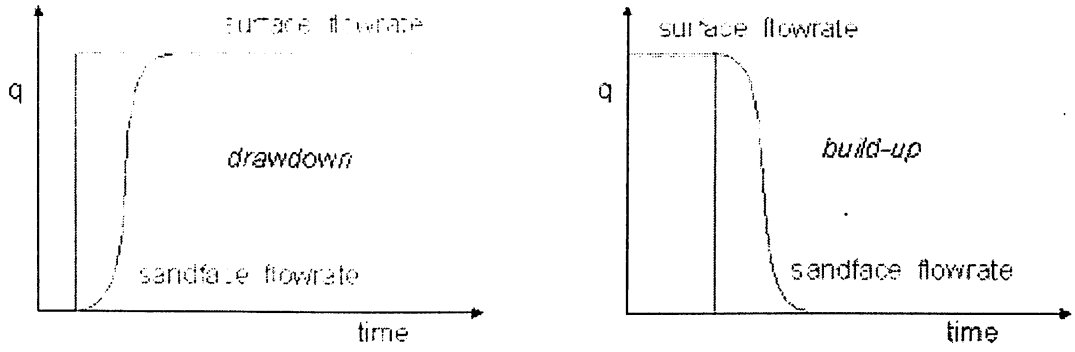

Fig 2.6 Downhole flowrates

The reverse happens during a build-up, as for a while 'the bottom of the well does not know what the top is doing', and the reservoir continues to flow into the well after it has been shut in. This is known as afterflow, and is also called wellbore storage. The principle is the same as for the drawdown, and it will be seen later that the effect on the pressure response is identical.

Until storage effects are over, the pressure response alone will contain no useful reservoir information.

2.2.2 Skin

If after drilling, completion, cementing and perforating, the overall pressure drop during production into the wellbore is identical to that for the ideal case, of a virgin, undamaged wellbore in an openhole completion, the well is said to have a zero skin. More often than not the reservoir near the wellbore has been invaded by (typically water-based) drilling fluid, and has undergone changes in permeability, absolute and/or relative to the reservoir fluid. Some of these changes are reversible during the 'clean-up' period, when the well is first put on production, but others are not:

$$S = \left[\frac{k}{k_s} - 1\right] \ln \frac{r_s}{r_w}$$

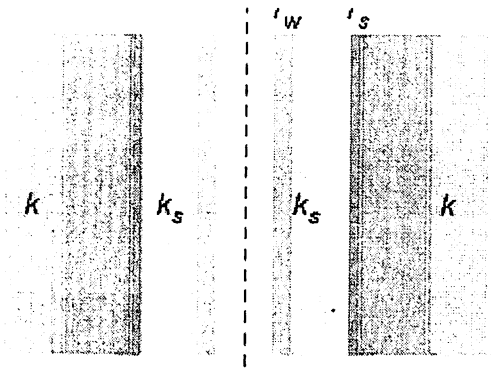

Fig 2.7 Skin openhole

The above definition of skin is seen to resolve to zero if the permeability of the invaded or 'skindamaged' zone, *k*s, is equal to the reservoir permeability *k*, or if the radius of the invaded zone, *r*s is equal to the wellbore radius, *r*w.

This mathematical description is not very realistic, as in real wells there will not be two discrete regions, each with homogeneous properties and with clear boundaries between the two. Also, it is possible to recreate a zero skin condition without removing the 'damage' around the wellbore. As long as the perforations are big enough, deep enough, and of a sufficiently high shot density and phasing, the pressure drop flowing into the well may still not exceed the pressure drop in the ideal case. If it does, the additional pressure drop due to skin, Δ*p*s , will serve no useful purpose, and will cause a reduction in the productivity index (PI) of the well. The situation can usually be improved by acidizing.

The skin value *S* is dimensionless, and in most cases independent of flowrate, but the corresponding pressure drop Δ*p*s is rate-dependent. A positive skin represents near-wellbore 'damage', whereas a negative skin historically denotes 'stimulation', and physically means that there is a smaller pressure drop close to the wellbore than would be expected in the ideal case.

If in the immediate vicinity close to the wellbore there is an additional pressure drop due to skin, the well is said to be damaged, and $S > 0$:

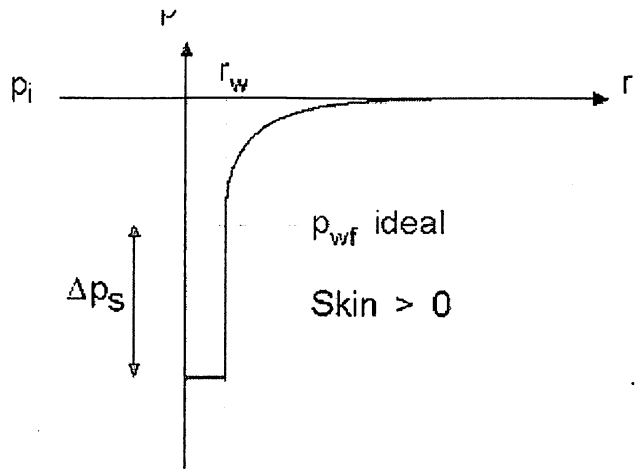

Fig 2.8 Positive skin

After stimulation, or a good TCP job, the pressure drop near the wellbore may be even less than in the 'ideal' case, so that $S < 0$:

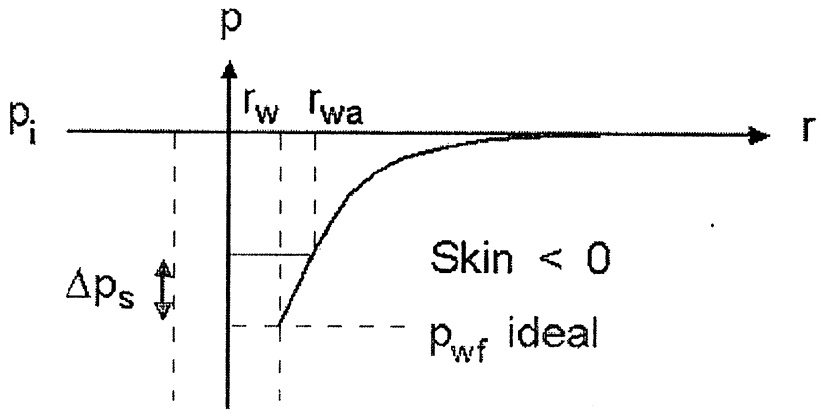

Fig 2.9 Negative skin

There is a mathematical equivalent to the negative skin, as shown above, which is a larger 'apparent' wellbore, *r*wa. In exceptional cases there may actually be an over-sized hole outside the casing, but typically this would not be the case. The skin value will be seen to do more than simply influence the pressure drop during production. For example, a high skin delays the onset of radial flow information in the pressure data, and a negative skin brings it forward. This is due to the inter-dependence of skin, productivity and wellbore storage effects.

2.2.3 Semi-Log Approach

During radial flow, the pressure change is related to the logarithm of the time. In other words, if pressure is plotted against the log of time, infinite-acting radial flow will give a straight line. For this reason the classical approach to well test interpretation has been the semi-log plot, of p versus log Δt:

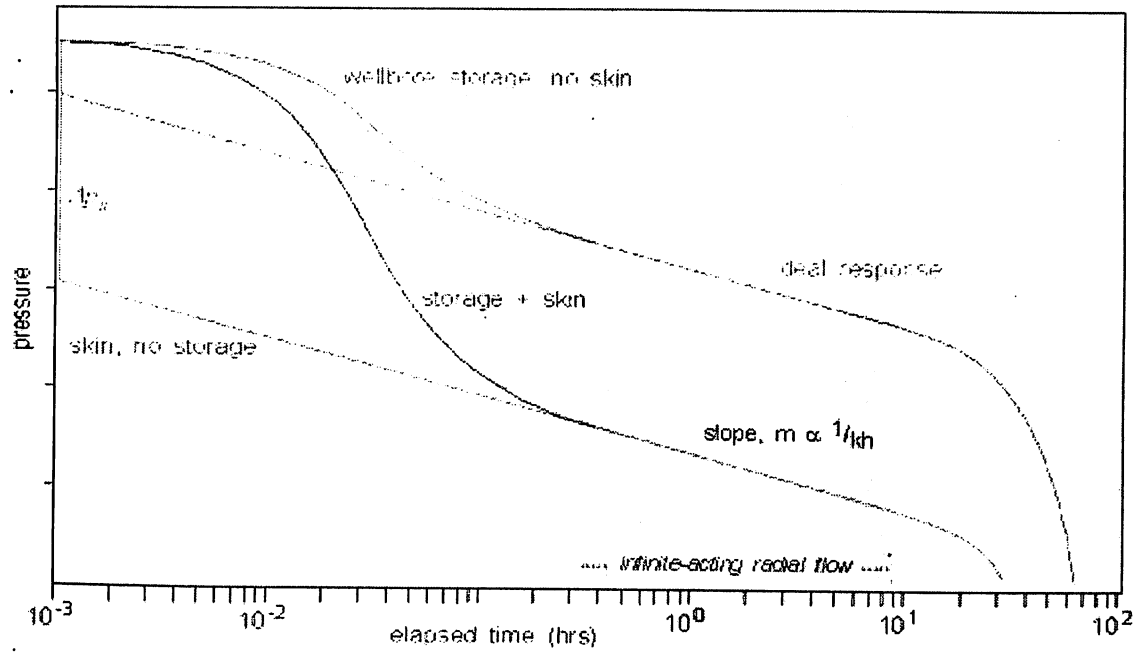

Fig 2.10 Semi-log approach

[The plot above is the 'MDH' (Miller-Dyes-Hutchinson) plot, for a drawdown, but the principles described below apply equally well to a build-up. Semi-log plots are discussed in detail in section 2.2.5].

- Considering the ideal case, of putting on production a well with no wellbore storage and no skin, the blue curve is obtained. The straight line representing radial flow is established almost instantaneously, and from the slope of the line the permeability-thickness product, kh, is obtained.

- With wellbore storage but no skin the red curve is obtained. Initially production is only from decompression of the wellbore fluid, so the bottomhole pressure remains constant for a short while, as if the well were still shut in. Once there is movement of fluid through the sand face, the bottom hole pressure starts to drop, and once the effects of storage are over the red curve transitions onto the ideal curve.

- With skin but no storage, the green curve shows radial flow immediately, parallel to but offset from the ideal blue line. The offset on the y-axis corresponds to Δps at this flowrate, and the slope of the straight line can not be different, as it represents the kh of the system.

- A typical test will reveal both wellbore storage and skin, corresponding to the black curve transitioning on to the green curve. The storage causes the delay, the skin the offset, and once again the final straight line slope is unchanged, as permeability is a reservoir property and is unaffected by near-wellbore effects.

In most cases the pressure curve will eventually drop below the radial flow line, as shown to the right of the grey window, if the well is tested long enough. This is because there is no such thing as an infinite reservoir, and as boundaries are seen, but the same flowrate is maintained from the well, the pressure will drop more rapidly. Sometimes the opposite happens, and the boundary is a supporting aquifer or gas cap, in which case the pressure curve tends to stabilize. What is certain is that the radial flow, and its corresponding straight line, can not last forever.Until the effects of wellbore storage become insignificant, the pressure response does not reveal information about the reservoir. The 'grey window', containing the radial flow data from which *kh* and skin are obtained, can be brought forward either physically, by way of downhole shut-in to reduce the wellbore storage, or mathematically, by way of convolution of downhole flowrate and

pressure data. As mentioned previously, this example is for the simplest semi-log plot, the MDH drawdown plot. However all of the principles described apply equally well to the other semi-log plots, as discussed in section 2.2.5.

2.2.4 Pressure Derivative

The introduction of the pressure derivative in 1983 transformed the science of well test interpretation, which until that time had been based upon the semi-log plot. By including the pressure derivative plot with the log-log plot, the 'diagnostic' plot was born, as just shown in the previous examples. The pressure derivative is essentially the rate of change of pressure with respect to the superposition time function – i.e., the slope of the semi-log plot:

Taking the example of a drawdown, the slope of the semi-log plot is evaluated at all points, of which 7 key points are shown in the plot.

The data starts at point 1, before eventually stabilizing at slope m in Infinite-Acting Radial Flow, points 6 and 7.

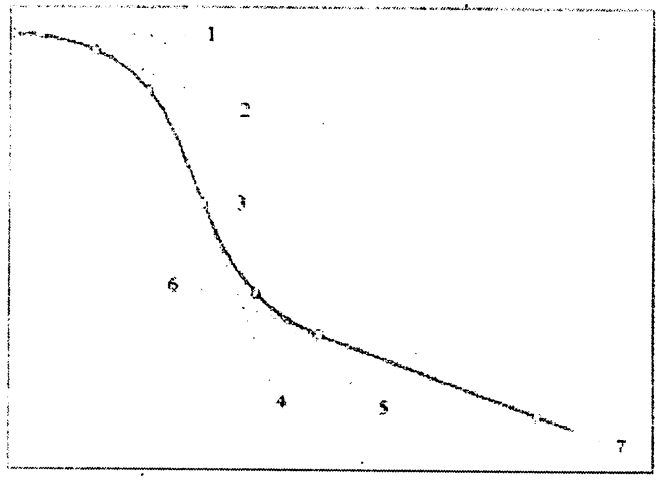

Points 1 and 2 fall on the wellbore storage unit-slope in early time and, during the transition to IARF, the derivative peaks at point 4. The transition is complete at point 6, as the derivative flattens to a value equivalent to m.

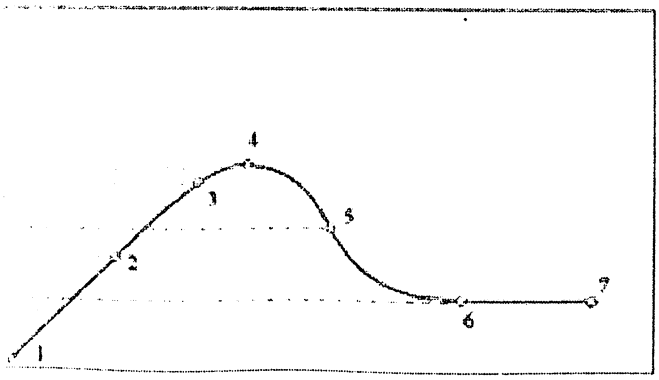

Fig 2.11 & Fig 2.12 Pressure derivative

So the basic idea of the derivative is to calculate the slope at each point of the pressure curve on the semi-log (superposition) plot, and to display it on the log-log plot.

The derivative has the expression:

$$\Delta p' = \frac{d\Delta p}{dsup.(\Delta t)}$$

Combined Pressure And Derivative Log-Log Plot

At early time, when the flow is dominated by fluid compression/ decompression in the wellbore (wellbore storage), the pressure change is linear with respect to elapsed time:

$$\Delta p = C\Delta t \Rightarrow \quad \Delta p' = \frac{d\Delta p}{dsup.(\Delta t)} \equiv \Delta t = \frac{d\Delta p}{d\ln\Delta t} = \Delta t = \frac{d\Delta p}{d\Delta t} = C\Delta t$$

[Note that in early-time the approximation can be made that dsup.Δt = dlnΔt].

- So when the flow at early time corresponds to pure wellbore storage, pressure and pressure derivative curves will merge on a unit slope straight line on the log-log plot.
- As already seen, in radial flow the derivative stabilises to a constant value, corresponding to the superposition slope m'.

For most other flow regimes, it will be seen that while the log-log plot reveals little or no relevant information, the pressure derivative always displays a characteristic response.

2.3 Superposition Theorem

2.3.1 Principle

If we start producing a well, from a reservoir initially at a uniform pressure pi, we will induce a distortion of the pressure profile at the wellbore, the slope of which is given by Darcy's Law. The 'bending' of the pressure profile in the case of a drawdown is described as concave, and the diffusivity equation will describe how quickly this distortion will evolve within the reservoir:

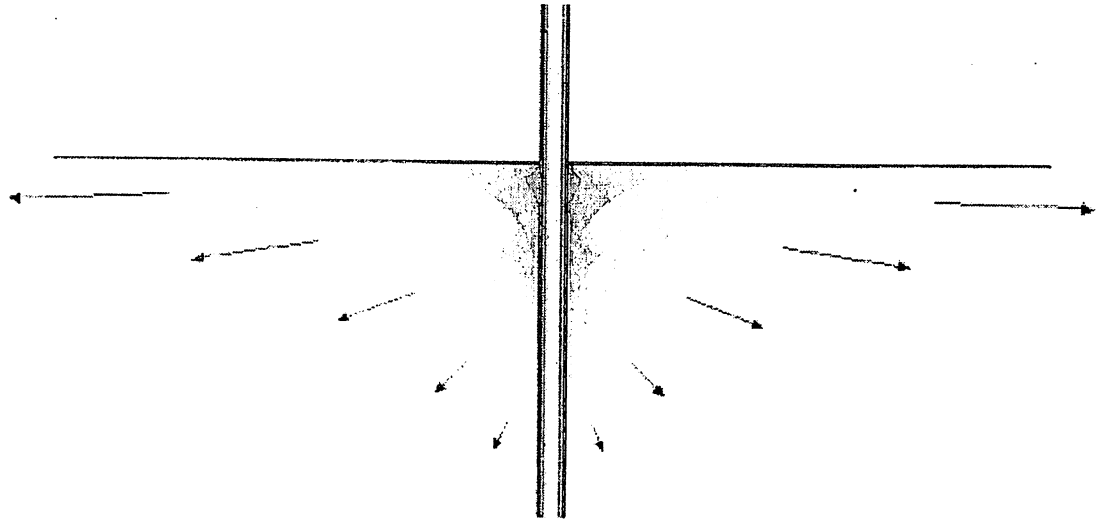

Fig 2.13 Drawdown sink

Throughout the production phase the profile will be concave, the pressure dropping everywhere, and it will be most concave close to the well. The concavity around the well will reduce in time, as more and more of the fluid is produced from further into the reservoir.

Build-Up

When the well is shut in, another distortion is induced in the pressure profile, and Darcy's Law shows that the profile has to be flat at the wellbore. Instantaneously the profile is 'bent' around the wellbore, while it is unaltered further from the well. This produces a build-up pressure profile which is convex around the wellbore (pressure increasing) and concave everywhere else (pressure still decreasing due

to the still-diffusing production signal). For radial flow the 'inflexion point' is a circle that moves away from the wellbore as the build-up progresses:

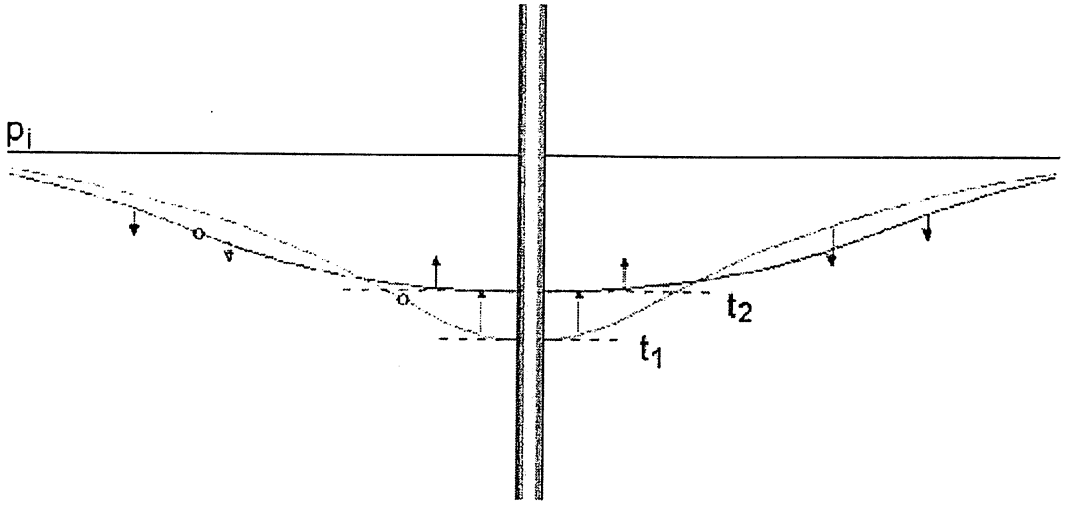

Fig 2.14 Superposition: Buildup

Physically, the part of the reservoir within the expanding 'inflexion circle' is 'recharged' by the outer part of the reservoir.

Considering an interference well, i.e. a nearby observation well which is passive, the pressure will continue to decrease until the inflexion circle reaches the interference well. At this point the pressure will start increasing again, to ultimately reach initial pressure (in the case of an ideal, infinite reservoir.)

2.3.2 Mathematical Approach

Earlier the log approximation to the solution to the diffusivity equation for infinite-acting radial flow was presented. This analytical model was developed assuming a single constant production rate, whereas in practice we need to obtain a model solution for more complex flow histories. In particular, due to the difficulty of maintaining a constant flow rate, interpretation methods have traditionally been based upon build-up data, preceded of course by one or more drawdowns. The superposition principle allows the multi-rate response to be calculated simply by adding drawdown responses.

Build-Up Solution

Consider a well producing at a rate *q* until time *tp*, and then shut in, and we want to find the pressure at time *tp* + Δ*t*, as seen below. The fact that the equations are linear allows us to use the principle of superposition: 'The pressure change due to a combination of production periods is equal to the combination of individual pressure changes due to each production phase'.

The shut-in at time *tp* is mathematically equivalent to a continuation of the drawdown at rate *q*, in combination with an injection at rate *-q* from time *tp*:

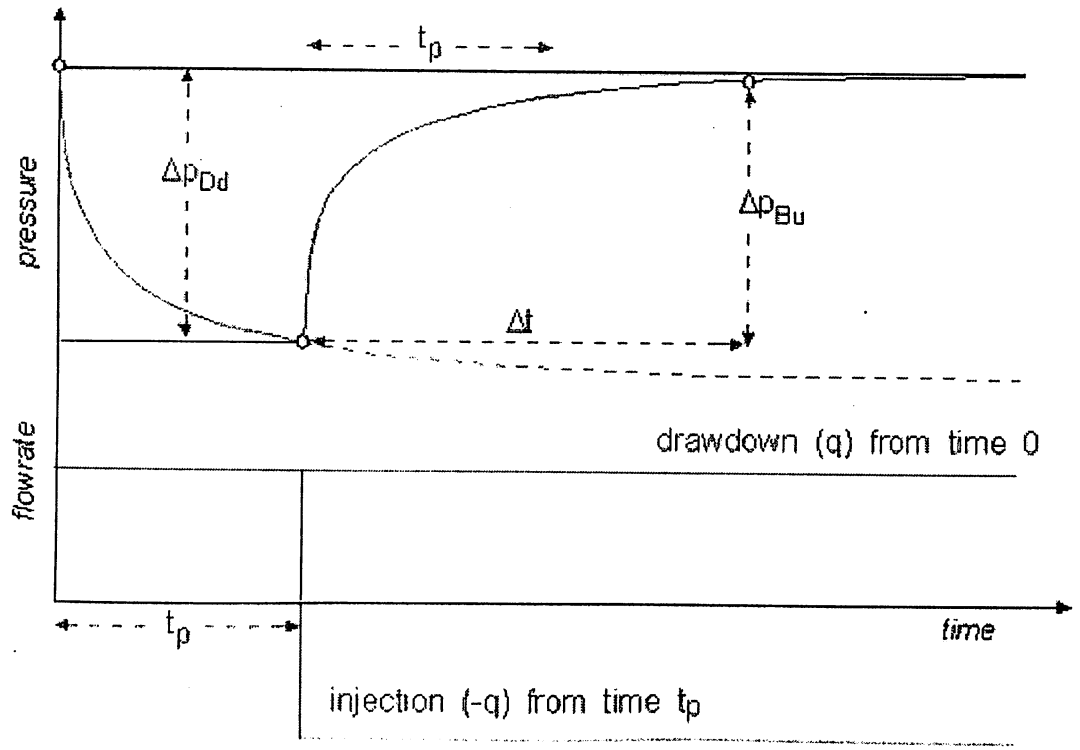

Fig 2.15 Buildup solution

In this case, the pressure change at *tp* + Δ*t* will be the sum of the pressure change due to the drawdown at rate q from time 0 to time *tp* + Δ*t*, and the pressure change due to an injection at rate –q from time tp to time *tp* + Δ*t*:

$$p_{BU}(\Delta t) = p_i - \Delta p_{DD}(t_p + \Delta t) + \Delta p_{DD}(\Delta t)$$

[Referring to the diagram again, note that after a build-up duration of *tp*, the pressure change due to the injection at *-q* is the same as the pressure change at the end of the drawdown, Δ*pDd*: So if it were not for the continued effect of the drawdown, the build-up pressure would follow the green curve and return to *Pi* after a time *tp* of the build-up. However this pressure change is superposed on a 'moving baseline', which is the continuing pressure decline due to the drawdown, and therefore the build-up can not return to *Pi* after a time *tp*.]

We are more concerned with the pressure changes than the actual pressure:

$$\Delta p_{BU}(\Delta t) = p_{BU}(\Delta t) - p_{@\Delta t=0}$$

Where

$$p_{@\Delta t=0} = p_i - \Delta p_{DD}(t_p)$$

Substituting pBU(Δ*t*) from above:

$$\Delta p_{BU}(\Delta t) = \Delta p_{DD}(t_p) + \Delta p_{DD}(\Delta t) - \Delta p_{DD}(t_p + \Delta t)$$

The general form of the build-up solution in dimensionless terms, with respect to its drawdown counterpart, becomes:

$$p_{D_{BU}}(t_D) = p_D(t_{pD}) + p_D(t_D) - p_D(t_{pD} + t_D)$$

As the drawdown solution is an inc reasing function of time, the negative term is greater than either of the positive terms, such that:

$$p_{D_{BU}}(t_D) < p_D(t_{pD})$$

And

$$p_{D_{BU}}(t_D) < p_D(t_D)$$

The first expression confirms that the build-up response will be 'flatter' than the drawdown response, and the second shows that the pressure can never exceed the initial pressure.

2.3.3 Superposition in Space: Boundaries

The principle of superposition, applied in time to flow periods in section 5.4, can also be applied in space, in order to reproduce the effects of nearby wells and/or boundaries. All wells in the same system can be added to obtain the total response at any point in the system. This principle is used in interference testing, and can also be used to model sealing and constant pressure boundaries:

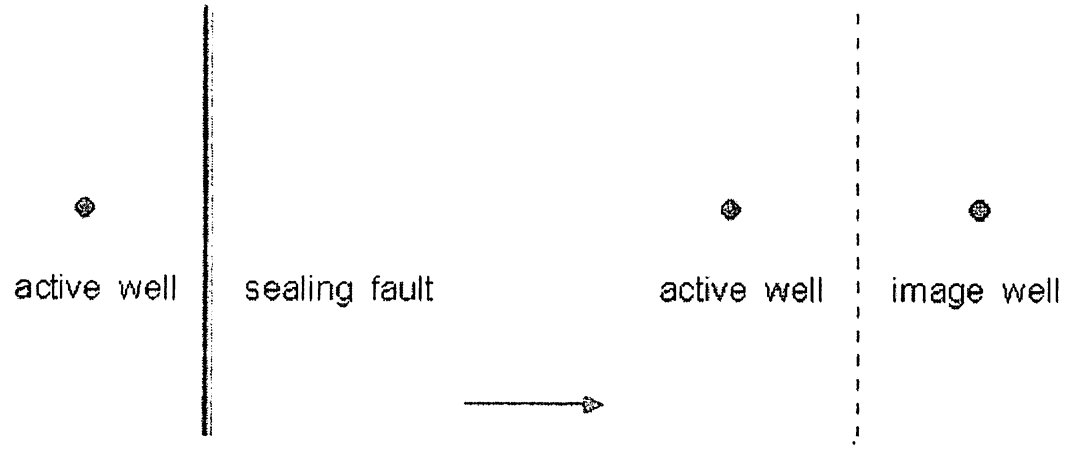

Fig 2.16 Superposition in Space: Boundaries

The assumption is that the pressure response at the flowing well, due to a nearby fault, is physically equivalent to the pressure that would be observed at the active well in the presence of a nearby producing well. This is the 'method of images', with a virtual image well replacing the fault and creating the same effect.

Although not physically rigorous, the idea of a reflected signal can be used to explain the principle. In the real case, with one flowing well and a fault, the measured pressure response at the wellbore becomes a combination (superposition) of the drawdown response and the reflected response returning from the fault:

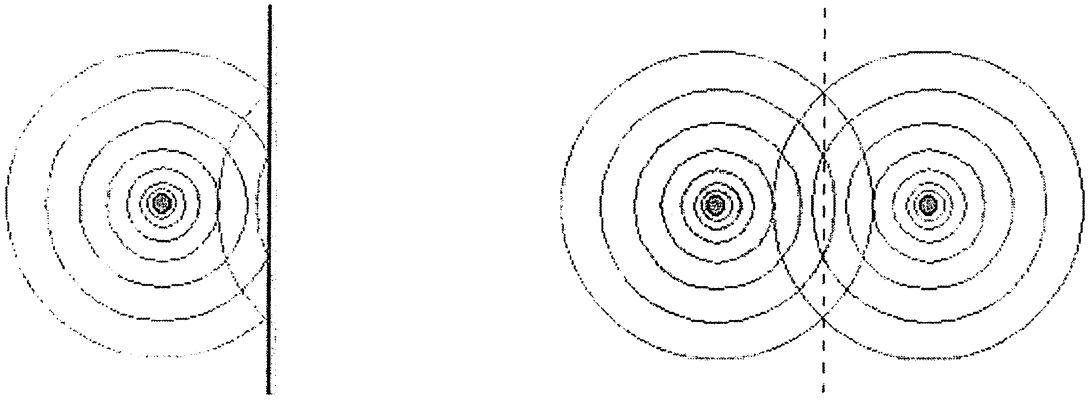

Fig 2.17 Method of Images

The analogy with the active well and the image well, at twice the distance from the active well as the fault, shows the wellbore response to be a superposition of the drawdown response and the effect of the drawdown from the image well – which is the same as the reflected response from the fault.

Anywhere in the reservoir, the pressure drop (Δp) is the sum of the Δps due to the real well and the image well. Each pressure change is a product of the diffusivity equation, as is the sum, so the Δp each side of the sealing boundary is symmetrical and the pressure gradient across the boundary is zero. The Δp sum respects all the conditions of the diffusion, the initial conditions and the boundary conditions of the physical problem, so the superposition is a rigorous solution.

In the case of a single plane boundary there is only one image well, which is producing at the same rate as the actual well for a sealing boundary, or injecting at the same rate for a constant pressure boundary.

When more than one sealing boundary is present, the solution can involve a large number (hundreds) of image wells, depending upon the geometry of the system, and the generation of theoretical solutions can take a long time even on a modern computer. On the other hand the presence of a single constant pressure boundary will mask the subsequent effect of any sealing boundaries further from the well.

2.4 Semi-Log Analysis

As seen in section 5.2.4, the late time approximation to the solution to the diffusivity equation for Infinite-Acting Radial Flow (IARF) is:

$$P_D = \frac{1}{2}\left[\ln(t_D) + 0.80907 + 2S\right]$$

and in decimal logarithms:

$$p_D = 1.151\ \log(t_D) + 0.40453 + S$$

In terms of real pressure, and converting to Oilfield Units:

$$\Delta p = 141.2\frac{q\mu B}{kh}\left[1.151\log\left(0.000264\frac{k\Delta t}{\phi\mu C_t r_w^2} + 0.40453 + S\right)\right]$$

which can be re-written as:

$$\Delta p = 162.6\frac{q\mu B}{kh}\left[\log(\Delta t) + \log\left(\frac{k}{\phi\mu C_t r_w^2}\right) - 3.23 + 0.87\ S\right]$$

When the semi-log approximation for infinite-acting radial flow is valid, a plot of Δp, or p, versus log (Δt) will yield a straight line, of slope 'm':

$$m = 162.6\frac{q\mu B}{kh}$$

The semi-log approach to well test interpretation is based upon the identification of this straight line portion of the drawdown or build-up data, from which the permeability-thickness product, kh, and the skin damage S are obtained.

- **kh** is obtained directly from the straight line slope m, as all other terms in the equation are known (flowrate q, fluid viscosity μ, and volume factor B).

- **S** is obtained by taking an arbitrary pressure point on the straight line, at Δt = 1 hour, so that log (Δt) = 0:

$$\frac{\Delta p_{1hr}}{m} = \left[\log\left(\frac{k}{\phi \mu C_t r_w^2}\right) - 3.23 + 0.87\ S\right]$$

All other terms are known, and the equation can be solved for the skin value, as will be seen in the next section.

2.4.1 MDH Plot (Dd #1)

The most simple semi-log plot, in which the time axis is log(Δt), is called the Miller-Dyes- Hutchinson or MDH plot. It is strictly valid only for the first ever drawdown on a well, but can in exceptional circumstances be used for analysis of a later drawdown or even a build-up. In 1998, with computers that can handle superposition rigorously, it should only be used for 'Drawdown #1':

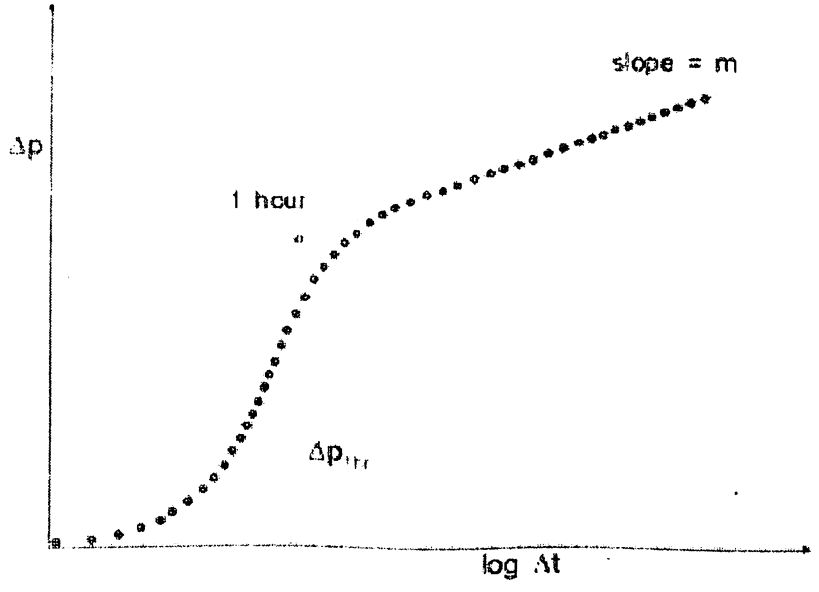

Fig 2.18 Semi-log plot

All of the semi-log plots are more conveniently plotted with pressure on the y-axis, as this makes no difference to the analysis. So for the MDH, a drawdown plot:

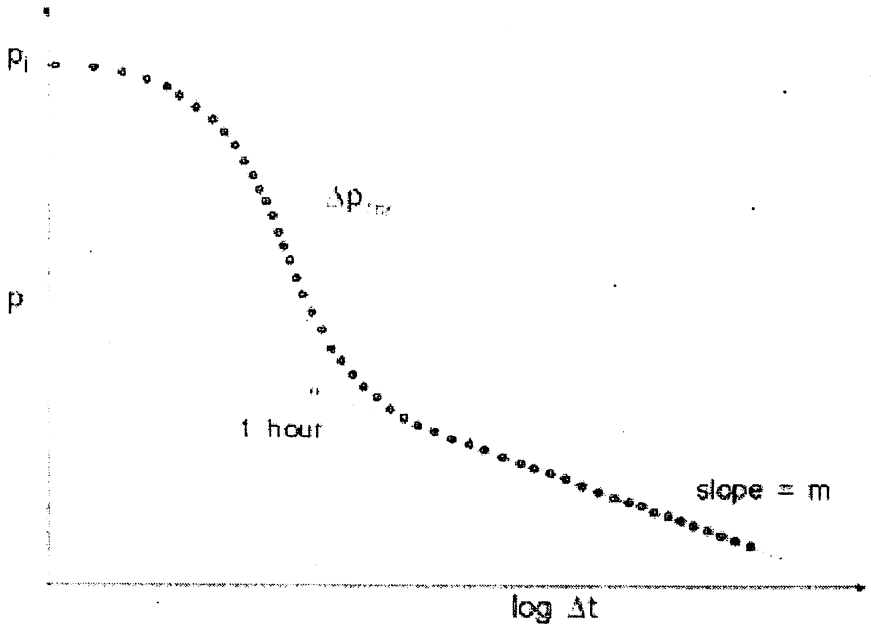

Fig 2.19 MDH plot

As already mentioned the slope of the straight line is:

$$m = 162.6\frac{q\mu B}{kh}$$

This gives the permeability-thickness product as:

$$kh = 162.6\frac{q\mu B}{m}$$

The value of the pressure on the line at $\Delta t = 1$ hour is used to evaluate the skin. Cross-multiplying the expression on the previous page:

$$S = 1.151\left[\frac{\Delta p_{1hr}}{m} - \log\left(\frac{k}{\phi\mu C_t r_w^2}\right) + 3.23\right]$$

2.4.2 Horner Plot (Bu #2)

The MDH plot, with the simple log(Δt) time function, results directly from the log approximation to the drawdown solution for infinite-acting radial flow. In order to use semi-log analysis for any flow period other than the first drawdown, it is necessary to take account of superposition effects, as discussed in earlier.

In the simplest superposition case of a build-up following a single drawdown, in which an 'elementary drawdown solution' of rate **-*q*** (i.e. an injection) overlays a drawdown of rate **+*q***, and assuming that both solutions reach IARF, we get the approximate build-up solution:

$$p = p_i - 162.6\frac{q\mu B}{kh}\log\left(\frac{t_p + \Delta t}{\Delta t}\right)$$

So infinite-acting radial flow will be characterized by a linearity between the pressure response and the Horner time function, *log (tp+Δt)/Δt*, which depends upon tp, the duration of the production period preceding the shut-in.

The coefficient in front of the log term is the same as for the MDH plot, so the straight line slope will again be 'm', and

$$\therefore kh = 162.6\frac{q\mu B}{m}$$

as before. The skin calculation requires that the drawdown had reached IARF in the reservoir prior to shut-in, as the last flowing pressure (at tp) is replaced by its log approximation:

$$\Delta p_{BU} = p_{BU} - p_{\Delta t=0} = 162.6\frac{q\mu B}{kh}\left[\log\left(\frac{t_p \Delta t}{t_p + \Delta t}\right) + \log\left(\frac{k}{\phi\mu C_t r_w^2}\right) - 3.23 + 0.87\,S\right]$$

Taking the pressure on the line again at 1 hour, the skin equation becomes:

$$S = 1.151\left[\frac{\Delta p_{1hr}}{m} - \log\left(\frac{k}{\phi\mu C_t r_w^2}\right) + \log\left(\frac{t_p + 1}{t_p}\right) + 3.23\right]$$

The only difference compared to the MDH solution is the second log term, which will typically be of little significance.

Note that the time function is such that the data plots 'backwards', as when Δt is small, at the start of the build-up, Horner time (log $(tp+\Delta t)/\Delta t$) will be large, and when Δt tends to infinite shut-in time the Horner time tends to 1, the log of which is 0:

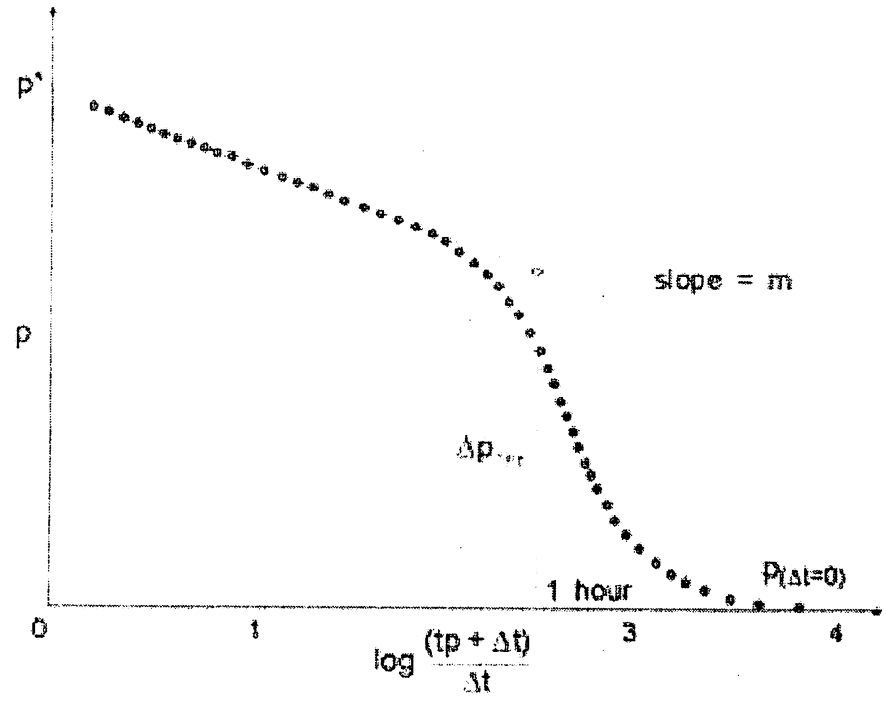

Fig 2.20 Horner's plot

If the reservoir were truly infinite, the pressure would continue to build-up in infinite-acting radial flow and eventually intercept the y-axis at pi, the initial pressure. However as no reservoir is infinite, the extrapolation of the radial flow line at infinite shut-in time is called p*, which is simply an extrapolated pressure. It may give a value very close to the eventual shut-in pressure, but to call this value the present reservoir pressure would be a mistake, as the only thing that is certain about the real data is that it would NOT follow the infinite-acting radial flow line forever. As the effects of

boundaries are seen, as they eventually must be, the data will deviate from the 'm' line. The Horner plot is only really valid for 'Build-Up #2', that is transient #2, the first transient being a single, constant-rate drawdown. However, with a more complex rate history, a good approximation can sometimes be made to the time function by using an 'equivalent production time', tpe , in which the cumulative production is assumed to have all occurred at the final flowrate prior to shut-in. Once again, it should be stressed that historical approximations born of necessity have no place in well test interpretation today. The correct approach for the analysis of a build-up (or drawdown) following a complex rate history is the superposition plot:

2.4.3 Superposition Plot (all transients)

The general, dimensionless multi-rate solution for the pressure response following various flows and shut-ins (transients) is:

$$p_{D_{MR}}(t_D) = p_D(t_D) + \sum_{i=1}^{N-1}\left[\frac{(q_i - q_{i-1})}{(q_N - q_{N-1})}\left\{p_D([t_N - t_i]_D + t_D) - p_D([t_N - t_i]_D)\right\}\right]$$

As with the Horner solution for build-up #2, it is possible to define a general logarithmic time function, applicable to all transients, by replacing each of the superposed responses with its semi-log approximation. This is the superposition time function:

$$Sm(\Delta t) = \sum_{i=1}^{n-1}(q_i - q_{i-1})\log\left[\sum_{i=1}^{n-1}\Delta t_j + \Delta t\right] + (q_{mi} - q_{n-1})\log(\Delta t)$$

A plot of pressure versus superposition time is the 'general semi-log' plot, as it applies to all transients:

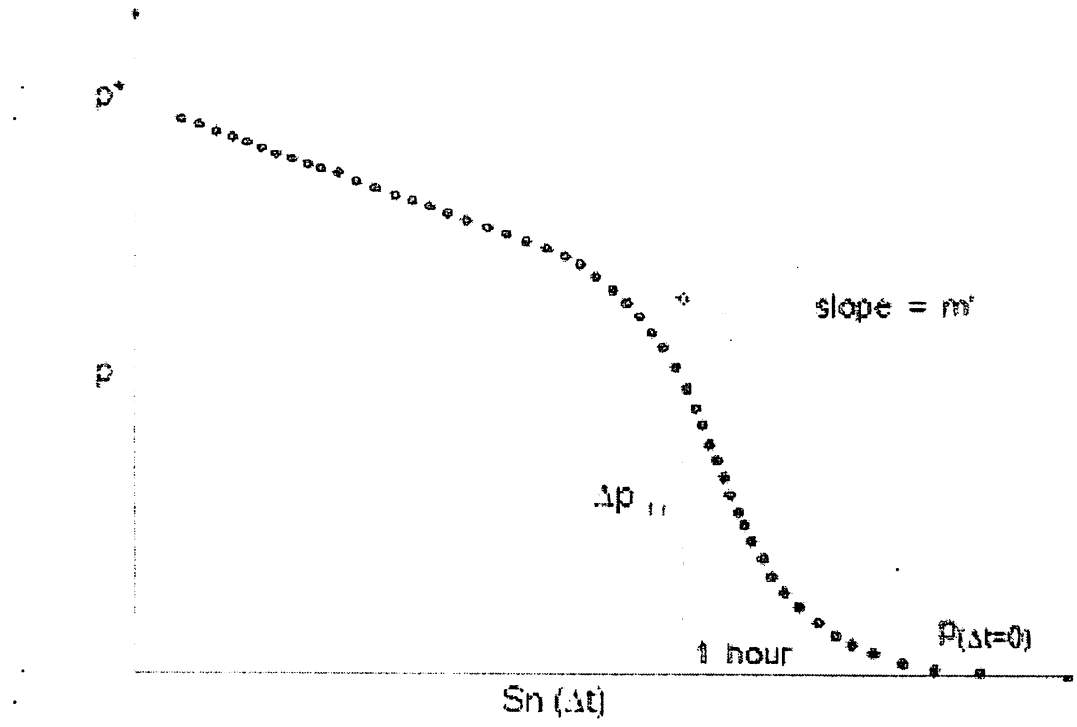

Fig 2.21 Superposition plot

The example shown is a build-up, and it can be seen that the superposition plot looks exactly like a Horner plot, with just 2 subtle differences:

- Firstly, the x-axis scale is cartesian. This is because the superposition time function is itself logarithmic, with all time values in the expression being log terms.
- Secondly, the slope of the IARF straight line is no longer m, as it was for MDH and Horner, it is now *m'*. In fact, $m'=m/q$, where *q (Δq)* is the change in rate of the transient under investigation. (In a build-up, this would be equivalent to the flowrate prior to shut-in.) This is because the superposition time function also incorporates the flowrates.

So although the superposition time function looks fundamentally different to MDH and Horner analysis, the solution equations are almost identical, with *m* replaced by m'/q:

$$kh = 162.6\frac{\mu B}{m'} \qquad S = 1.151\left[\frac{\Delta p_{1hr}}{m'q} - \log\left(\frac{k}{\phi\mu C_t r_w^2}\right) + 3.23\right]$$

As with Horner analysis, the extrapolated radial flow line would give the final shut-in pressure in an infinite reservoir, and is known in as p*. Some literature refers to p* as the 'false pressure', which is a good way to think of it! (In the case of drawdowns, whether in MDH or superposition analysis, there is no meaning to extrapolating the radial flow line to infinite time.) Δp(1 hr) can be difficult to evaluate in superposition analysis, at least by hand, as it involves calculating the value of the time function at 1 hour. Modern software computes it automatically when a line is drawn on the data Δp(1 hr) is evaluated at 1 hour on the line, even if the real data is not in radial flow), and typically flags the user with the computed value for reference purposes.

Chapter 3

Drill Stem Test –Methodology and Equipments

3.1 Introduction

Drill stem testing is a method of gathering data on the potential productivity of a reservoir before a permanent completion string is installed .It is aimed to answer certain questions about the profitability and most important of the reservoir extent and hydrocarbon in place. Basic parameters needed to be determined by well test are: -

1. Inflow performance of the well (PI /AOFP)
2. Reservoir pressure and temperature.
3. Reservoir fluid type and sampling.
4. Skin factor and Permeability.
5. Commercial viability of the well.
6. GOR, API gravity.
7. Critical flow rate for sand production.
8. Fluid gradient and reserve estimates.

Formation fluid samples are taken and are used for PVT analysis, which reveals how hydrocarbon phases coexist at different pressures and temperatures. PVT analysis also provides fluid physical properties required for well test analysis and fluid flow simulation. Reservoir deliverability is a key concern for commercial exploitation.

Estimating a reservoir's productivity requires relating flow rates to drawdown pressures. This can be achieved by flowing the well at several flow rates (different choke sizes) and measuring the stabilized bottomhole pressure and temperature prior to changing the choke.

The plot of flow data versus drawdown pressure is known as the inflow performance relationship (IPR). For single phase oil conditions, the IPR is a straight line whose intersection with the vertical axis yields the static reservoir pressure. For gas wells, IPR curves exhibit certain curvature due to extra inertial and turbulent flow effects in the vicinity of the wellbore and changes of gas properties with pressure. Oil wells flowing below the bubble point also display similar curvature, but these are due to changes in relative permeability created by variations in saturation distributions. The inverse of the slope represents the productivity index of the well. The IPR is governed by properties of the rock-fluid system and near wellbore conditions.

Estimation of the formation's flow capacity, characterization of wellbore damage, etc. require a transient test because a stabilized test is unable to provide unique values for mobility-thickness and skin. Transient tests are performed by introducing abrupt changes in surface production rates and recording the associated changes in bottomhole pressure. Production changes, carried out during a transient well test, induce pressure disturbances in the wellbore and surrounding rock. These pressure disturbances travel into the formation and are affected in various ways by rock features. For example, a pressure disturbance will have difficulty entering a tight reservoir zone, but will pass unhindered through an area of high permeability. It may diminish or even vanish upon entering a gas cap. Therefore, a record of wellbore pressure response over time produces a curve whose shape is defined by the reservoir's unique characteristics. Unlocking the information contained in pressure transient curves is the fundamental objective of well test interpretation.

Pressure transient curve analysis provides very useful information about reservoir characteristics. Horizontal and vertical permeability,

well damage and fracture length flow are just a few of the characteristics that can be determined. In addition pressure transient curves can indicate the reservoir's extent and boundary details. The shape of the curve, however, is also affected by the reservoir's production history. Each change in production rate generates a new pressure transient that passes into the reservoir and merges with previous pressure effects. The observed pressure at the wellbore is a result of the superposition of all these pressure changes.

3.2 Sequence Of Events

1. Flex Run

- To check the tubing integrity
- To clean the tubing of any scaling and rusting

2. Dummy Run

- Depth Correlation
- Sub-sea tree spacing

3. Main Run

- Set the packer after the depth is matched
- Activation of necessary valves after pressure testing
- Perforate the well after safety meeting

4. Flow the well as per the program

- Initial build up
- Clean up flow
- First build up
- Main flow
- Final build up
- Commercial flow(if planned)

5. Reverse circulate the h/c out of the wellbore

6. Kill the well as per the program

Typical Drill Stem Test design

Flow Period	Duration	Cumulative hours	Remarks
Initial Flow	10 minutes	10 minutes	
Initial Buildup	110 minutes	2 hours	
Cleanup Flow (48/64" choke maximum)	6 hours	8 hours	Clean up to increase gradually from 16/64 choke to 48/64 choke. The cleanup flow to continue till the stabilisation of Well head pressure and BS&W < 1%.
First Buildup	8 hours	16 hours	Data latch to be run in to get the readings. The actual time may vary depending upon the data latch operation.
First Drawdown (24/64" choke)	6 hours	22 hours	The actual timing of the flow period and buildup along with the choke sizes may be modified depending upon the results of the first buildup data (obtained from the data latch operation).
Second Drawdown (36/64" choke)	6 hours	28 hours	
Third Drawdown (48/64" choke)	6 hours	34 hours	
Final buildup	24 hours	58 hours	

Choke changes to take place gradullay in 10-15 minutes

Table 3.1

3.3 Methodology

Drill stem testing is a temporary well completion test undertaken before or after casing is run. It enables us to look "deeper" into the reservoir than the other wellbore measurement methods. In its simplest form, the DST assembly is a set of measurement, control, and sample tools placed on the drill stem (in limited cases, at the bottom of tubing). It consists of one or more packers which isolate the test zone, a flow control valve, a continuous pressure recording device, a fluid sample chamber, and a perforated anchor for the fluids entering the tool string.

The test tools are run into the hole with empty drillpipe or tubing (in some cases a carefully designed water, diesel, or nitrogen cushion is used). The sequence of a typical test is shown in Figures 1 to 6. As the tool string is run into the hole, the increasing hydrostatic pressure of the mud column is recorded by the pressure gauge (Figure 3.1).

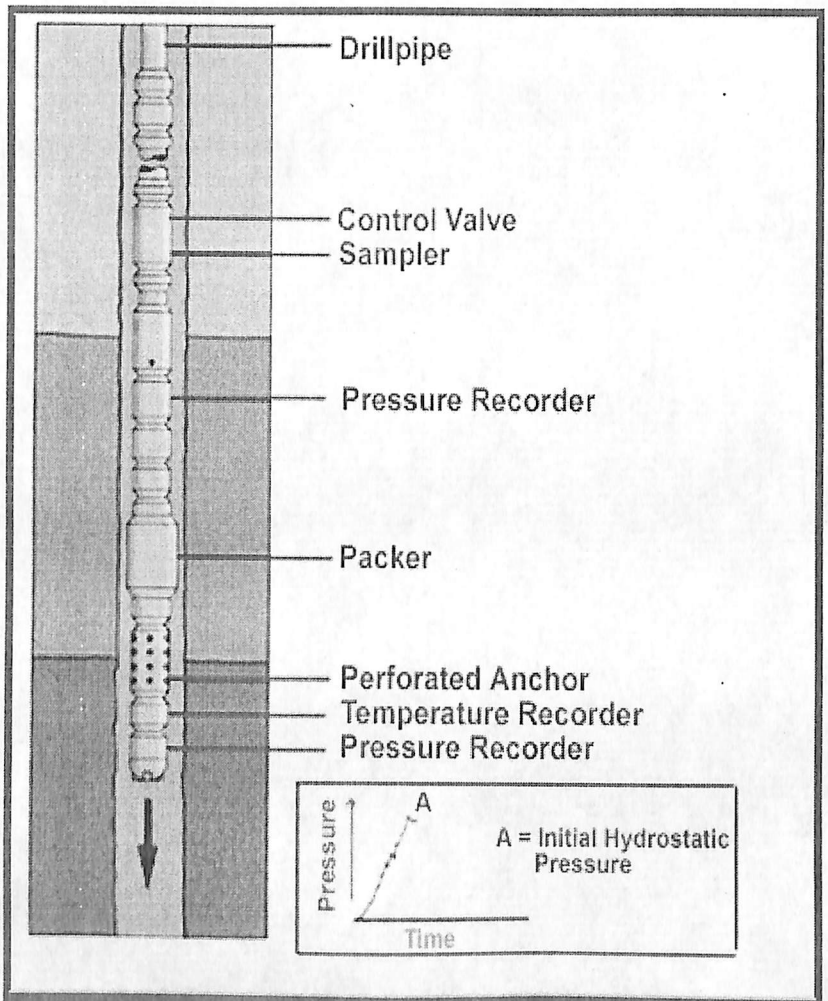

Figure 3.1

When the test tools reach the depth of the test formation, the packer is set against the walls of the hole or casing, thereby isolating the pressure of the mud column from the pressure in the test zone. Pressure is measured at the very bottom of the tool string and within the tool string itself. The gauge records the pressure imposed by the

hydrostatic head and any "squeeze" pressure developed when setting the packer.

The hydraulic valve is then opened and the formation fluids are free to flow into the low-pressure drillpipe (Figure 3.2).

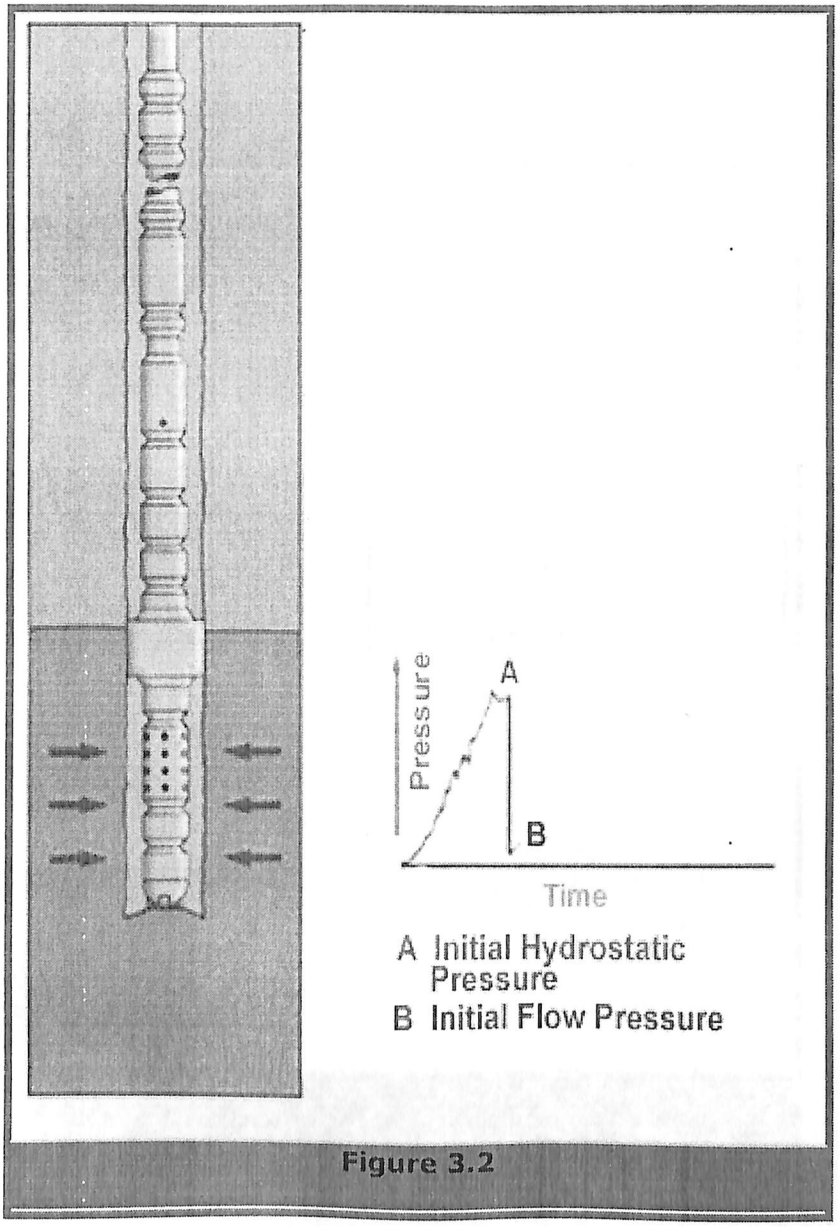

Figure 3.2

This initial flow, or pre-flow period, is usually short in duration, say 5 to 10 minutes. Its purpose is to relieve any buildup in pressure that may have occurred due to setting the packer(s), or supercharging. If the formation being tested is permeable and a large overbalance in

drilling mud hydrostatic pressure is present during drilling, the formation may be ""supercharged'' with mud filtrate. In this case, a longer flow period (perhaps 30 minutes) may be necessary in order to obtain an accurate estimate of initial pressure. The control valve is then closed and, because fluids may no longer flow into the drillpipe, the recorded pressure normally approaches the original formation pressure (Figure 3.3). This shut-in period typically lasts for 30 to 60 minutes.

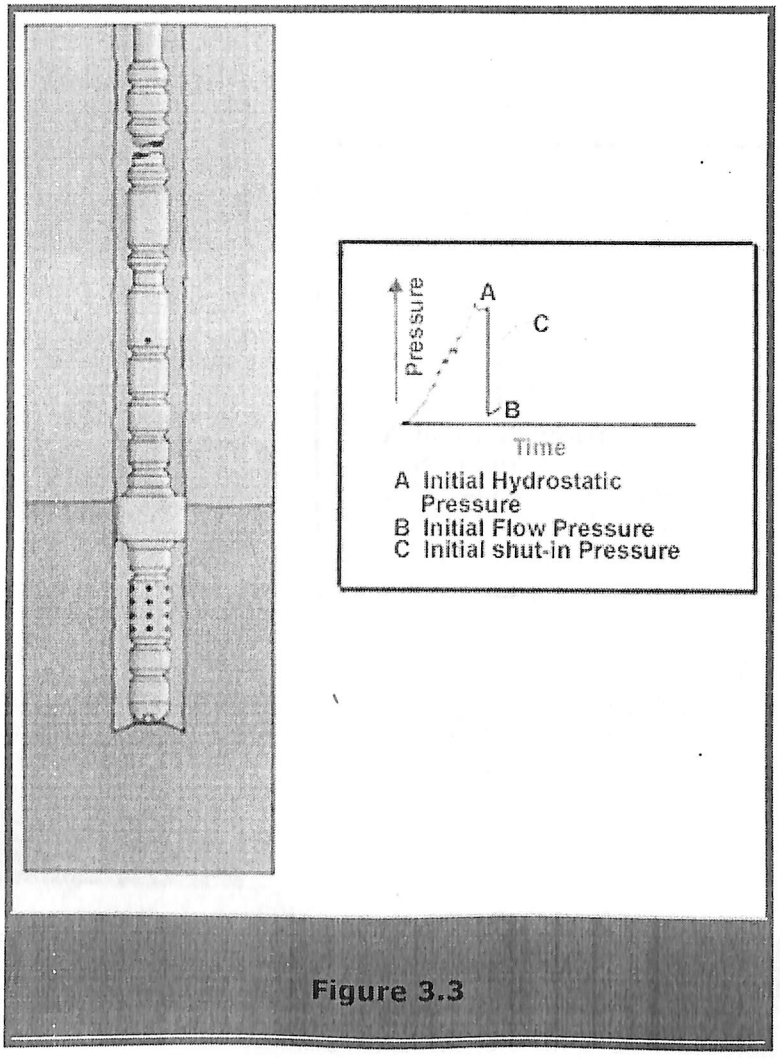

Figure 3.3

The control valve is then opened once again for the second, more important flow period.Typically, an openhole test will last for 60 to 180 minutes and a cased hole test will last for 8 to 10 hours(Figure 3.4).

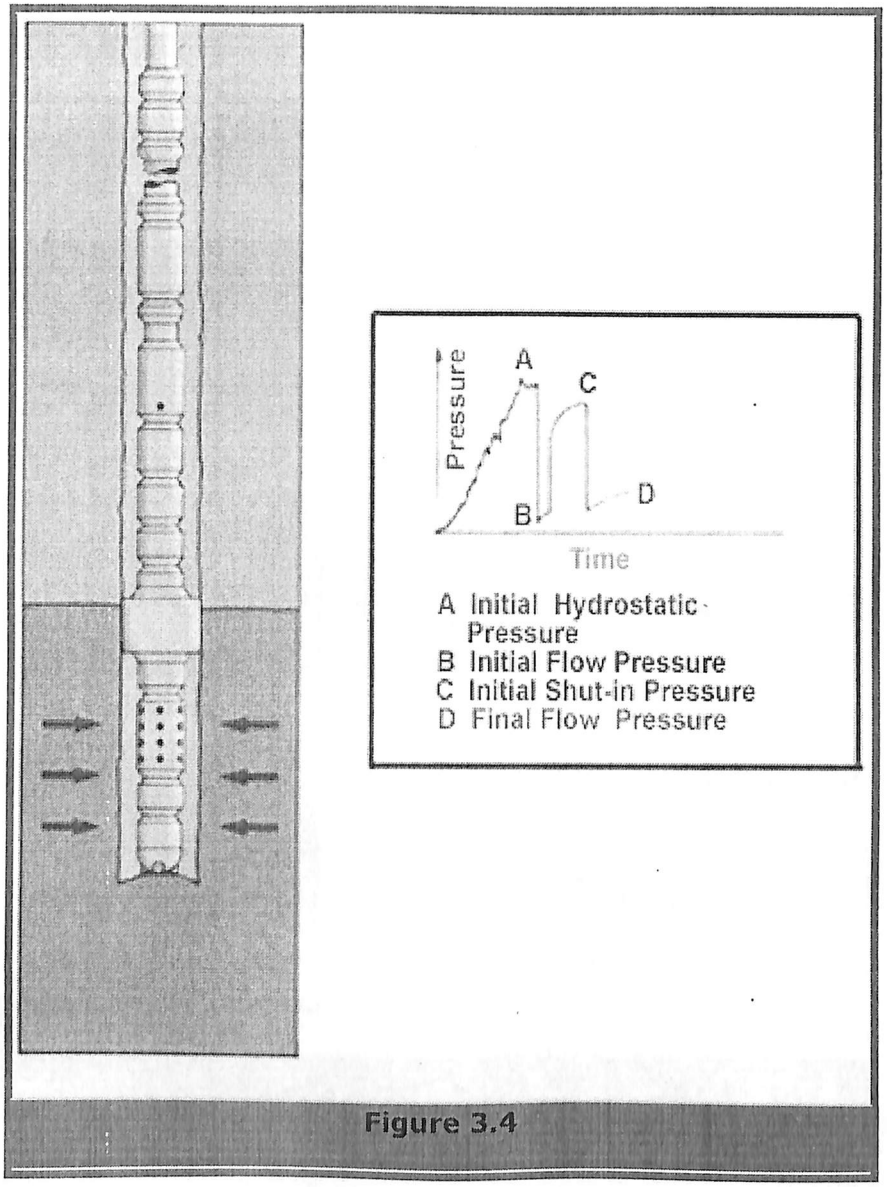

Figure 3.4

At the end of this flow period, a fluid sample is collected and isolated in the sample chamber. Additional samples are collected at the surface for wells that flow to surface. The final flow period is followed by a final shut-in period (Figure 3.5), which lasts approximately twice as long as the final flow period.

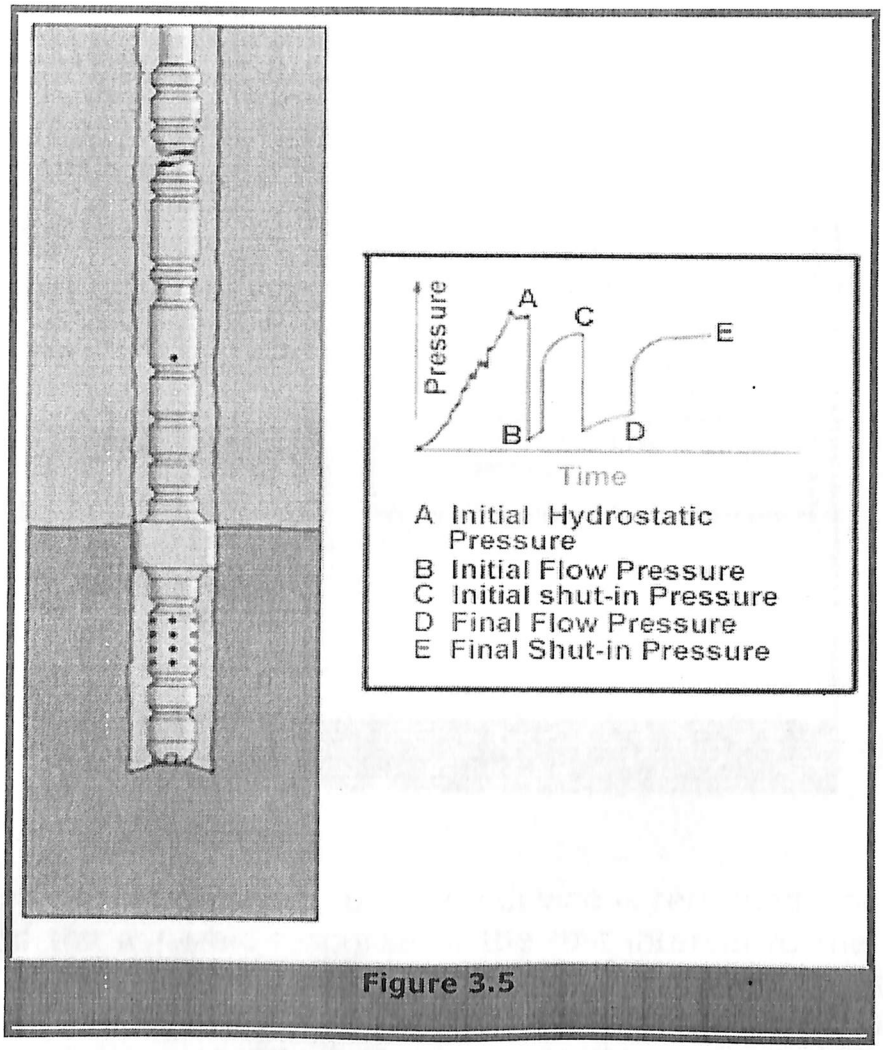

Figure 3.5

This provides a final shut-in pressure value. Any produced hydrocarbons are then reversed out of the test string, the packer is carefully released, and the tool string is pulled to the surface. Note that as soon as the packer is released, the hydrostatic pressure imposed by the mud column at the bottom of the drillstem is reduced as the tool string is pulled out of the hole (Figure 3.6).

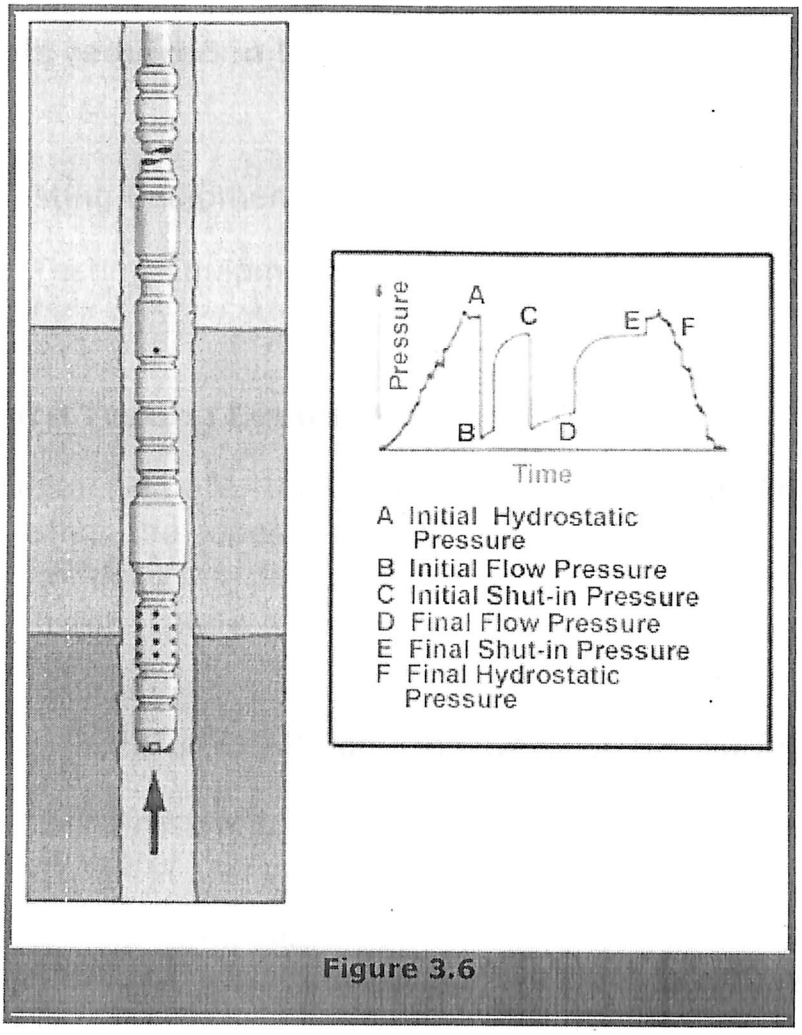

Figure 3.6

At the surface, the pressure recording device is retrieved from the tool string, and the dynamic response of the test interval to the alternate pressure drawdown and buildup periods is analyzed. If the test tools did not operate properly, the test must be repeated. To avoid this potentially costly remedy, it is now possible to display and record bottom hole pressures at the surface while the test is being run. This provides immediate information on the quality of the test, the opportunity to analyze the data before the tool string is retrieved, and the ability to terminate the test when sufficient data has been collected.

3.4 The tools required in DST can be categorized under the following:

1. Surface Testing Equipments

2. Downhole Testing Equipments (drill stem testing tools)

3.4.1 Surface Testing Equipments

Surface equipments are temporary installed to handle the fluids produced during the operation; this is because, in most cases, permanent production facilities have not yet been installed. These equipments must safely and reliably perform a wide range of functions:

- Quickly control pressure and flowrates at the surface and shut the well.
- Separate the resulting effluent into three separate phases and accurately meter these fluids.

- Collect surface samples.
- Dispose of the resulting fluids in an environmentally safe manner.

Surface equipments can further be subdivided as:

1 Flowhead

It is located directly on top of the well and equipped with master valve, flow wing valve, kill line valve, swab valve and a swivel. Coflex hose is connected with flow line and killing hose with kill line.

2 Coflex Hose

It is a flexible hose through which the effluent flows from flowhead to data header and is also used to compensate for the movement of the semisubmersible or drillship.

3 Data Header

It has 4 ports for pressure and temperature gauges, sampling and dead weight tester all connected to the flowline.

4 Sand Filter Unit

The dual-pot sand filter removes sand and other solid particles from well effluent. It is usually located upstream of the choke manifold.

5 Choke Manifold

The choke manifold controls the fluid from the well by reducing the flowing pressure and achieving a constant flow rate before the fluid enters the processing equipment on the surface. It consists of valves and fittings arranged to direct the flow through one of two choke boxes.

6 Heat Exchanger

Heat exchangers raise the temperature of well effluents, which prevents hydrate formation, reduces viscosity and breaks down emulsions to facilitate the separation of oil and water.

7 Separator

Test separators are used to separate, meter and sample all phases of the effluent. Orificemeter/ Daniel plate is used to measure the flowrate of gas while fluccometer or rotoron is used for oil flowrate measurement.

8 Surge Tank

The surge tank is a pressurized vessel used to measure liquid flow rates and obtain an accurate measurement of shrinkage and the meter factor. It is also used to calibrate the separator during the test.

9 Oil and Gas manifold

The oil produced by the separator can be directed through an oil manifold to the gauge tank, surge tank, production flowline or burner depending on the test circumstances while the gas from the separator is directed through the gas manifold to one of the burners depending on the prevailing wind during the test.

10 Transfer Pump

A transfer pump connected to the gauge tank outlet is used to empty one of the tank compartments while the other is being filled. It is also used for pressure boosting when there is insufficient pressure to achieve atomization at the burner.

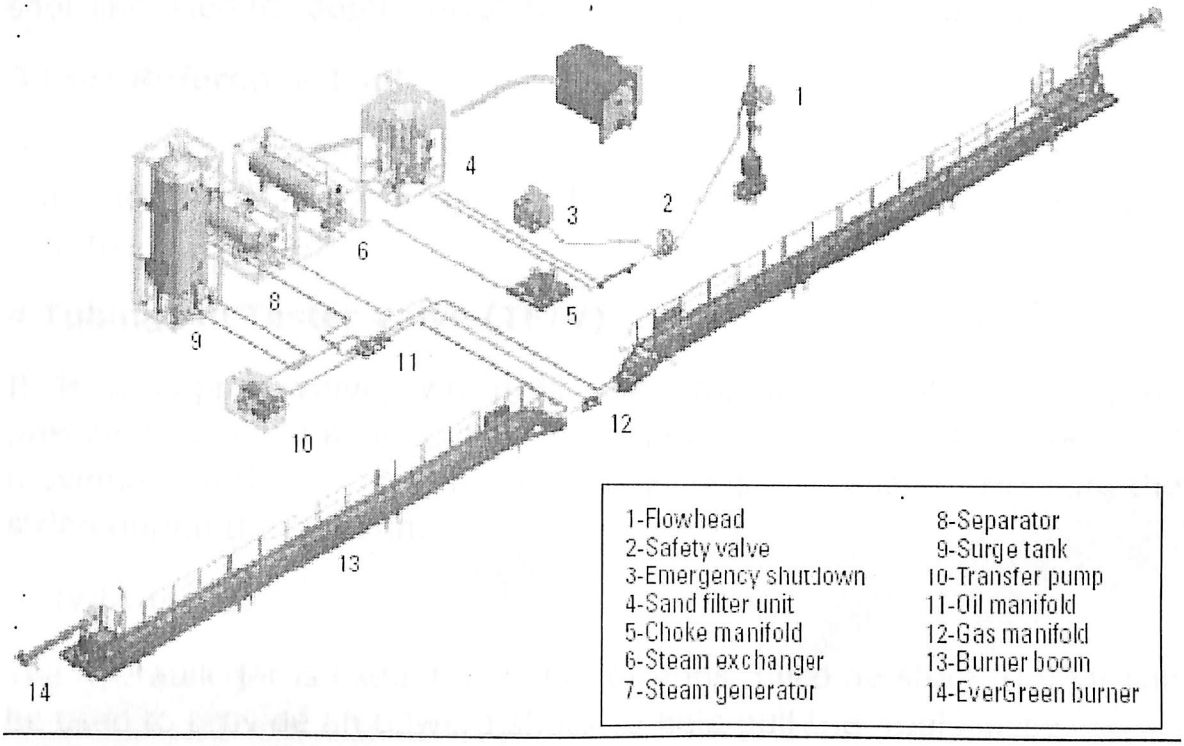

3.6 Surface Testing Equipments

3.4.2 Down Hole testing Equipments

The Downhole test string is a key of well testing and it is an efficient means of temporarily completing the well while maintaining maximum flexibility. It includes the following components:

1 Slip Joint

The slip joint is an expansion/contraction compensating tool. It accommodates any changes in string length caused by temperature and pressure during the test.

2 Radioactive Marker (RA)

It is placed in the string at a precisely known distance from the top shot and used for depth correlation of DST string during dummy run.

3 Port Reference Tool

It is used for capturing hydrostatic pressure, which can be used as reference pressure for opening of PCT. It is normally run in conjunction with the PCT valve.

4 Tubing Fill Tester Valve (TFTV)

It is a flapper valve, which is used for testing DST string by pressurizing string against it. It is a one way valve, which allows fluid movement in the upward direction only. It is also used in cleaning the string during the flex run.

5 Hydraulic Jar

The hydraulic jar is used if a packer or guns become stuck.The jar can be used to provide an upward shock to help pull the tools loose.

6 Safety Joint

The safety joint allows quick release of the test string if the packer Or anything below the packer becomes stuck. It is located on top of the packer and made up to the same torque as the other tools in the string.

7 Packers

Packers are designed to isolate the perforated interval from the mud column. The packer has three main sections: the drag block and slip assembly, packer elements and the bypass.

Depending on their settingmechanism packers can be categorized as:

- Flexpac packer
- Positest packer
- Positrieve packer

8 Sand Screen

Sand screens are used to prevent sand particles from entering the DST string upto the surface.
There are generally two types:

- Prepacked screen (For Gas Wells)
- Wire Wrapped screen (For oil wells)

9 Perforating Gun

Perforating gun is the bottommost part of the DST string. TCP guns are used for overbalance as well as underbalance perforation but preferred in case of underbalance perforation.

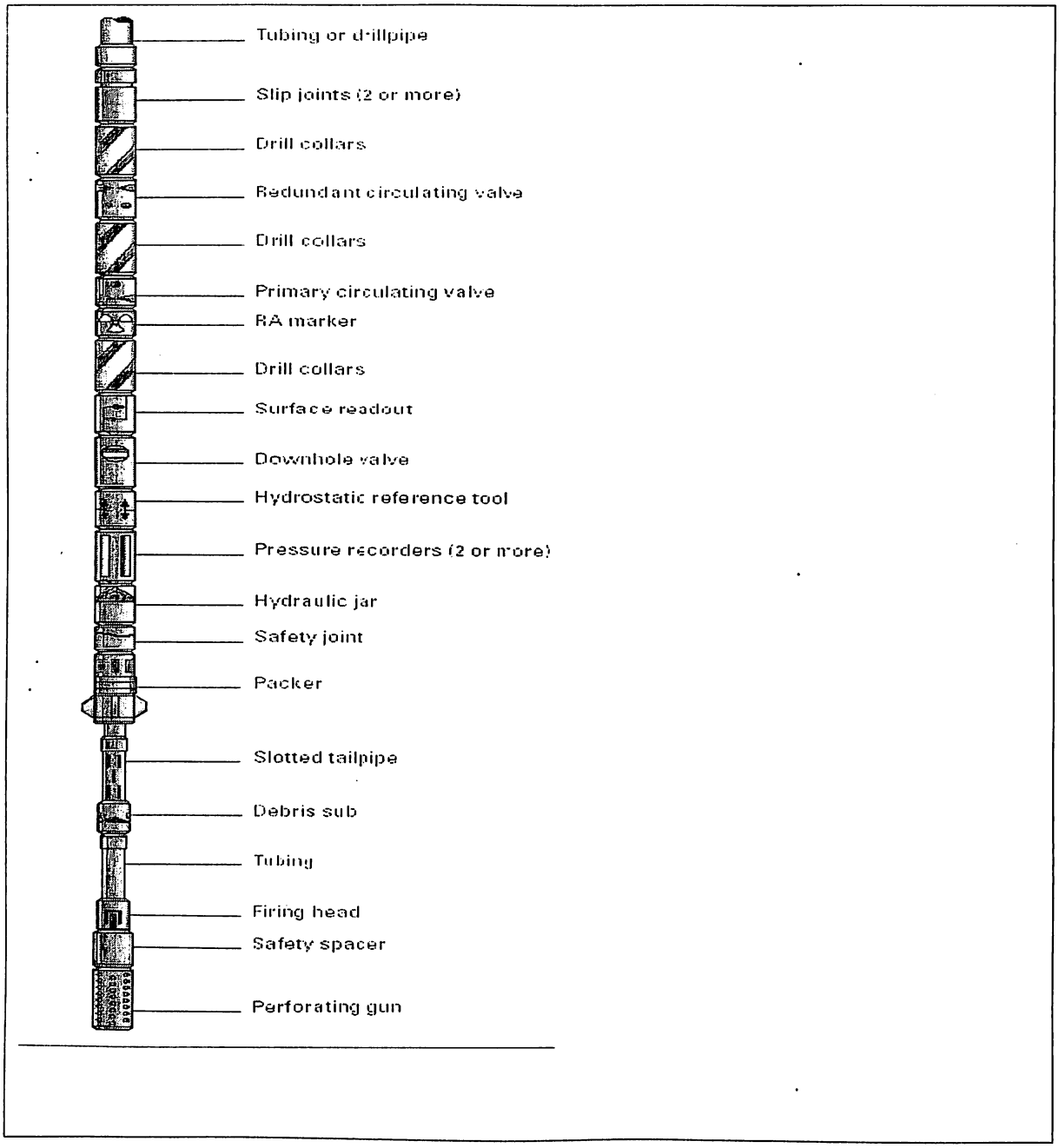

3.7 Down Hole testing Equipments

Chapter 4

Advanced Well Test Interpretation Method

4.1 Well Models

4.1.1 Line Source Solution

Also known as the Theis Curve and the Exponential Integral solution, the Line Source solution describes the observation well response due to one active well in a homogeneous reservoir: Although used in Interference testing, this is the most basic model, homogeneous with no wellbore storage and no skin. The pressure match on the horizontal derivative will give the 'kh' corresponding to radial flow, as usual, but the time match gives the storativity, 'ΦhCt'. This model introduces the standard definitions for dimensionless time and dimensionless pressure, as will be used in most of the single-well models, and has an additional 'dimensionless distance', which relates the separation of the 2 wells to the wellbore radius of the observation well:

4.1.2 Wellbore Storage and Skin

When a well is opened at surface, the first flow at the wellhead is due to the expansion of wellbore fluid alone. This expansion continues after the reservoir fluid starts to contribute to the production, until the sandface flowrate equals the surface flowrate (when expressed at the same conditions). This effect is called wellbore storage, as is the reverse effect, also known as afterflow, observed during a shut-in. Wellbore storage is quantified by the constant C, defined as ΔV/ΔP, and expressed in STB/psi. The immediate vicinity close to the wellbore usually does not have the same characteristics as the surrounding formation, typically being less permeable due to the invasion of mud filtrate during drilling, but possibly due to other causes. This causes an additional pressure drop close to the wellbore, Δps, and is represented by the skin factor, S. The skin factor is a dimensionless variable:

$$r_D = \frac{kh}{141.2\ q\mu B}\Delta p_s$$

A positive skin corresponds to a damaged well, and a negative skin corresponds to a stimulated well.

Dimensionless Variables and Groups

C_D, the dimensionless wellbore storage constant,

is given by:

$$C_D = \frac{0.8937C}{\phi C_t h r_w^2} \Delta t$$

and the dimensionless time is defined as:

$$\frac{t_D}{C_D} = \frac{0.000295\, kh\, \Delta t}{\mu C} \Delta t$$

Any dimensionless solution for a well with wellbore storage and skin in a homogeneous reservoir is completely determined by the value of C_De2S, and for this reason is usually called a C_De2S curve. As seen later, an increase in the C_De2S value has the effect of increasing the separation of the log-log and derivative curves. As the C_De2S function is dominated by the skin value in the exponent, it follows that an increasing skin causes the curves to move apart. A useful rule of thumb is that when radial flow is first seen in the derivative, a separation between the 2 curves of one log cycle is approximately equivalent to a zero skin - less than a log cycle is a negative skin, more is skin damage.

Homogeneous Reservoir, Wellbore Storage and Skin

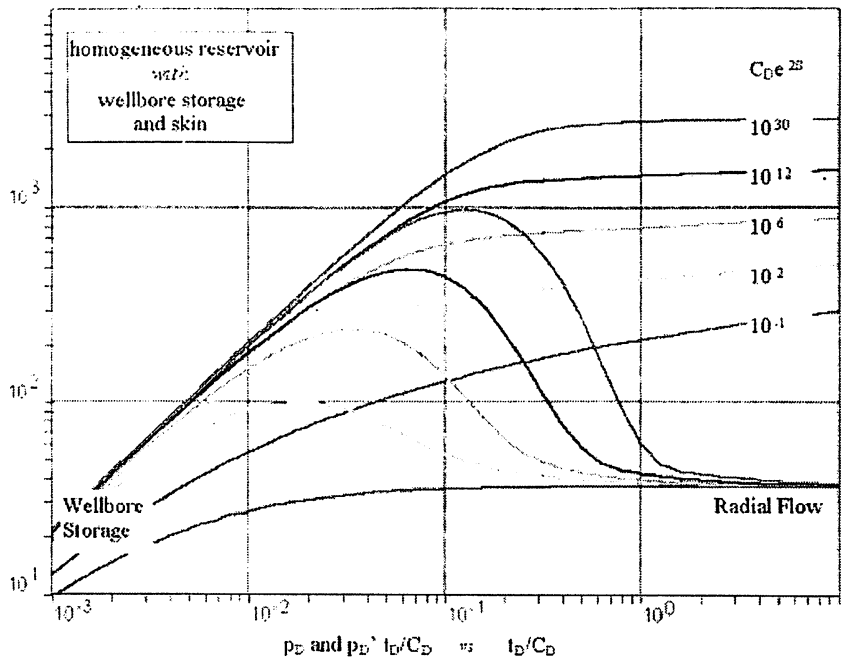

Dimensionless Groups:

$$p_D = \frac{kh}{141.2\ q\mu B}\Delta p$$

$$t_D = \frac{0.0002637\ k}{\varphi\mu C_t r_w^2}\Delta t$$

$$C_D = \frac{0.8936C}{\varphi C_t h r_w^2}$$

S

Type-Curve Analysis:

$$kh = 141.2\ q\mu B\left(\frac{p_D}{\Delta p}\right)_{match}$$

$$C = \frac{0.0002637\ kh}{\mu\left(\frac{t_D/C_D}{\Delta t}\right)_{match}}$$

$$S = 0.5\ \ln\left[\frac{(C_De^{2S})_{match}}{C_D}\right]$$

Fig 4.1 Wellbore Storage and skin

Specialized Analysis

During pure wellbore storage, a straight line will be diagnosed on a Cartesian plot of Δp vs Δt, and C can be obtained from its slope *m*:

$$C = \frac{qB}{24m}$$

The skin is obtained from the specialized analysis applicable to radial flow (semi-log) covered earlier.

4.1.3 Infinite-Conductivity or Uniform Flux Vertical Fracture

To improve the productivity of a well, there are 2 basic choices; acidising or fracturing. There are many factors to consider when selecting a stimulation treatment, but the general rule is 'high permeability, acidise, low permeability, fracture'.

To acidize, you need injectivity, so that the fluid will enter the formation without too much difficulty. To fracture a well, the opposite is true; you need to pump fluid against a high resistance, so that the bottomhole pressure rises above the formation breakdown pressure and the rock cracks. Once the fracture is initiated, the key is to maintain a high bottomhole pressure by pumping rapidly, so that the fracture propagates away from the wellbore. During the treatment a 'proppant' is included in the injection fluid, so that when pumping stops the fracture faces can not close back together. Rock mechanics suggests that the fracture is always a 'bi-wing' symmetrical geometry, although our assumption in well testing that the fracture wings are 2 perfect rectangles is an oversimplification:

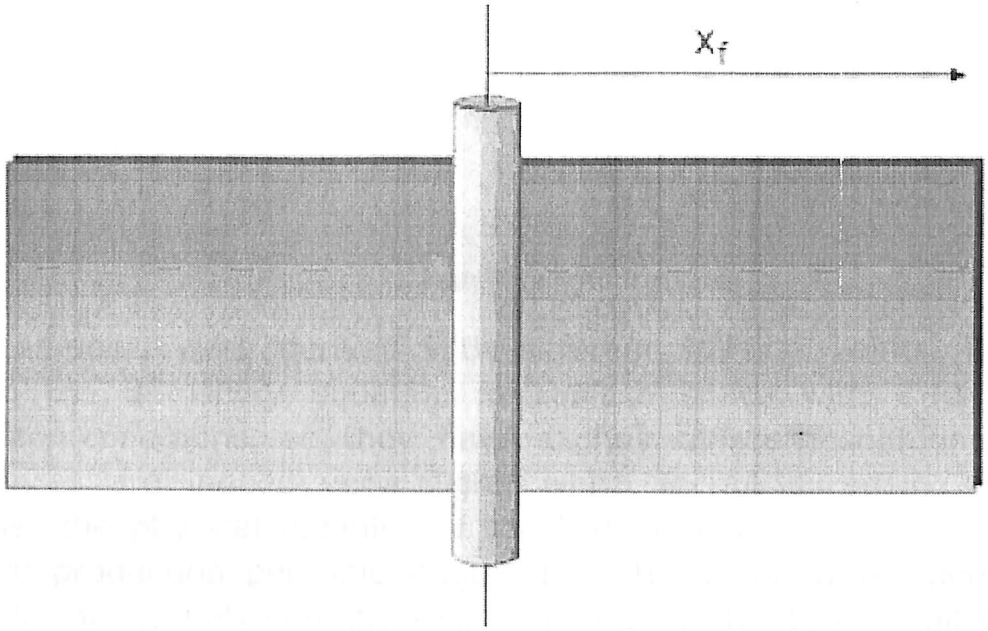

Fig 4.2 Infinite-Conductivity Vertical Fracture

It is also assumed in the analysis of the fracture behavior that it is internally propped to a constant dimension, i.e. that there is no variation in fracture width with height or length. At present there is no way to know if this is true or not, but like all mathematical models, the fracture models are as good as can be handled analytically, and they typically reproduce the pressure response due to the fracture quite accurately.

There are 2 basic fracture models, of which one assumes 'high conductivity', in which the pressure drop along the inside of the fracture is negligible, and the other is 'low conductivity', in which the pressure drop along the fracture is significant.

The high conductivity fracture model can be divided into 2 sub-categories:

- **Infinite-Conductivity Fracture**

  Assumes that there is no pressure drop along the fracture.

- **Uniform Flux Fracture**

  Assumes a uniform production per unit length of fracture.

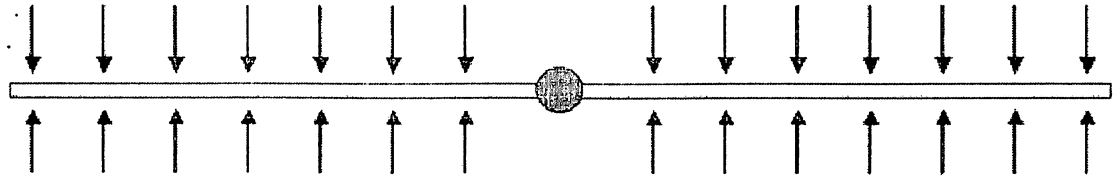

Fig 4.3 Linear Flow into fracture

The 2 models were derived with different starting points, i.e. by solving the diffusivity equation in Laplace space with 2 different boundary conditions, so they have slightly different solutions. The differences are indeed very slight, which is not surprising if you consider the physical meaning of the 2 definitions: In order to have uniform production per unit length of fracture, you would need the same linear Δp between the reservoir and the fracture at all points along its length – which means no pressure drop inside the fracture. The same argument can be used in reverse, and the conclusion is that the 2 models are in fact equivalent. The mathematical model is different to the non-fractured models, as skin drops out of the equation. Any localized formation damage close to the wellbore becomes irrelevant if the flow is linear into a fracture plane hundreds of feet long, so skin simply isn't considered. Similarly, the wellbore radius is now an irrelevance, and in the dimensionless variables all 'rw' terms are replaced by another length term, 'xf', the fracture-half length. More surprisingly, wellbore storage tends to be absent in the solution. This is not because there is no wellbore storage, and in fact there should be additional 'fracture storage' due to the volume of fluid contained in the fracture itself, but the productivity of fractured wells is so high that wellbore storage just isn't seen in most cases. The first flow regime seen in the pressure response is linear flow into

the fracture, which is characterized by 1/2-unit slope lines in both the pressure and derivative curves:

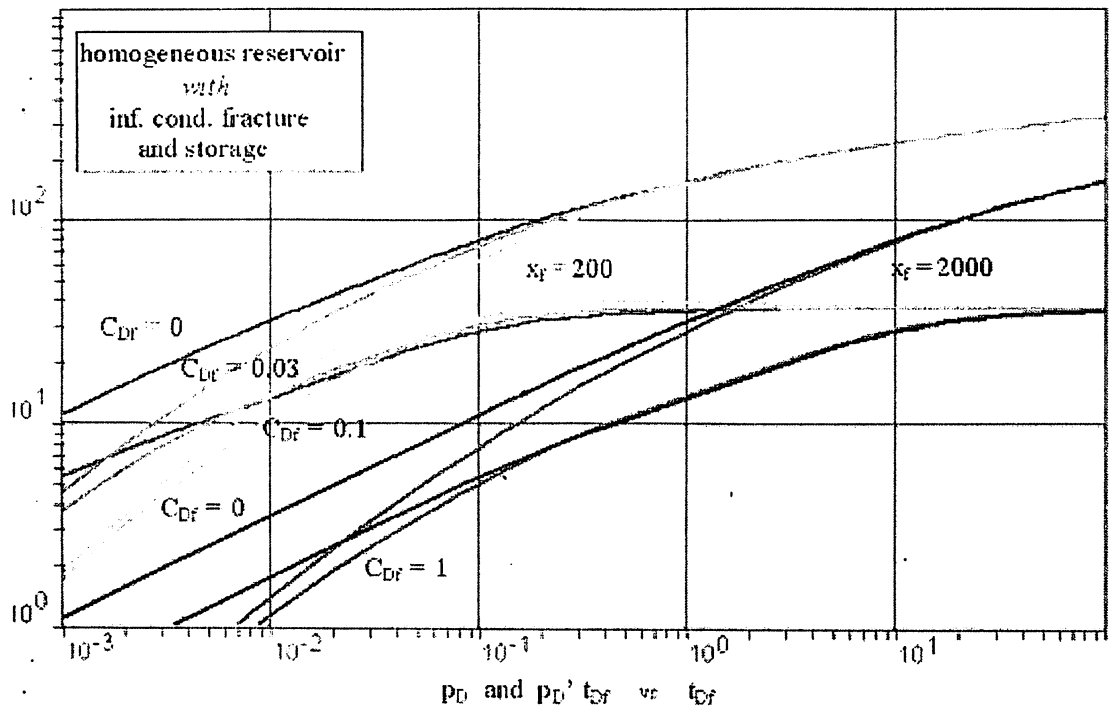

Dimensionless Groups:

$$p_D = \frac{kh}{141.2\ q\mu B}\Delta p$$

$$t_{Df} = \frac{0.0002637\ k}{\varphi\mu C_t x_f^2}\Delta t$$

$$C_{Df} = \frac{0.8936C}{\varphi C_t h x_f^2}$$

Type-Curve Analysis:

$$kh = 141.2\ q\mu B\left(\frac{p_D}{\Delta p}\right)_{match}$$

$$kh = 141.2\ q\mu B\sqrt{\frac{0.0002637\ k}{\varphi\mu C_t\left[\frac{t_{Df}}{\Delta t}\right]_{match}}}$$

$$C = \frac{\varphi C_t h x_f^2 (C_{Df})_{match}}{0.8936}$$

Fig 4.4 Infinite-conductivity fracture model

4.1.4 Finite-Conductivity Fracture

The fracture geometry is the same as for the 'high-conductivity' models, but the assumption is now that there is a significant pressure gradient along the fracture:

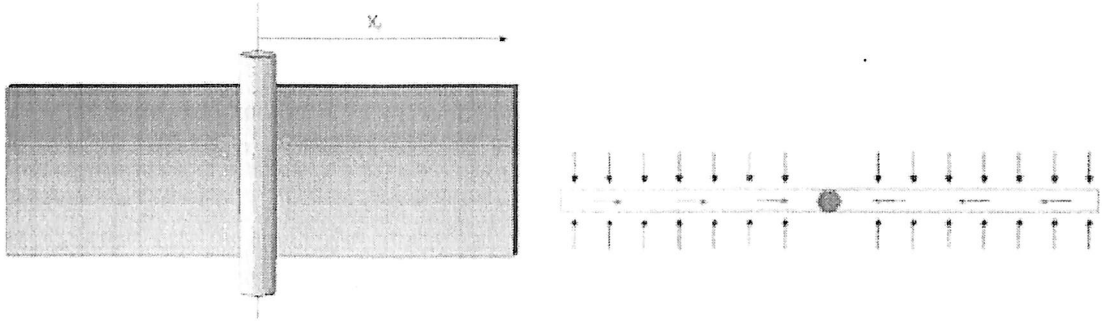

Fig 4.5 Infinite-conductivity fracture

In the absence of storage, the first flow regime is a linear flow along the fracture axis (red arrows), which simultaneously induces a linear flow orthogonal to the fracture (blue arrows), the amplitude of which changes along the fracture length – i.e., there is a non-uniform flux into the fracture, in contrast to the high-conductivity models.

This bi-linear flow regime, with linear flow along 2 axes, gives a pressure response proportional to the fourth root of time. Both the log-log and derivative plots exhibit a quarter slope during bi-linear flow. Bi-linear flow is followed by the usual linear flow, characterized by a 1/2-unit slope on log-log. The bi-linear flow regime is a very early time feature, and is almost never seen. It represents the time at which the pressure drop along the fracture is significant, and in reality this time is very short indeed. Even when there is no storage the data does not exhibit a 1/4-unit slope, and can be matched on a high-conductivity fracture type-curve with an immediate 1/2-unit slope. The general model for a fractured well must surely be the finite-conductivity fracture, as there must always be a pressure drop along the fracture, however small; but it just isn't significant compared to the linear pressure drop in the reservoir, into the fracture.

There is an additional dimensionless term in this model, FCD, the dimensionless fracture conductivity, which takes account of the fracture width (w) and the fracture permeability (kf) and is compared to 'kh':

$$F_{CD} = \frac{k_f w}{kh}$$

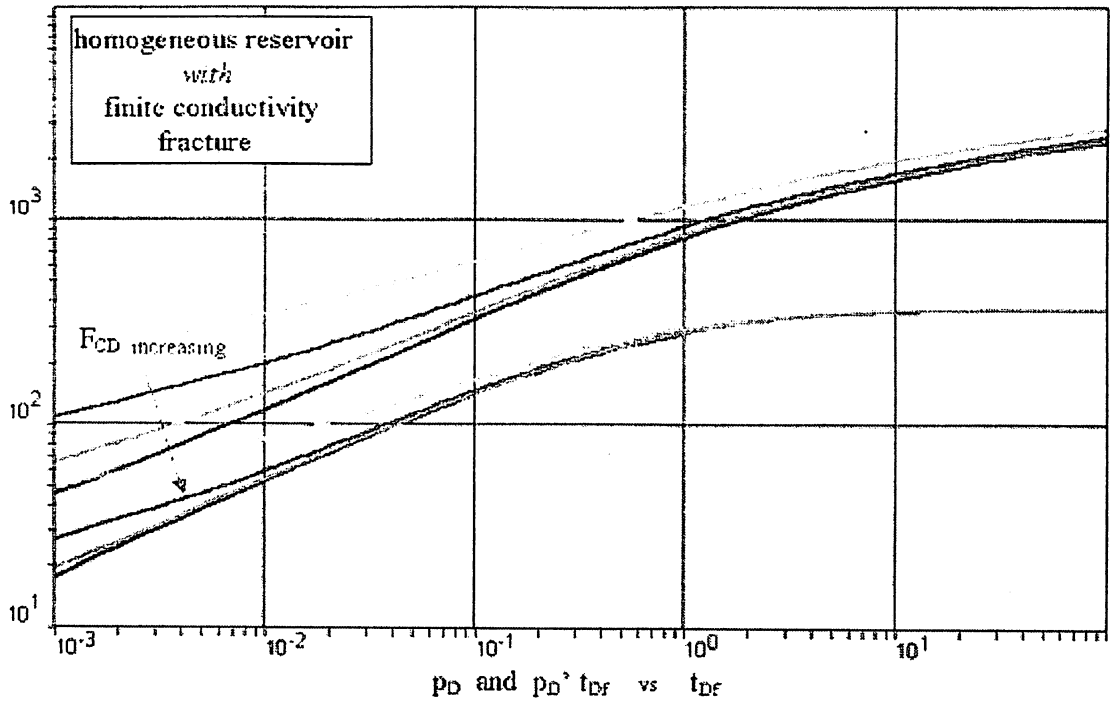

Fig 4.6 Finite Conductivity Fracture Model

Note that for a very high fracture conductivity, FCD, the model approaches an infinite-conductivity response, with a 1/2-unit slope developed instantaneously. Conversely, with a very low FCD the pressure drop along the fracture is significant almost to the onset of radial flow.

Specialized Analysis

The specialized plot for the linear flow regime is the 'fourth-root delta-t' plot, Δp versus $4\sqrt{\Delta t}$.

4.1.5 Limited-Entry Well

This model assumes that the well produces from a perforated interval smaller than the interval thickness:

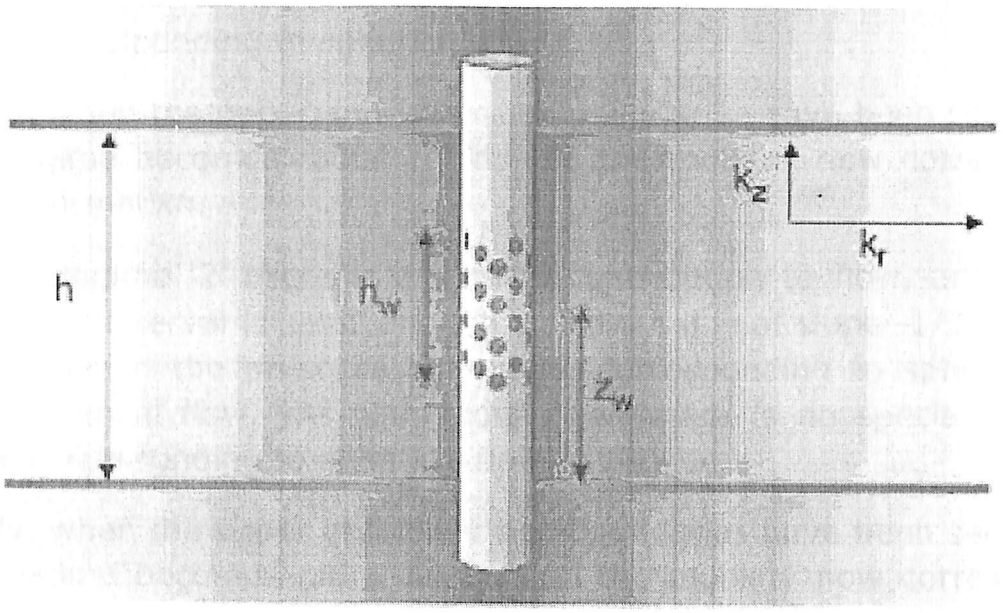

Fig 4.7 Limited Entry Well

In theory, after wellbore storage, the response can be initially radial in the perforated interval thickness *hw*, shown as '1' below. This will give a derivative match equivalent to the small mobility *k hw*, and it can be imagined that if there were no vertical permeability this would be the only flow regime. In practice this flow regime is often masked by storage.

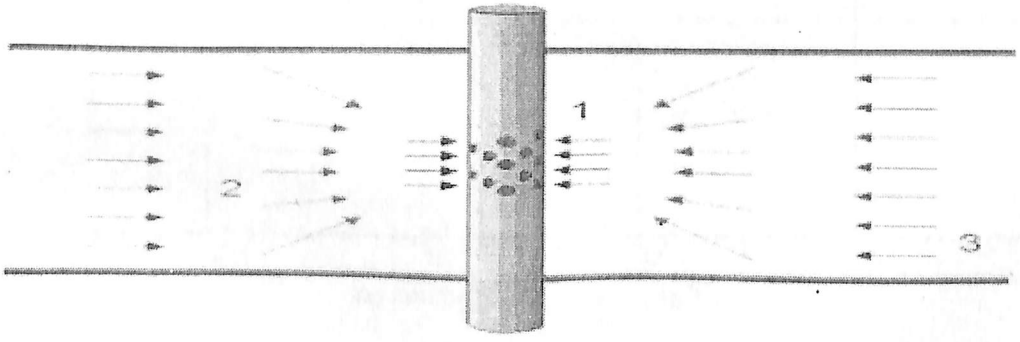

Fig 4.8 Limited Entry Flow Regimes

In flow regime '2' there is a vertical contribution to flow, and if the perforated interval is small enough a straight line of slope -1/2 may be established in the pressure derivative, corresponding to spherical or

hemi-spherical flow. (As with radial flow, there is no special log-log shape corresponding to spherical flow.)

Finally, when the upper and lower bed boundaries have been seen, the flow regime becomes radial again, and the mobility now corresponds to the normal *kh*.

In flow regime '2' there is a vertical contribution to flow, and if the perforated interval is small enough a straight line of slope -1/2 may be established in the pressure derivative, corresponding to spherical or hemi-spherical flow. (As with radial flow, there is no special log-log shape corresponding to spherical flow.)

Finally, when the upper and lower bed boundaries have been seen, the flow regime becomes radial again, and the mobility now corresponds to the normal *kh*.

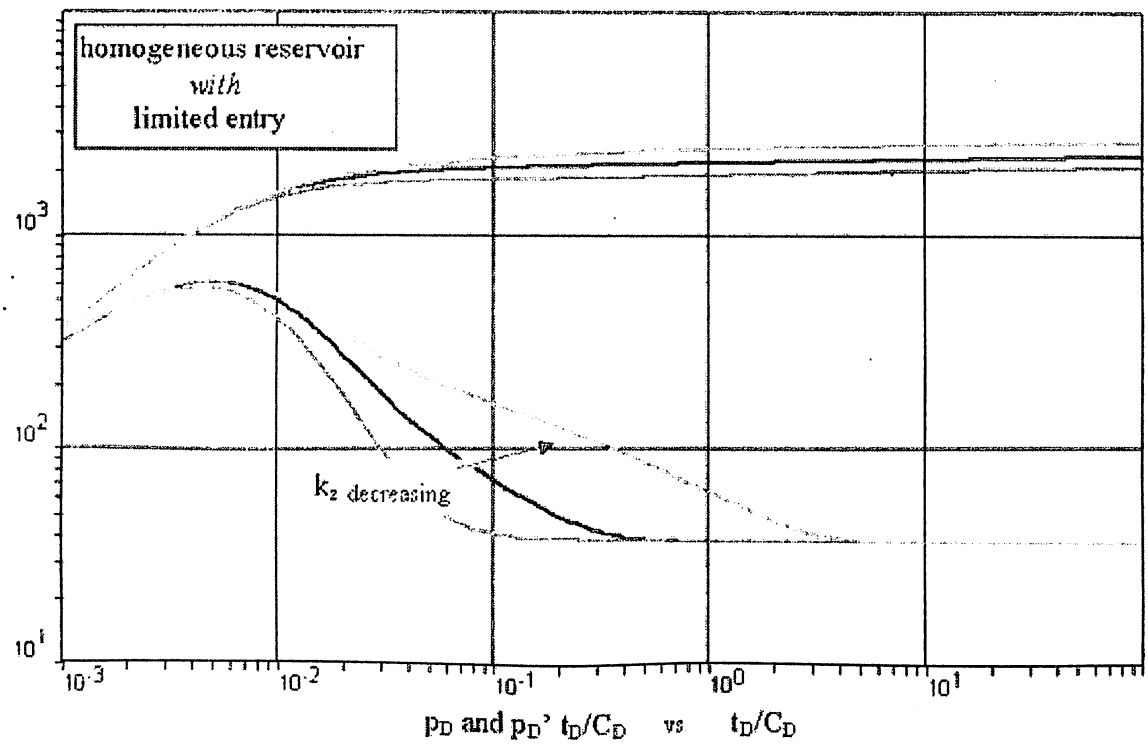

Fig 4.9 Limited Entry Response

With a high enough vertical permeability the spherical flow may not be seen at all, as shown by the green curve, but this also depends on hw /h, the fraction of the producing interval that is perforated, and of course the storage. As kz decreases the -1/2 spherical flow derivative

becomes evident, as the duration of the spherical flow regime increases, and does the overall pressure drop increases, shown by the log-log curve moving up the page. The apparent skin also increases, as shown by the separation of the log-log and derivative curves.

Specialized Analysis

The specialized plot for the spherical or hemi-spherical flow regime is the 'one over-root delta-t' plot, Δp versus $1/\sqrt{\Delta t}$.

4.1.6 Horizontal Well

The well is assumed to be strictly horizontal, and is defined with the same parameters as a limited entry well:

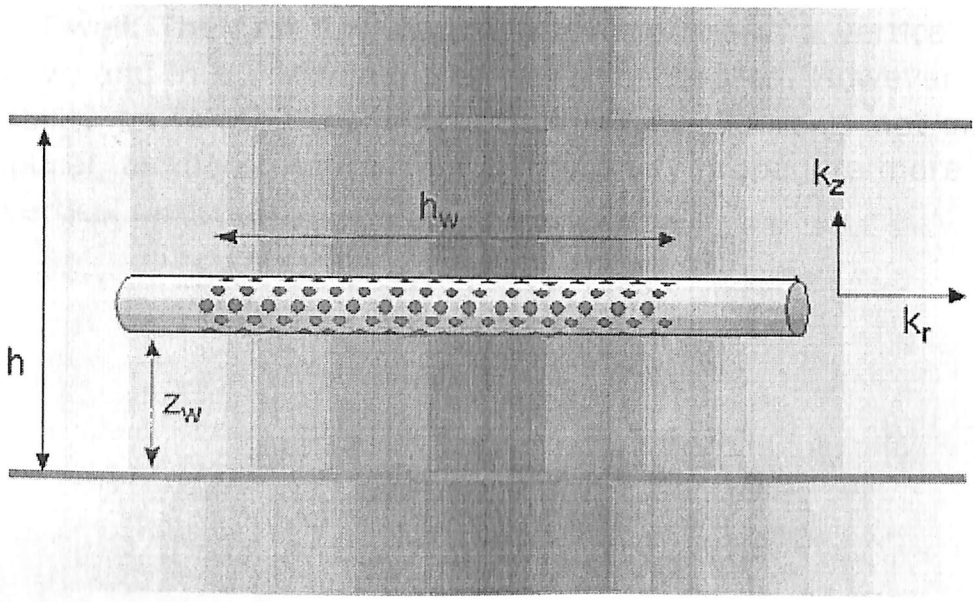

Fig 4.10 Horizontal well

The first flow regime, often obscured by wellbore storage, is pseudo-radial flow in the vertical sense, analogous to radial flow in a vertical well. The average permeability combines a vertical and a radial (horizontal) component, and the 'thickness' corresponds to the producing well length. The horizontal derivative therefore represents a high mobility:

$$(kh)_{early} = h_w \sqrt{k_r k_z}$$

The second flow regime is linear flow, corresponding to horizontal flow between the upper and lower bed boundaries. Both log-log and derivative curves will follow a 1/2 -unit slope. The final flow regime is radial flow equivalent to that in a vertical well, with the derivative representing the usual *kh*, where in this case:

$$(kh)_{late} = k_r h$$

The flow regimes are summarized next:

Horizontal Well Flow Regimes

Looking end-on into a horizontal well is equivalent to looking down on a vertical well. The first flow regime after storage in a vertical well is radial flow, and in a horizontal well the same applies. However due to permeability anisotropy the flow around the wellbore is not circular, but elliptical, as the pressure front will typically propagate more slowly in the vertical direction:

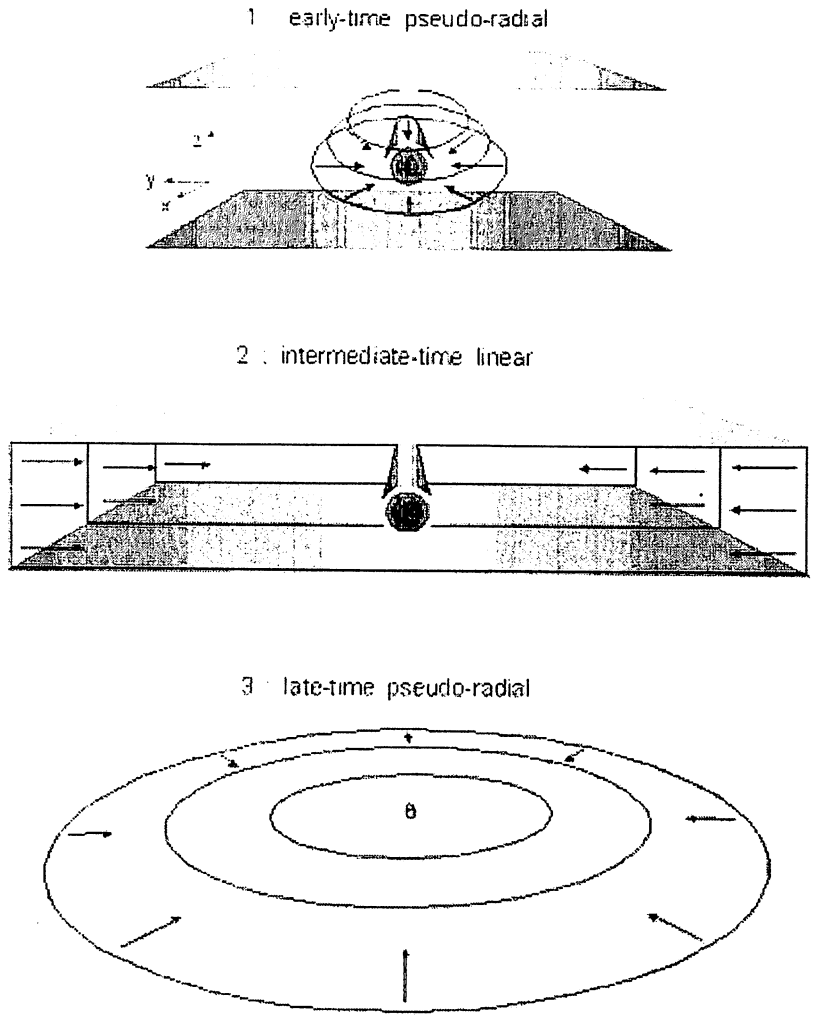

Fig 4.11 Horizontal well flow regimes

Once the pressure front has reached the upper and lower bed boundaries the flow becomes linear, equivalent to the parallel faults geometry in a vertical well, but because of the finite length of the horizontal wellbore it can not stay linear. Eventually the pressure front is sufficiently far from the wellbore that the dimensions of the horizontal section become irrelevant, and the flow again becomes radial, equivalent to normal radial flow in a vertical well.

Horizontal Well Log-Log Responses

In a reservoir with no gas cap or aquifer, the well would typically be positioned as centrally aspossible between the upper and lower bed boundaries, in which case the boundaries would be seensimultaneously and there would be a clean transition from radial to linear flow:

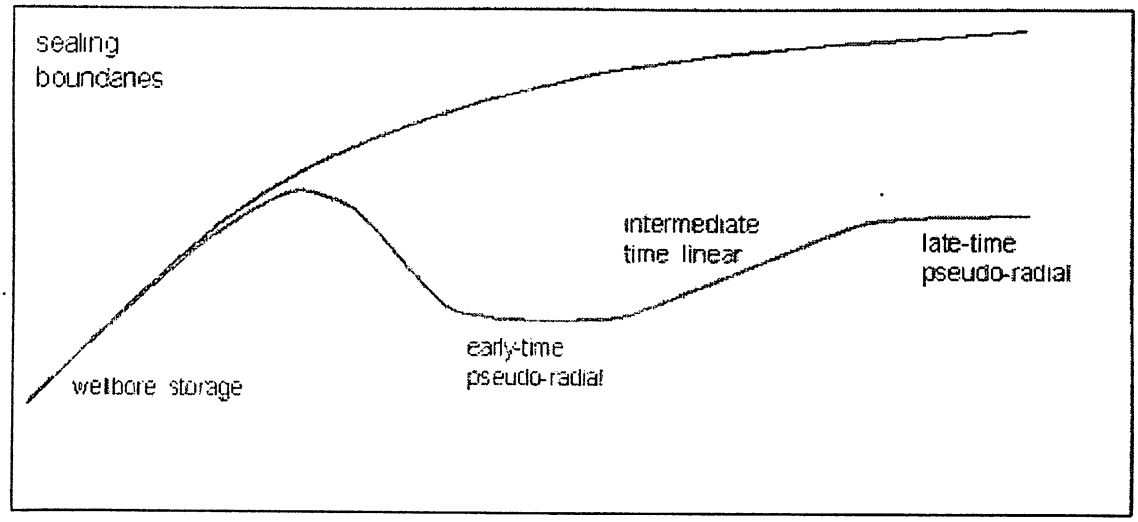

Fig 4.11 Horizontal well log-log responses (1)

However, it can be imagined that if the well is closer to one or other boundary, there will first be a doubling of the derivative, as if seeing a fault in a vertical well, before the second boundary brings on the linear flow.

If the upper or lower boundary is a gas cap or an aquifer, the well will probably be positioned close to the other, sealing boundary. In that case there will again be a doubling of the derivative, similar to the 'fault' response in a vertical well, followed by a constant pressure response:

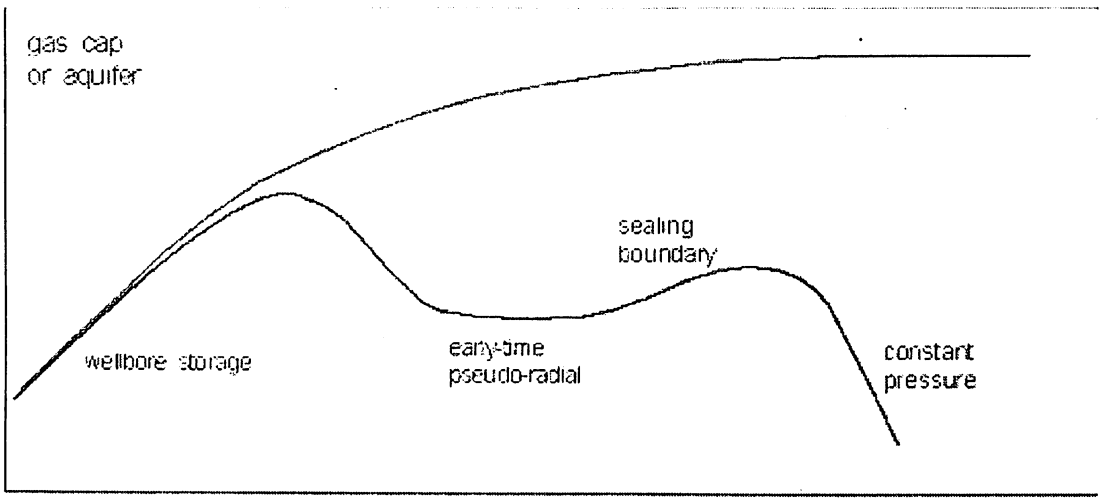

Fig 4.13 Horizontal well log-log responses (2)

In each case the doubling of the derivative will almost certainly not be fully developed before the arrival of the next flow regime, be it linear flow or a constant pressure boundary.

4.1.7 Changing Wellbore Storage

The well is characterized by 2 different wellbore storage constants during a single transient.

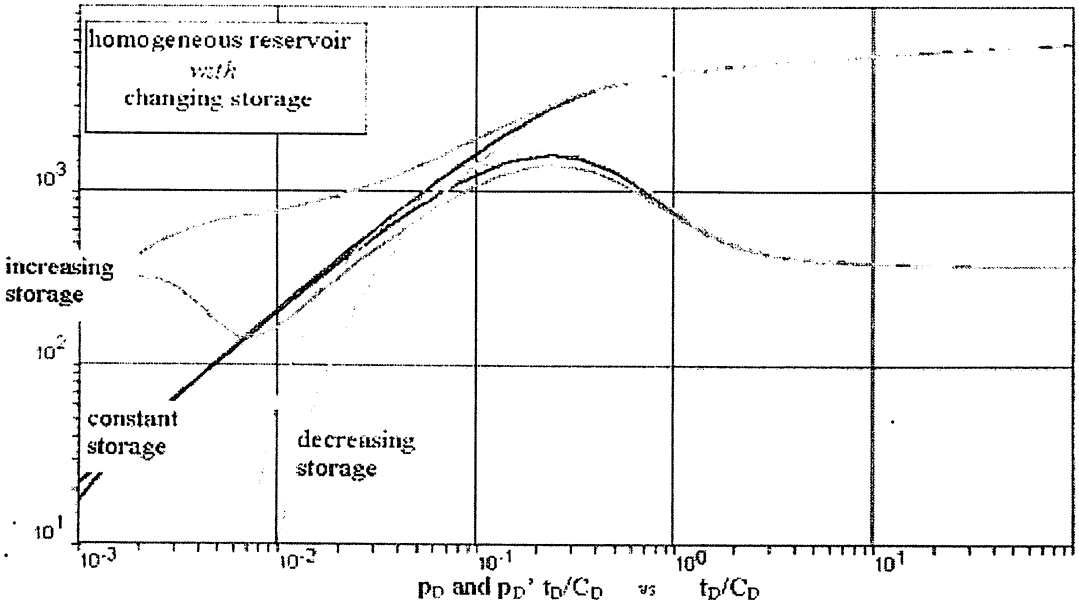

Fig 4.14 Changing Wellbore Storage

Decreasing Wellbore Storage
The most common application of the changing storage model is for decreasing storage during build-ups in gas wells.

As the pressure increases the gas compressibility increases, so C decreases and the log-log and derivative curves move back on the X-axis in early time.

Only wellbore effects, such as this, can make the derivative cross above the log-log curve.

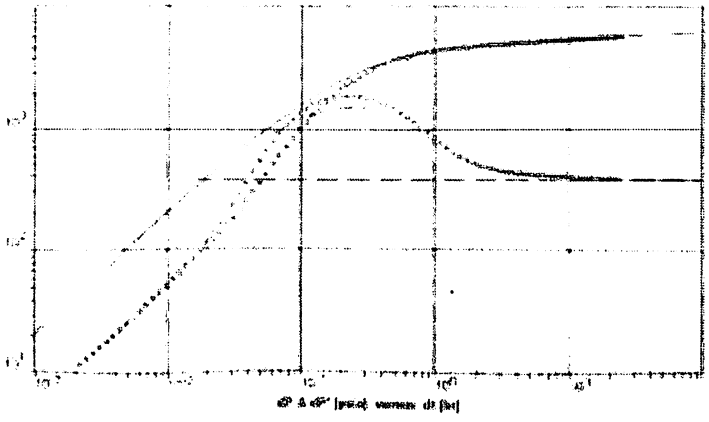

Fig 4.15 Decreasing Wellbore Storage

In the example shown, decreasing storage build-up data are poorly matched by a constant storage type-curve. They could be perfectly matched using the CWBS model.

4.2 Reservoir Models

Dual Porosity Response

The double-porosity (2Φ) models assume that the reservoir is not homogeneous, but made up of rock matrix blocks, with high storativity and low permeability, connecting to the well by natural fissures of low storativity and high permeability. The matrix blocks can not flow to the well directly, so even though most of the hydrocarbon is stored in the matrix blocks it has to enter the fissure system in order to be produced.

The dual-porosity model is described by 2 additional variables compared to the homogeneous model:

ω is the **storativity ratio**, and is essentially the fraction of oil or gas stored in the fissure system; e.g. ω= 0.05 means 5%.

λ is the **interporosity flow coefficient** and characterizes the ability of the matrix blocks to flow into the fissure system; it is dominated by the matrix/fissures permeability contrast, km/kf.

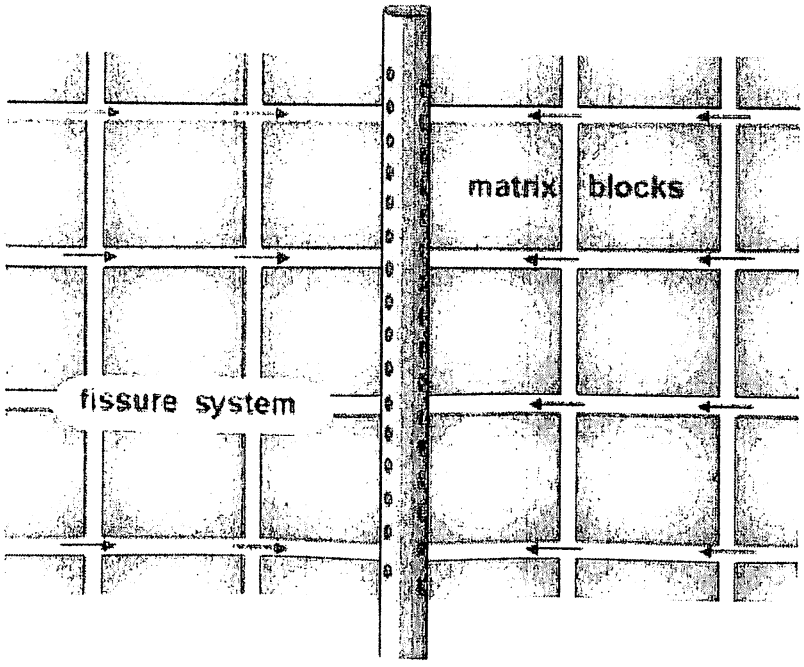

Fig 4.16 Dual Porosity model- fissure system flow

When the well is first put on production, the first flow regime will be fissure system radial flow – i.e. the fissure system is producing, and

there is no change in pressure inside the matrix blocks. This first flow regime is typically over very quickly, and is frequently masked by wellbore storage. If not, it will be manifested by an IARF response on the pressure derivative.

Once the fissure system has started to produce, a pressure differential is established between the matrix blocks, still at initial pressure pi, and the fissure system, which at the wellbore has a pressure pwf . The matrix blocks then start to produce into the fissure system, effectively providing pressure support, and the drawdown briefly slows down, creating a transitional 'dip' in the derivative.

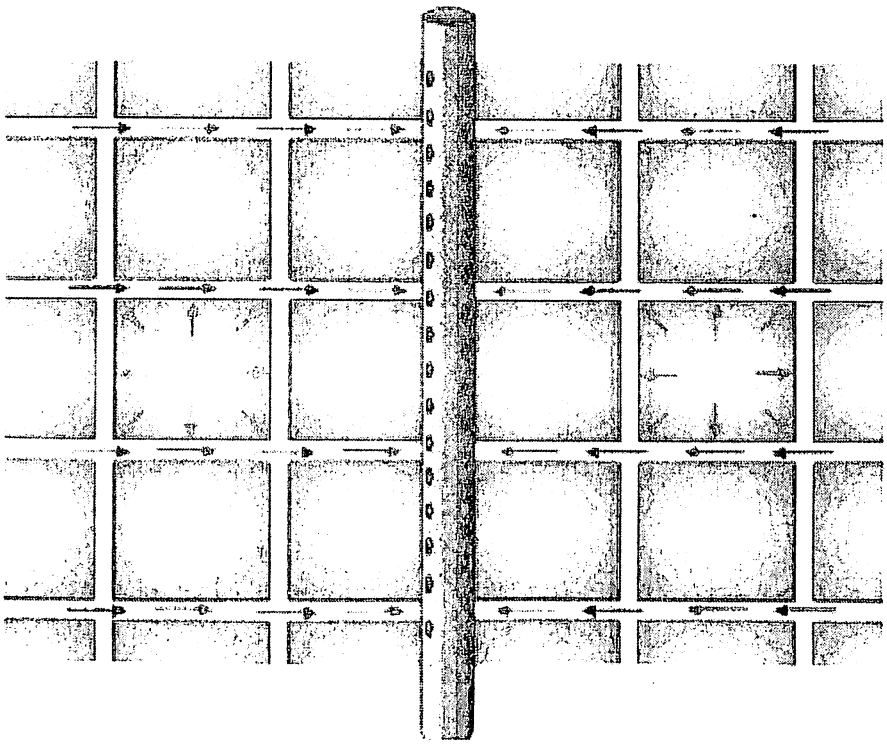

Fig 4.17 Matrix Contribution

'Total system' radial flow is established when any pressure differential between the matrix blocks and the fissure system is no longer significant, and the 'equivalent homogeneous' radial flow response is observed - the second IARF line in the pressure derivative.

(According to the mathematics, this takes place when the pressure inside the matrix blocks is the same as in the fissure system – but this

could never be true at all points in the reservoir, as there would be no production into the fissure system.)

4.2.1 Dual Porosity PSS (pseudo-steady state interporosity flow)

In this case it is assumed that the pressure distribution in the matrix blocks is uniform, i.e. there is no pressure drop inside the matrix blocks. (A physical explanation for this might be that the matrix blocks are small, so that any pressure drop inside them is insignificant compared to the pressure diffusion in the reservoir away from the wellbore.)

All of the pressure drop takes place at the surface of the blocks, as a 'discontinuity', and the resulting pressure response gives a sharp 'dip' during the transition:

The dual-porosity dip in the derivative is defined by 2 parameters:

Storativity ratio:

(fraction of oil in the fissures)

Ω determines the depth of the dip –

$$\omega = \frac{(\varphi V C_t)_f}{(\varphi V C_t)_f + (\varphi V C_t)_m}$$

For small ω values, corresponding to a very high proportion of the hydrocarbon stored in the fissure system, the 'support' during the transition is substantial, and the dip is deeper and longer, as seen on the previous page.

Interporosity flow coefficient:

(ability to flow from matrix to fissures)

[α is a function of the matrix block size.]

$$\lambda = \alpha r_w^2 \frac{k_m}{k_f}$$

λ determines the time of the transition –

λ controls the speed at which the matrix will react, and therefore determines the time of the transition: For a high λ, the matrix permeability is comparatively high, so it will start to give up its oil (or gas) almost as soon as the fissure system starts to produce. Conversely a low λ means a very tight matrix, and more of a drawdown will have to be established in the fissure system before the matrix blocks will appreciably give up their oil, and the transition is seen later.

Although there are theoretically 2 IARF lines on the pressure derivative, corresponding to 2 parallel straight lines on the semi-log plot, the first is almost invariably obscured by wellbore storage.

If seen, the 2 lines would each correspond to kfh, radial flow in the fissure system, as in the first case only the fissure system is producing. In the second case, although the total system is producing, any pressure differential between the matrix blocks and the fissure system is now negligible, and the only pressure drop in the system is in the fissures, as fluids flow to the wellbore. Imagine a droplet of oil in a matrix block 50 meters from the wellbore; it lazily travels a few centimeters to enter the fissure system, expelled by a negligible Δp, then travels 50 meters through the fissure network, accelerating as it approaches the wellbore as the pressure gradient increases (and flow area decreases). It is this pressure gradient, in the fissure system, that creates the measured wellbore response.

4.2.2 Dual Porosity (transient interporosity flow)

This model assumes that there is a pressure gradient, and therefore diffusivity, within the matrix blocks. If the pressure profile inside the blocks is important, then the shape of the blocks has to be taken into consideration, and for this reason there are 2 solution models available, each corresponding to different matrix block geometries. The 2 responses are very similar:

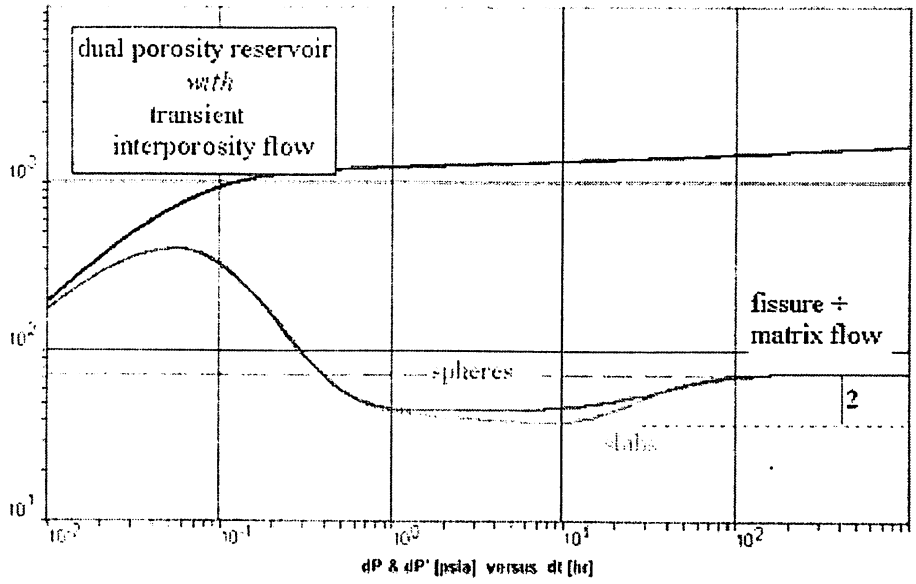

Fig 4.18 Dual porosity Transient Interporosity Flow

The 'slab' geometry model assumes rectangular matrix blocks, which is what we have been considering so far with the dual-porosity models. The 'spheres' model, realistically or not, represents another simple geometry with which to define the boundary conditions for the mathematical solution. It is difficult to visualize a reservoir consisting of spherical matrix blocks, but perhaps due to fluid movements over geological times the fissure network can get 'vuggy', the edges of the matrix blocks can become rounded – for whatever reason, dual-porosity data sets sometimes match the 'spheres' model better than any other. (As before, our mathematical models will not be an accurate representation of what nature has provided in the reservoir, but the performance from these models is very close to the measured pressures from these wells.)

As shown in the plots, the fissure system radial flow is very short-lived, and in practice is not seen. During the transition, the semi-log slope/derivative value is half of the total system radial flow value. As seen overleaf, ω in this model has a more subtle effect on the shape of the derivative, and λ defines the time at which the response transitions to total system IARF:

4.2.3 Double Permeability

When is a layered reservoir not a layered reservoir? When each layer has the same properties, in which case the behavior of the system will be the equivalent behavior of the summed interval. In the double-permeability (2K) model the reservoir consists of 2 layers of different permeabilities, each of which may be perforated. Crossflow between the layers is proportional to the pressure difference between them.

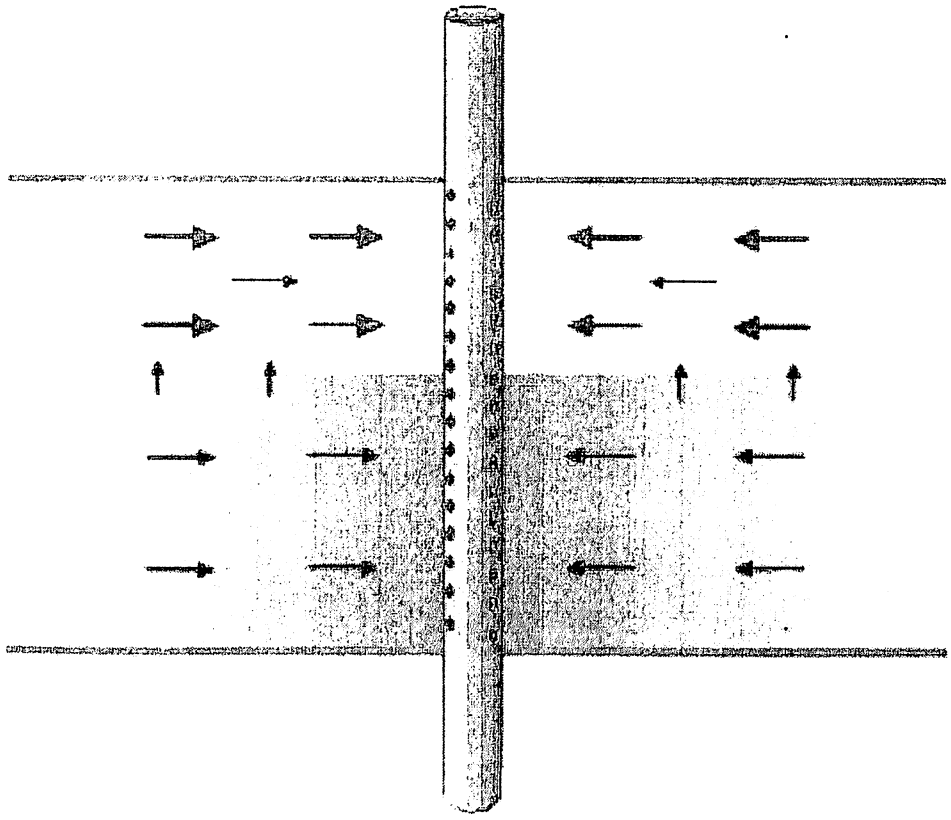

Fig 4.19 Double permeability model

In addition to the storativity ratio ω and the interporosity flow coefficient λ, another coefficient is introduced: κ is the ratio of the permeability-thickness product of the first layer to the total for both layers:

$$\kappa = \frac{k_1 h_1}{k_1 h_1 + k_2 h_2}$$

Usually the high permeability layer is considered as layer 1, so κ will be close to 1.

At early time there is no pressure difference between the layers and the system behaves as 2 homogeneous layers without crossflow, in infinite-acting radial flow, with the total *kh* of the 2 layers. As the most permeable layer produces more rapidly than the less permeable layer, a Δp develops between the layers and crossflow begins to occur. Eventually the system behaves again as a homogeneous reservoir, with the total *kh* and storativity of the 2 layers.

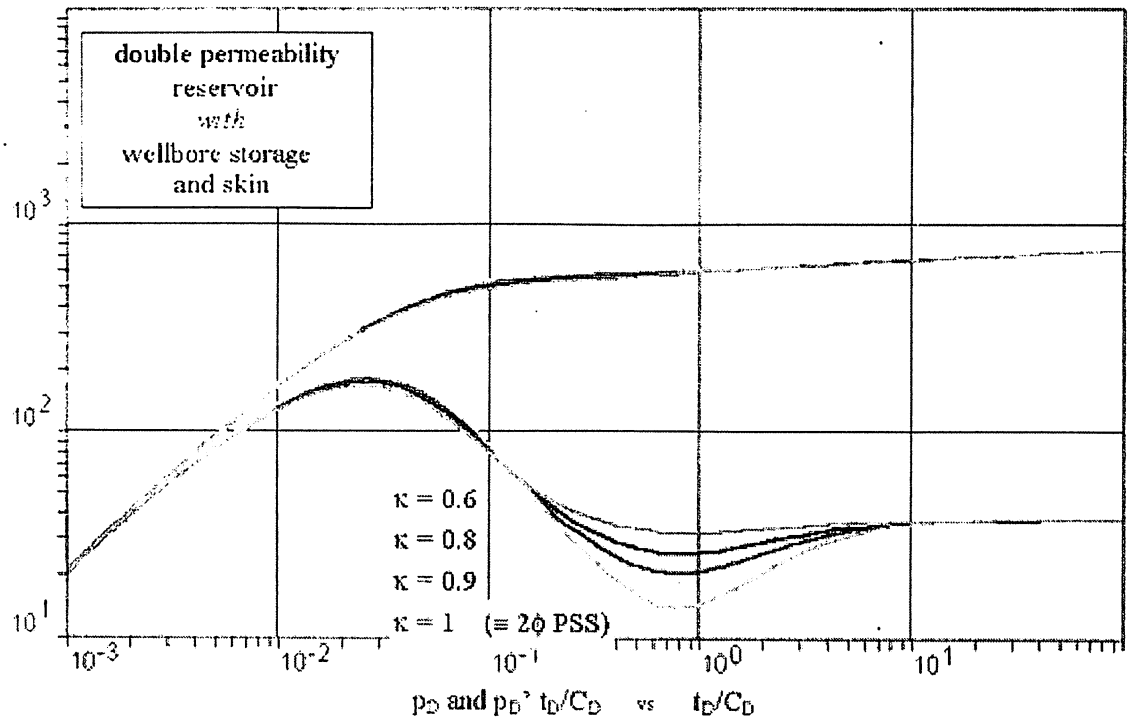

Dimensionless Groups:

$$p_D = \frac{k_1 h_1 + k_2 h_2}{141.2\, q\, \mu B}\,\Delta p$$

$$t_D = \frac{0.0002637\, k\,(k_1 h_1 + k_2 h_2)}{[(\varphi C_t h)_1 + (\varphi C_t h)_2]\,\mu r_w^2}\,\Delta t$$

$$C_D = \frac{0.8936\, C}{[(\varphi C_t h)_1 + (\varphi C_t h)_2]\, r_w^2}$$

S

Type-Curve Analysis:

$$(kh)_t = 141.2\, q\, \mu B \left(\frac{p_D}{\Delta p}\right)_{match}$$

$$C = \frac{0.000295(k_1 h_1 + k_2 h_2)}{\mu \left(\frac{t_D / C_D}{\Delta t}\right)_{match}}$$

$$S = 0.5 \ln\left[\frac{(C_D e^{2S})_{match}}{C_D}\right]$$

Fig 4.20 Double permeability model flow type curve

The transitional dip is governed by ω and λ, which have the same effect as in the 2Ø models, and κ, which reduces the depth of the dip compared to κ=1, which gives the dual-porosity pseudo-steady state solution.

That is because if κ=1 then $k_{2h2}=0$, and the oil or gas in the low permeability layer, equivalent to the matrix blocks, can only be produced by entering the high-permeability layer, equivalent to the fissure system. Not surprisingly it behaves like the dual-porosity model.

4.2.4 Radial Composite

With composite models, the reservoir is divided into 2 regions of different mobilities and/or storativities:

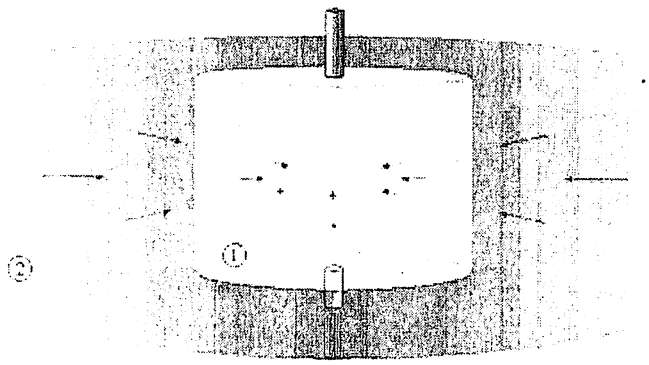

Fig 4.21 Radial composite model

In the case of the radial composite model, there is a circular inner zone, with the well located at the center, and an infinite outer zone.

$$M = \frac{[k/\mu]_1}{[k/\mu]_2}$$

$$D = \frac{[k/\phi\mu C_t]_1}{[k/\phi\mu C_t]_2}$$

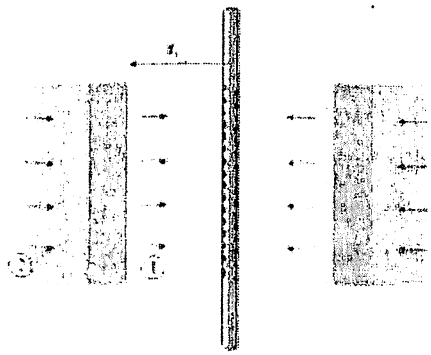

Fig 4.22 Mobility and diffusivity ratios

Each zone has the characteristics of a homogeneous reservoir. The parameters defining the change in properties from one zone to the other are the mobility and diffusivity ratios, M and D above. There is no pressure loss at the interface, which is at a distance ri from the wellbore.

In the pressure response, the early time corresponds to the inner zone, and the late time behavior depends upon the properties of the outer zone:

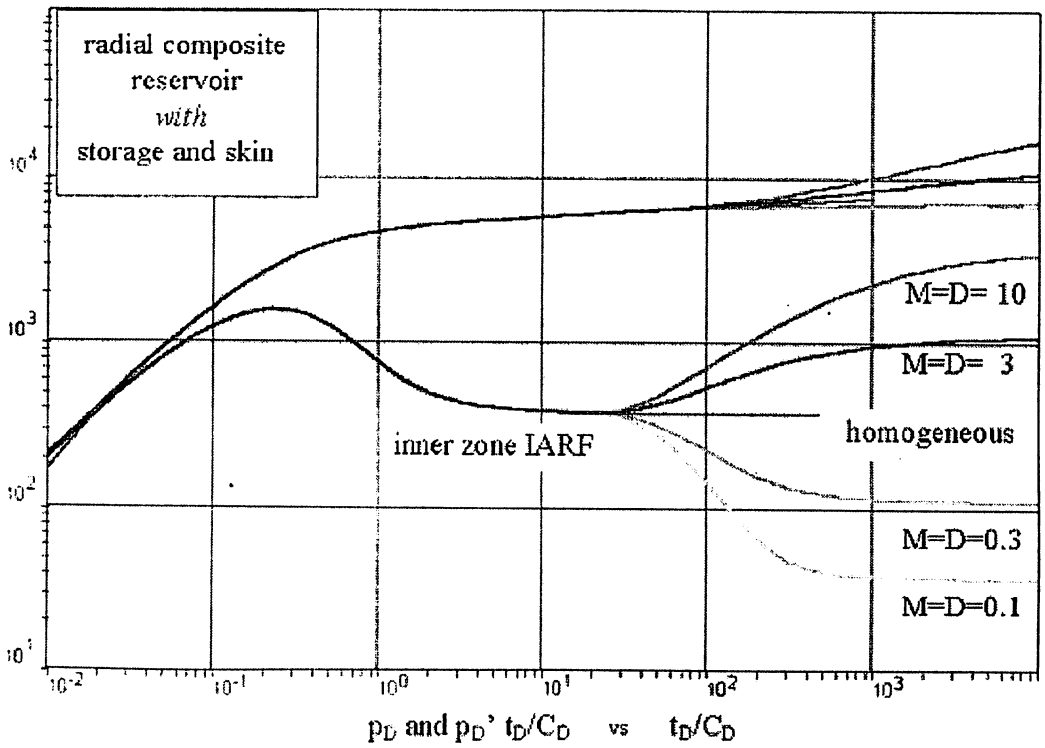

Fig 4.23 Radial composite model pressure response

This model has a practical use in injection wells, where the injection fluid has a different viscosity to the reservoir fluid.

With any model, the direction of movement of the derivative can be remembered as 'down = good', as a downward movement means a slowing down of the drawdown due to some kind of improvement to the flow mechanism, whether a support boundary, an increase in kh, or in this case an increase in mobility. (With one exception, the build-

up derivative always moves in the same direction as the drawdown derivative.)

For example, with water injecting into oil, the mobility of the oil will typically be greater than the water mobility, and the derivative will move down at the interface. Interestingly, water injected into an aquifer will do the same thing, as the cool injection water is more viscous than the reservoir water.

As will be seen in the next section, this model can be considered as the general circular boundary model, and if the second mobility is zero it corresponds to a closed circular boundary, and if it is infinite it corresponds to a constant pressure circular boundary.

4.2.5 Linear Composite

The producing well is in a homogeneous reservoir, infinite in all directions but one, where the reservoir and/or fluid characteristics change across a linear front. Again there is no pressure loss at the interface. On the other side of the interface the reservoir is again homogeneous and infinite, with different properties:

After wellbore storage effects, the derivative will correspond to homogeneous radial flow in the first zone.

After the transition, the second homogeneous response is semi-radial flow in the 2 parts of the reservoir.

Mobility and Diffusivity ratios, M and D, are as for the radial composite model:

$$M = \frac{[k/\mu]_1}{[k/\mu]_2}$$

$$D = \frac{[k/\phi\mu C_t]_1}{[k/\phi\mu C_t]_2}$$

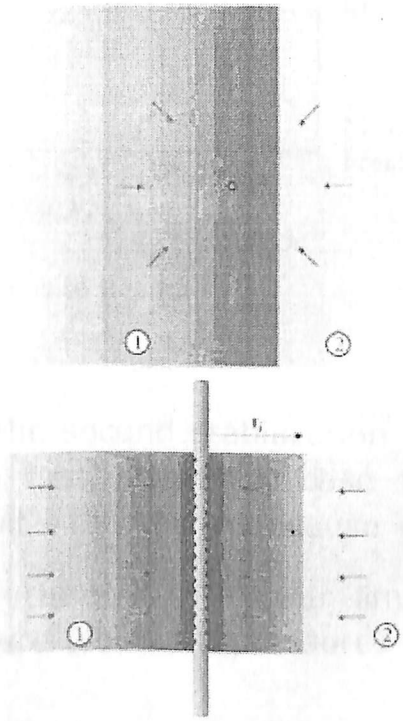

Fig 4.24 Linear Composite

Assuming a constant bed thickness, *h*, the first derivative stabilization will correspond to k1/μ1.

The second will be the average mobility of the 2 zones: ((kl/mu1) + (k2/mu2)) /2.

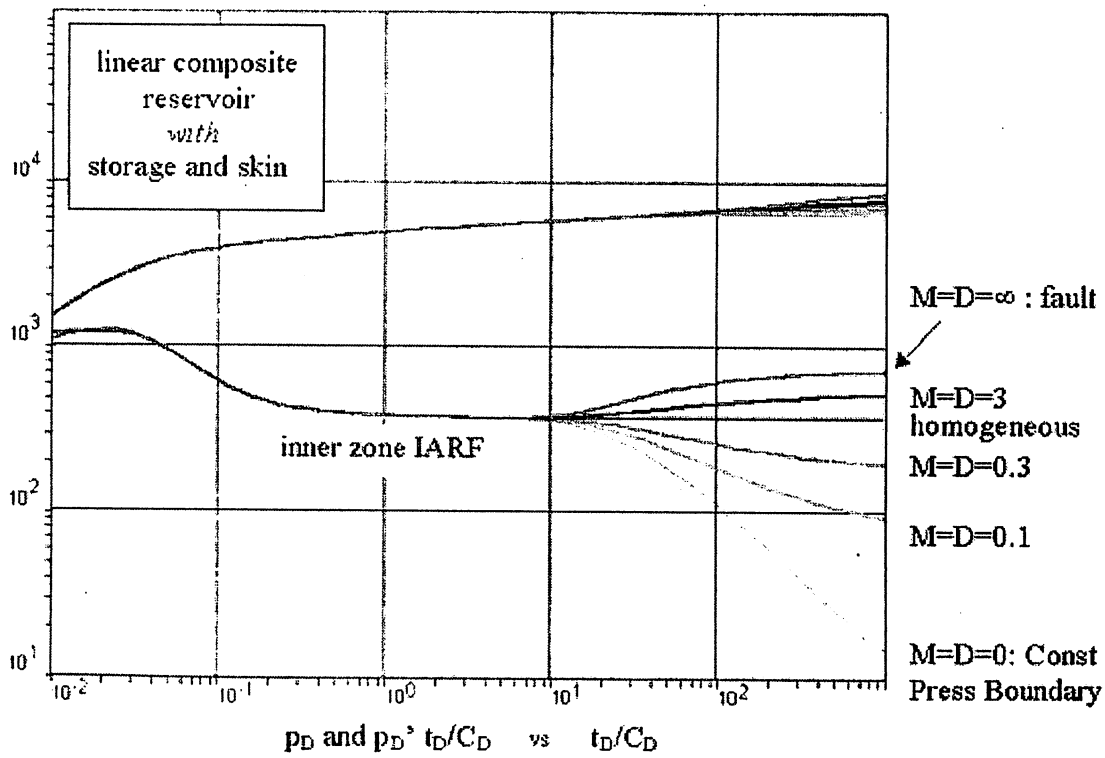

Fig 4.25 Linear Composite Response

In the case of decreasing mobility, the second stabilization can never be more than double that of the first, in which case the linear discontinuity represents a sealing fault – i.e. M =∞,because k2mu2=0.

In the case of increasing mobility, there is no lower limit for the second stabilization which tends to zero (constant pressure) when M = 0, meaning that k2 mu 2 = ∞.

4.3 Boundary Models

1 Pressure front has not reached the fault:

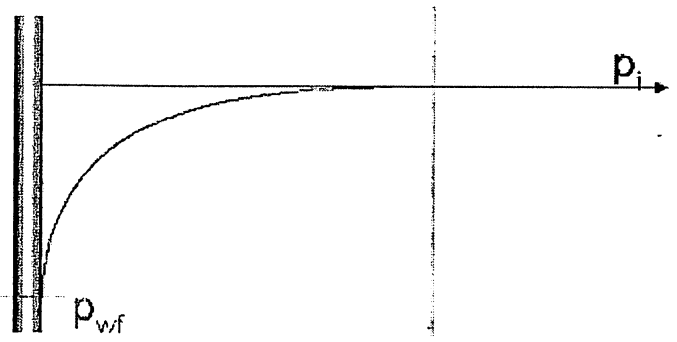

2 Reflection has not yet reached the wellbore:

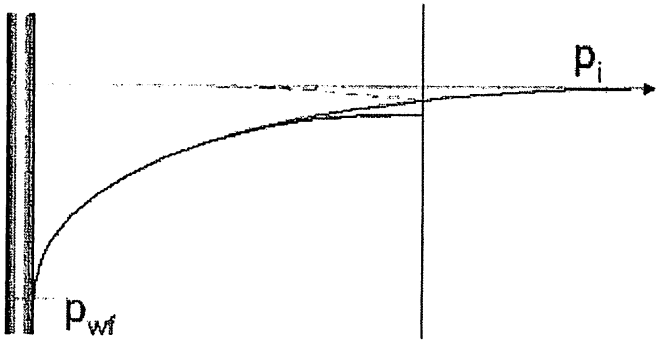

3 Boundary is seen at the wellbore:

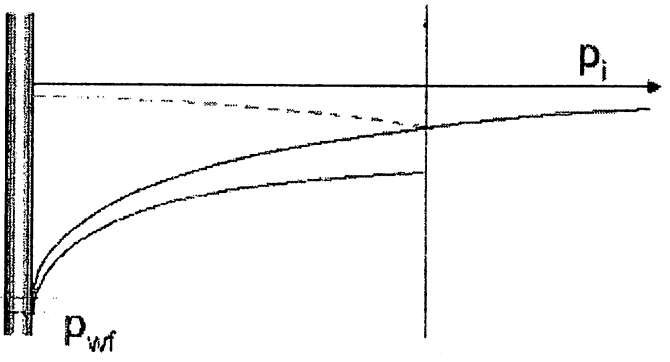

Fig 4.26 Boundary Modeling

The wellbore pressure corresponds to the superposition of the infinite response and its own 'reflection' from the fault. The reflection is equivalent to the infinite-acting response of an 'image' well, at an equal distance on the other side of the fault.

Single boundaries are modeled with a single image well, multiple boundaries with an escalating number of image wells.

4.3.1 Linear Boundaries

Sealing Fault

As discussed in section 4, the solution is constructed by superposing 2 infinite responses. In reality, the nature of the reservoir beyond the fault is irrelevant, but in the model the reservoir is replaced by an infinite virtual reservoir, which extends beyond the fault. The virtual image well has the same production history as the active well, so that the Δp each side of the boundary is symmetrical, and nothing will flow across it:

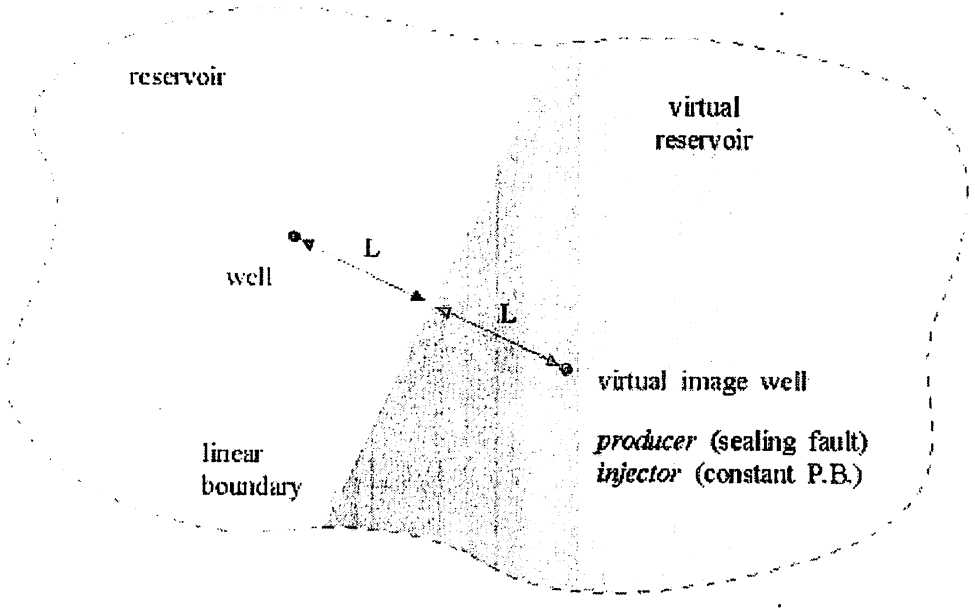

Fig 4.27 Linear Boundaries

Constant Pressure Boundary

The configuration is exactly as above, except the production history at the image well is the inverse of the active well; i.e., if the active well is a producer the image well is an injector, and vice versa. Any point on the boundary is equidistant from the 2 wells, so the Δp from one is balanced by the - Δp from the other, and the pressure along the boundary is constant. Note that for the image well approach to be rigorous, the image well(s) should have the same wellbore storage, skin, etc. as the active well. However, the image wells are typically represented by straightforward line sources, which is technically incorrect. Fortunately, the pressure regime around any well, outside

the skin-damaged zone, will be almost identical to that around a line source well, with no storage and no skin, as the inner boundary conditions affect only the pressure internal to the wellbore. The deliverability of the reservoir is not changed by the presence of a well, and the only distortion will be the effect on the early-time flowrate in the reservoir, which will not change instantaneously.

Pressure Response

When the semi-log approximation holds for both active and image wells, the overall derivative, which is the sum of the individual derivatives, becomes:

Sealing fault : twice that of infinite system
Constant pressure boundary : tending to 0

In the sealing fault case, the late-time response is identical to the response of an infinite system with a permeability of half the actual reservoir permeability.

In the constant pressure response, the derivative is tending to zero, as the pressure stabilizes.

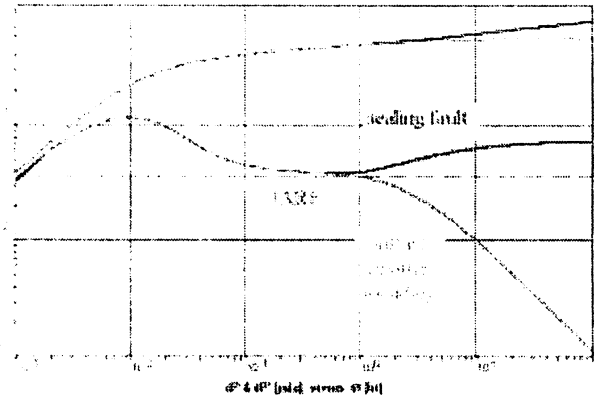

Fig 4.28 Linear Boundary Response

The semi-log response for the sealing fault is a second straight line with double the slope of the IARF line, as seen in the doubling of the derivative.

The constant pressure response is seen to be stabilizing to a value sometimes called the 'average reservoir pressure'

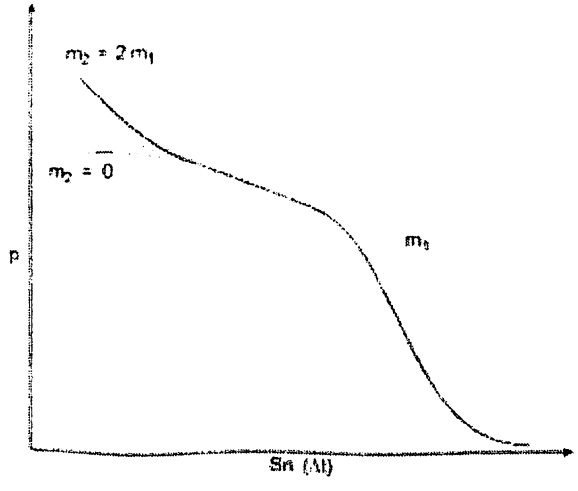

Fig 4.29 Semi-log Response for linear boundary

4.3.2 Circular Boundaries

Closed Circle

The well is at the center of a reservoir limited by a sealing circular boundary, radius re. Unlike linear faults, this model has a radial symmetry and can be solved without the need for image wells:

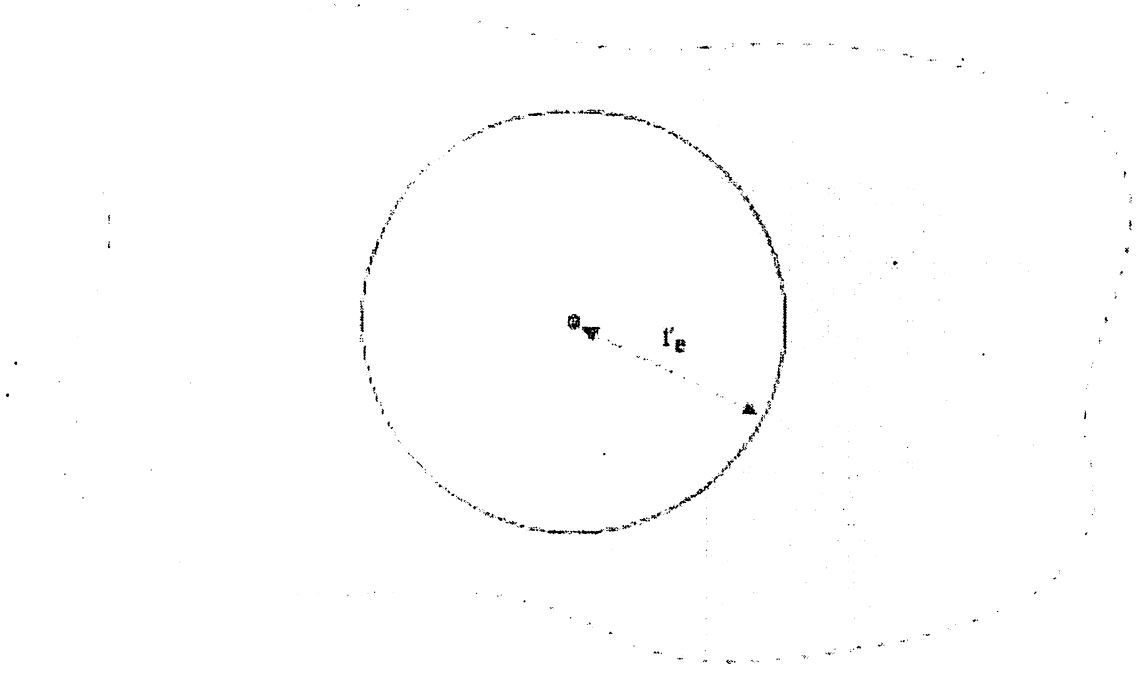

Fig 4.30 Circular Boundaries

When the boundary is seen during a drawdown, the pressure response will transition from radial flow to pseudo-steady state flow, corresponding to depletion and approximated in dimensionless terms by:

$$p_D = 2\pi t_{DA} + a$$

where *a* is a constant, and tDA is the dimensionless time, in which rw 2 is replaced by the reservoir area 'A'. During pseudo-steady state flow, Δp is proportional Δt, for a constant flowrate, so there will be a straight line on a linear plot and a unit slope straight line on the log-log plot. The derivative, 2ΠtDA, is also proportional to Δt, and also follows a unit-slope straight line, as seen overleaf.

The build-up response is actually the difference between 2 drawdown responses, at the same point in space but shifted in time. When the pseudo-steady state approximation holds for both responses the pressure becomes constant, equal to the average reservoir pressure, and the derivative tends to zero. This is precisely the response of a reservoir with a constant pressure boundary:

The drawdown response in a closed circle (or any closed reservoir) is unmistakable, a unit-slope straight line in late time, on both the log-log and the derivative.

The build-up response is the same as for a constant pressure circular boundary, as seen below. (It is too steep to be a linear constant pressure.)

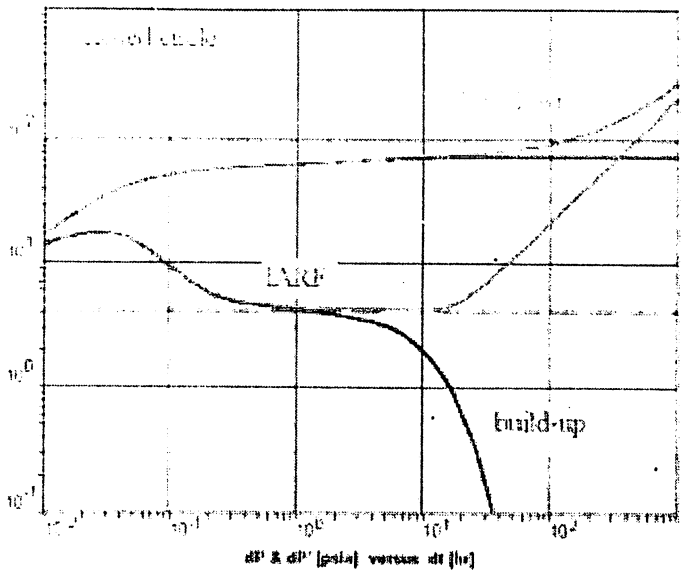

Fig 4.31 Closed Circular Boundary

Constant Pressure Circle:

The geometry is the same as for the closed circle, but the pressure at the boundary radius (re) is constant. The model again has radial symmetry, and is solved with no image wells.

The qualitative behavior is the same as for a constant pressure linear boundary, namely a pressure stabilization indicated by a plunging derivative, but for a circular boundary the trend is sharper. Drawdowns and build-ups look the same:

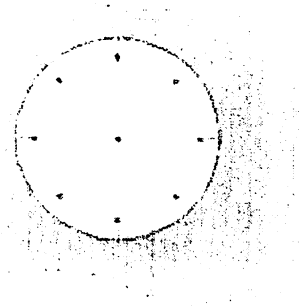

Fig 4.32 Constant pressure circle

4.3.3 Intersecting Faults

If the first fault is far enough away, infinite-acting radial flow is established after wellbore storage. Until a fault is seen, it will have no effect on the pressure curve. Similarly, the first fault will always cause the derivative to double, as until it is seen the second fault will have no effect. The final stabilization level is determined by the angle between the faults, θ:

If the well is centered (1), there will be a single jump to the final stabilization, at a value $\frac{360}{\theta}$ times the initial radial flow stabilization. If the well is much closer to one fault (2), the single fault doubling of the derivative may be seen before a second jump.

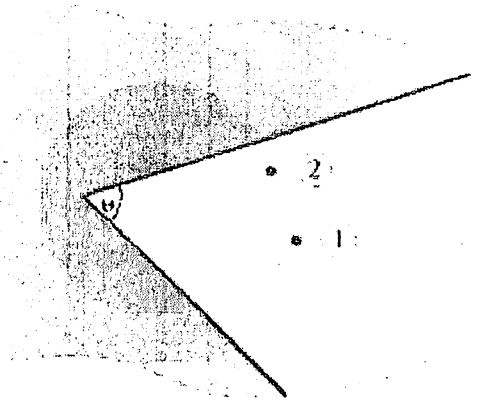

When at least one of the 'faults' is a constant pressure, the pressure will stabilize and the derivative will tend to zero. The constant pressure boundary will dominate the pressure response, so that nothing more distant will be observed

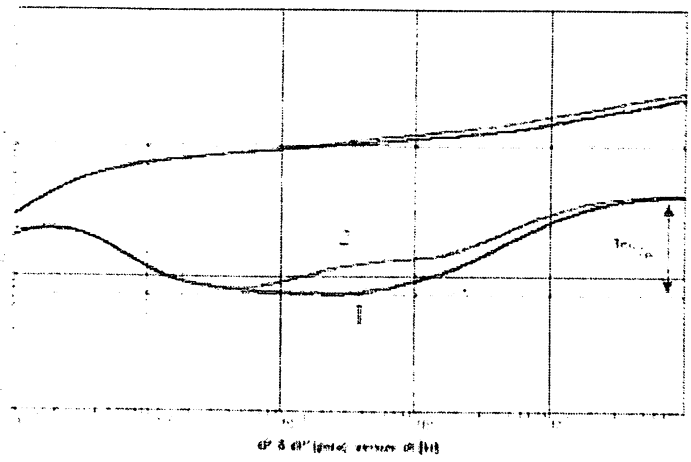

Fig 4.33 Intersecting Faults

The total jump in the derivative, between infinite-acting radial flow and the final stabilization, is equal to 360/θ. The flow structure in the 'wedge' is a fraction of radial flow, so the flow capacity of the system has reduced by that fraction. Just as a single fault reduces the 'infinite' reservoir by a factor of 2, and the derivative doubles, faults at 60°would reduce it by a factor of 6, for example, so the total increase in the derivative from the IARF value would be 6. Interestingly, the same rule applies for parallel faults.

4.3.4 Parallel Faults (Channel)

The well is either between parallel faults or in a channel:

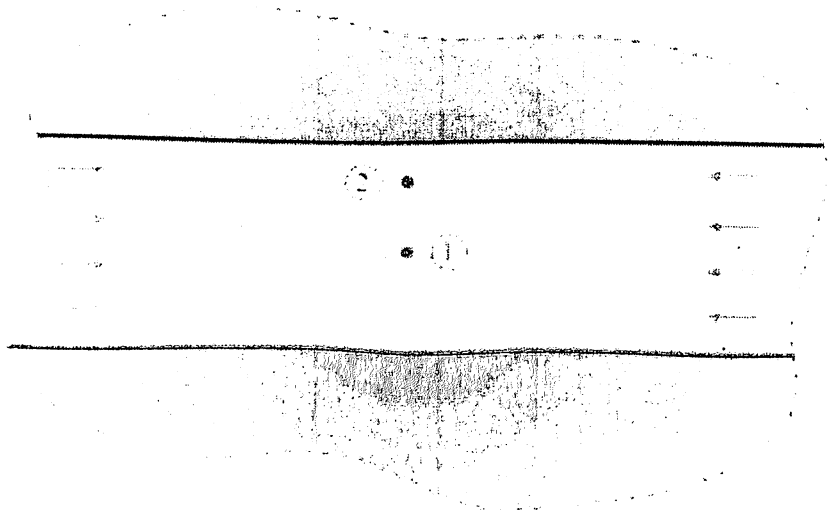

Fig 4.33 Parallel faults

The late time behavior will be linear flow, resulting in a 1/2-unit slope on both the log-log and derivative plots, as for a fracture in early time. Before that there may be infinite-acting radial flow, and there may be a doubling of the derivative due to the first fault being a lot closer than the second:

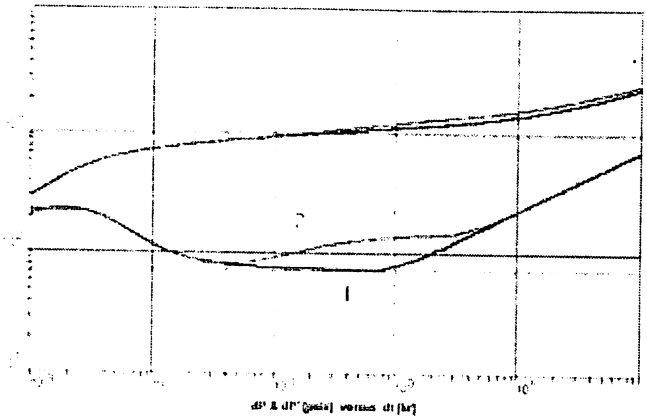

Fig 4.34 Parallel faults response

Note that the 360/θrule still applies to the total jump in the derivative; in this case, when θis 0^0, it is infinite, and the derivative increases continually at a 1/2-unit slope.

4.3.5 Mixed Boundary Rectangle

The mixed boundary or composite rectangle has each of the 4 sides either sealing, constant pressure or infinite:

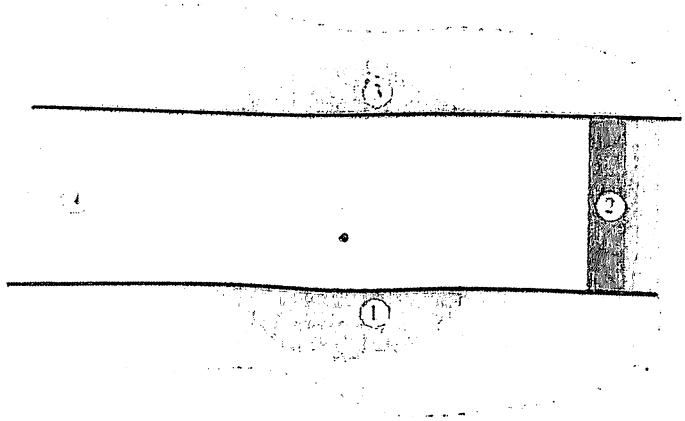

Fig 4.35 Mixed Boundary Rectangle

In this case sides 1 and 3 are sealing faults, 2 is constant pressure and 4 is infinite. The derivative response clearly depends upon the nature of the boundaries and their configuration, but in this case it would be as shown below:

4.4 Gas Well Testing

4.4.1 Pseudopressure and Pseudotime

In solving the diffusivity equation certain assumptions are made about the fluid properties, some of which are not applicable to gas – in particular, that the reservoir fluid is slightly compressible and that both viscosity and compressibility are independent of pressure:

Above bubble point, most oil properties are fairly constant. Compressibility decreases slightly with pressure, but it is assumed to be constant over the range of test pressures. Viscosity will increase slightly with pressure.

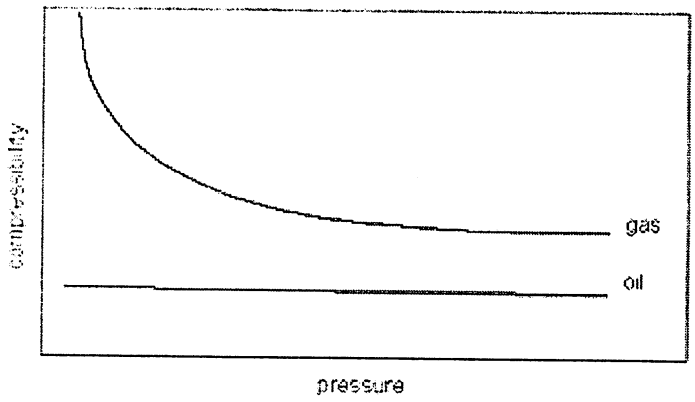

For gas, compressibility is inversely proportional to pressure - it is initially very easy to compress, and becomes increasingly difficult. Gas viscosity increases with pressure, as the molecules are forced closer together and collide more frequently.

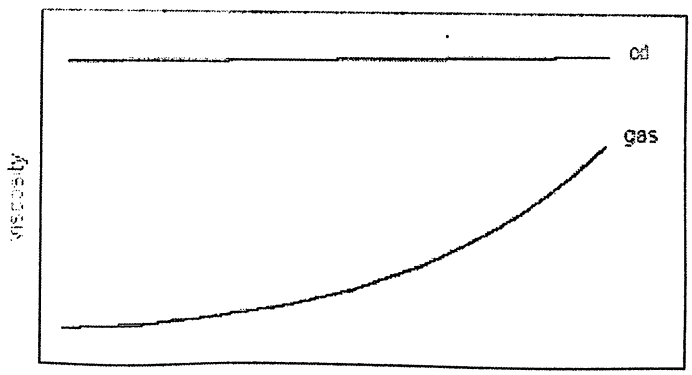

Fig 4.36 Gas well Testing

The simplest equation of state that can be used for a gas is the Ideal Gas Law: $PV = nRT$

The behavior of real gases is not quite that simple, and a compressibility term is required, the 'deviation factor', Z:

$PV = nZRT$

Assuming this equation of state, it is possible to express the diffusivity equation in the same form as for a slightly compressible fluid, by introducing the pseudo-pressure (or Real Gas Potential, defined by Al-Hussainy in 1966):

$$m(p) = \int_{P_0}^{p} \frac{2p}{\mu(p)\, z(p)}$$

where p_0 is a reference pressure that must be below the lowest measured pressure during the transient under investigation. It is generally taken as 0.

The diffusivity equation is expressed as:

$$\Delta m(p) = \frac{\phi \mu C_t}{k} \frac{\partial m(p)}{\partial t}$$

For gas well test analysis, the pressure terms are replaced by m(p). Analysis based on pseudopressure is valid in all cases, and today we have no reason not to use it, but historically it was of interest to make approximations, based upon the variation of μz with pressure:

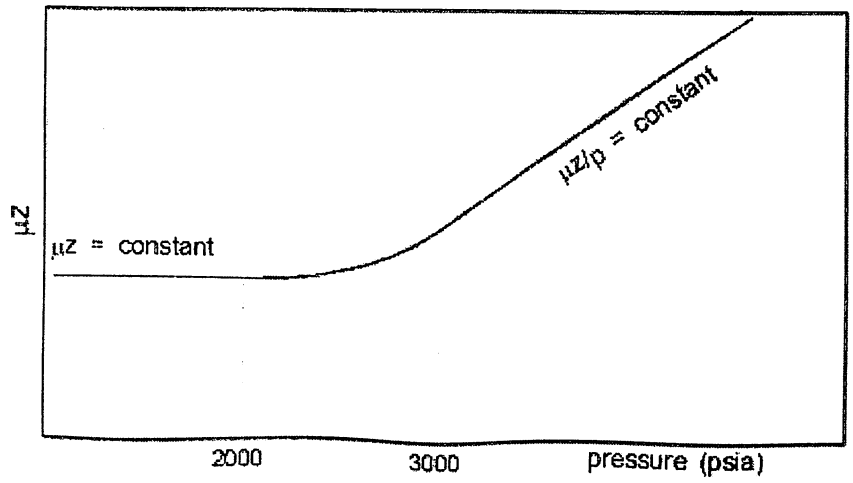

Fig 4.37 Pseudo-Pressure

At low pressures, the gas tends to behave as an ideal gas, and μz is constant. Considering the integral solution, this means that m(p) is proportional to p2. At high pressures μz is proportional to p, so m(p) is proportional to p.

So before the advent of computers, the rules of thumb were:

- pmax < 2000 psi: use p2
- pmin > 3000 psi: use p

In between these values no approximation was available, and m(p) had to be used.

In the diffusivity equation on the previous page, the factor μCt is a function of pressure, but for practical purposes it can often be assumed to be constant during the test. However where pressure variations are large, such as in a tight formation and/or a very damaged well, this assumption is no longer valid, as will be seen in the next section.

Assuming that μCt is constant, the dimensionless pseudo-pressure becomes:

$$m_D = \frac{1.987 \times 10^{-5}\, kh\, T_{sc} \left[m(p_i) - m(p) \right]}{p_{sc}\, T\, q_{sc}}$$

where TSC is the temperature at standard conditions, expressed in ^{0}Rankine (520), pSC is the pressure at standard conditions, in psia (14.7), T is the reservoir temperature in ^{0}R and qSC is the gas flowrate at standard conditions, in MSCF/day. The difference between this expression and the oil equations is that the downhole gas flowrate is computed from the surface rate by way of an equation of state, rather than a formation volume factor. (B is replaced by T, p and z terms).

The equations for evaluating gas reservoir parameters depend upon which pressure function is used:

$$kh = 711 \Delta qT \left(\frac{\overline{\mu . z}}{p}\right) \left(\frac{p_D}{\Delta p}\right)_{match}$$

$$kh = 1442\ \Delta qT \left(\frac{\overline{\mu . z}}{p}\right) \left(\frac{p_D}{\Delta p^2}\right)_{match}$$

$$kh = 1442\ \Delta qT \left(\frac{p_D}{\Delta m(p)}\right)_{match}$$

Normalized Pseudopressure

The pressure function can be normalized, and given dimensions of pressure:

$$p_{pn} = p_i + \frac{\mu_i z_i}{p_i} \int_{P_i}^{p} \frac{p}{\mu(p)\, z(p)} dp$$

The normalized pseudopressure, normalized with reference to gas properties at static conditions, pi, enables the equations for oil solutions to be used.

Pseudotime

In a tight reservoir, with large drawdowns, the assumption that μCt is constant leads to a distortion in the early time of the log-log and derivative data:

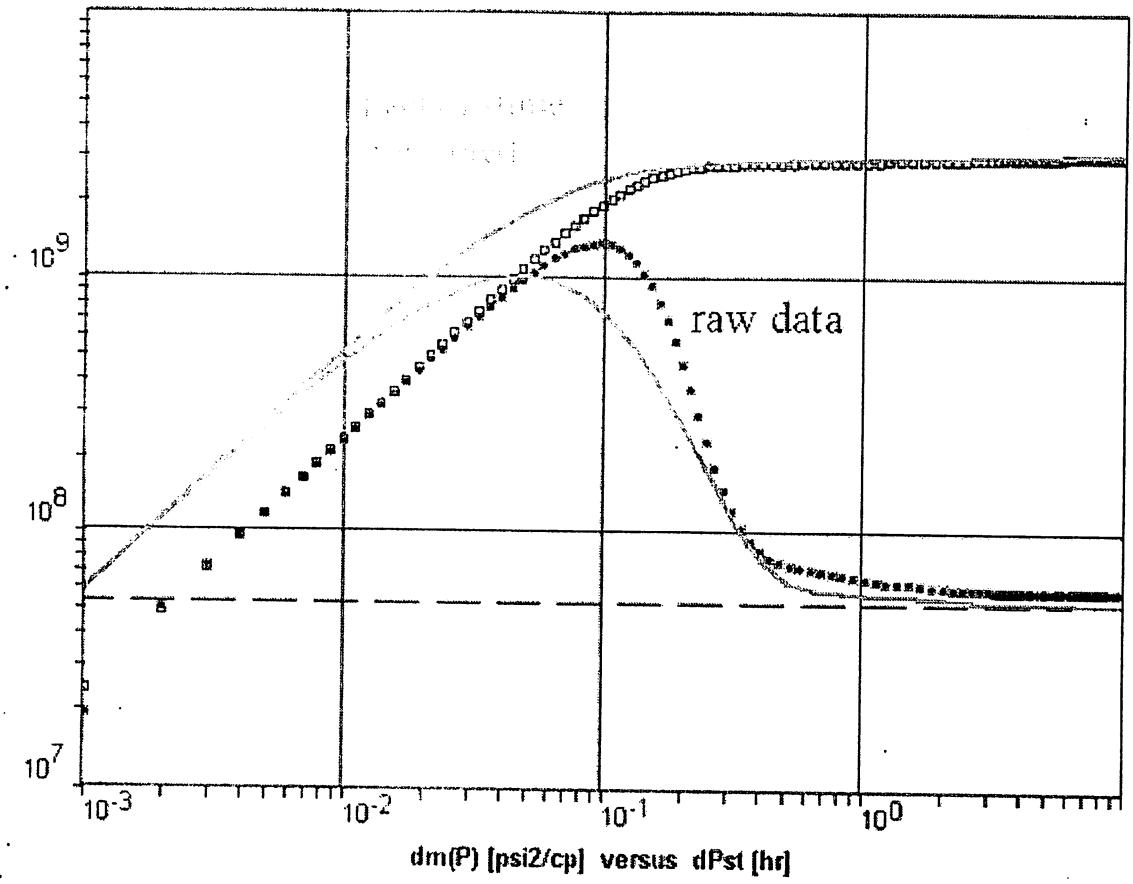

Fig 4.37 Pseudo-Time

The raw data shows is re-plotted (as above, solid green line) using the gas pseudo-time function developed by Agarwal, 1979:

$$t(p, t) = \int_{t0,P0}^{t,p} \frac{dt}{\mu(p)\, C_t(p)}$$

Normalized Pseudotime

In a tight reservoir, with large drawdowns, the assumption that □Ct is constant leads to a distortion in the early time of the log-log and derivative data:

$$t_{pn} = \mu_i \mu_{t_i} \int_0^t \frac{dt}{\mu C_t}$$

4.4.2 Pseudo-Skin, S'

In oil well testing, the skin measured during each transient will be the same, whatever it consists of:
– true formation damage, convergent flow due to partial penetration, inadequate perforations, etc. In gas wells this is not the case.

In fluid mechanics, the Reynolds number determines whether fluid flow will be laminar, which in well testing we call Darcy flow, or turbulent, which we call non-Darcy flow. In oil wells, with the possible exception of some extremely high rate producers, the combination of certain parameters, such as fluid density and flow velocity, is such that the critical Reynolds number is never exceeded, and the flow remains laminar. However, in gas wells the Reynolds number frequently exceeds 2000-3000, and turbulent flow results.

The significance of turbulent flow in well testing is that it creates an additional, rate-dependent pressure drop. The turbulence occurs where the fluid velocity is highest, which is where the flow area in the reservoir converges to a minimum – i.e. at the wellbore. This additional pressure drop very close to the wellbore looks like skin, and can not be separated from the true skin in a single transient. The total measured skin will be a combination of the true and rate-dependent skins.

To obtain the true skin, the solution is simply to test the well on a number of different flow rates, as the 'pseudo-skin' is related to the true skin by a simple straight-line equation:

$$S' = S0 + Dq$$

where :

S' is the pseudo-skin
S0 is the true skin
D is the non-Darcy flow coefficient
q is the gas flowrate

The pseudo-skin (S') measured during any transient is such that for a higher flowrate there will be higher apparent skin. The true 'damage' skin is obtained by extrapolating the measured skins to zero flowrate, as shown overleaf.

(Due to superposition effects it is actually the change in flowrate, Dq, which determines the apparent skin value, so that any build-up will have the same S' as the preceding drawdown.)

It is mainly for this reason that the standard gas test is multiple-rate. The most typical is a modified isochronal test, in which each drawdown is the same duration (except the last), and each build-up is the same duration, but build-ups can be longer than drawdowns.

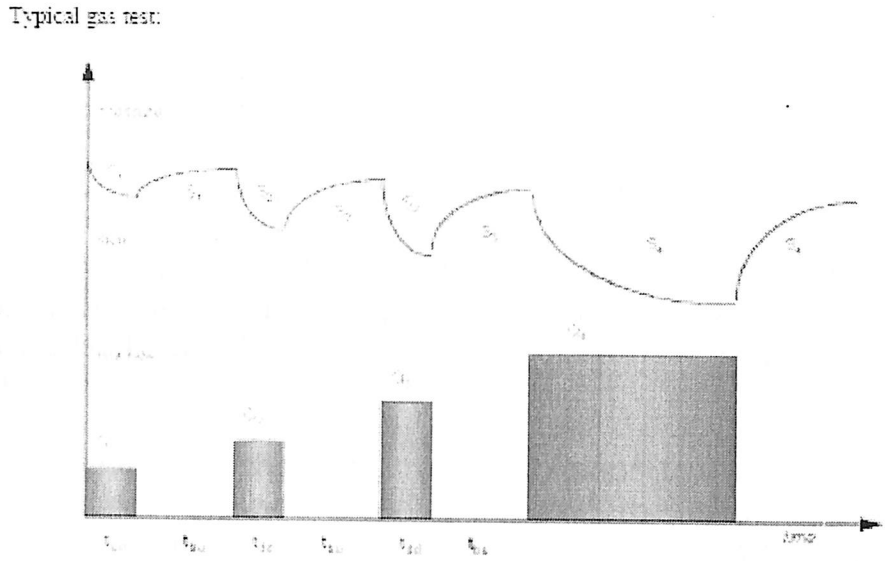

Fig. 4-38 Typical Gas Test

By utilizing the superposition principle it would not matter if each transient were a different duration, but there is another reason for trying to keep the drawdowns and build-ups to fixed times, and for extending the final flow, as will be seen in the next section.
To obtain the true skin, S' = S + Dq is the same as 'y = mx + C':

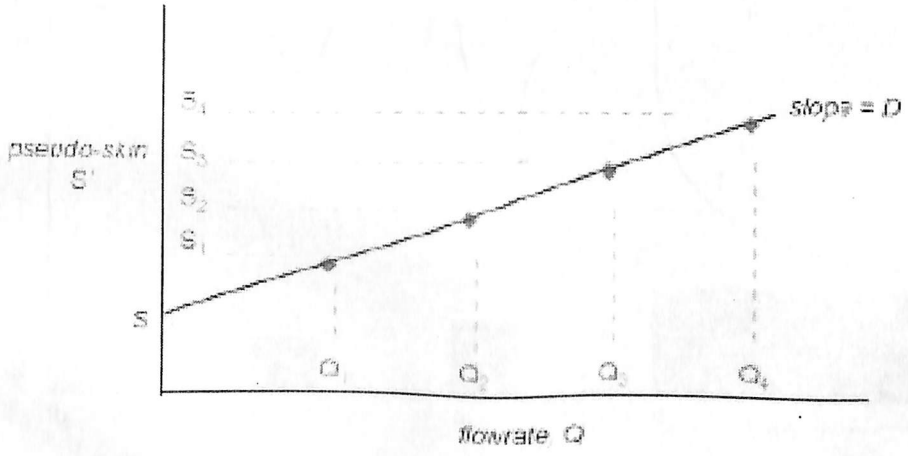

Fig. 4-39 Pseudo-Skin

If S' is plotted against q, the slope of the line is D and the intercept is the true skin, S (or S0, the skinat zero flowrate.) A high pseudo-skin

will probably benefit little from an acid job, but may be significantly reduced by adding more perforations.

4.4.3 Absolute Open Flow

A common measure of the performance of any gas well is its ability to deliver against 'zero' bottomhole pressure, or more accurately against atmospheric pressure. How hard could it flow with a flowing bottomhole pressure of 1 atmosphere? This may sound like a pointless calculation, as it is certainly unrealistic; a gas well could not even blow out at this rate, the bottomhole pressure would be too high. However this measurement provides an input value for the reservoir engineer working with IPR calculations, and is an accepted 'universal indicator' for gas wells. It is called the 'absolute open flow' potential of the well, the AOF.

In order to evaluate the AOF, the well needs to be tested at multiple rates – as has already been done for the skin calculation. The bottomhole pressure must be measured during each drawdown, after the same time – for example 2 hours into each drawdown, 4 hours, etc.

The final drawdown is extended, as this will provide a single 'stabilized' value for the calculation, pwf5 in the plot below:

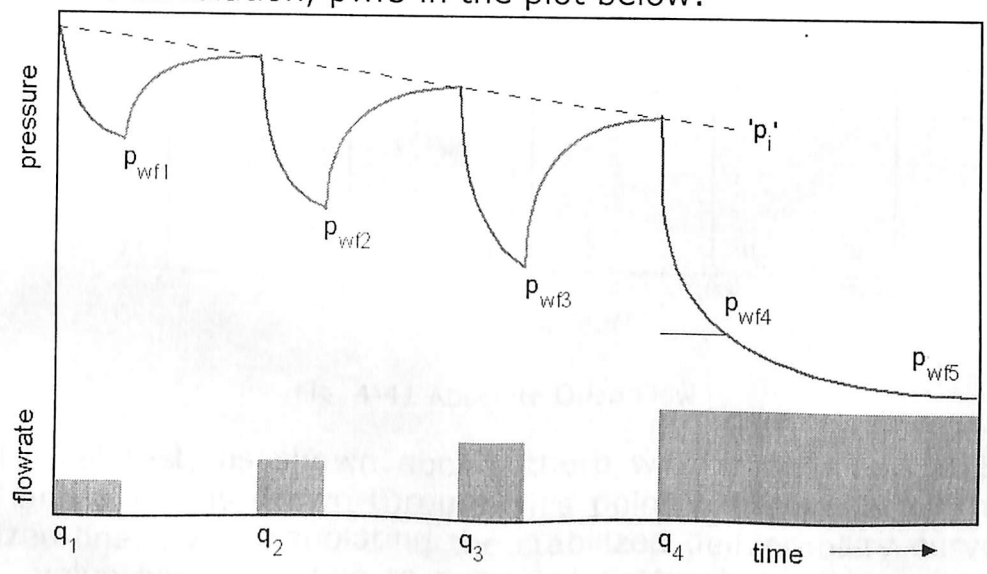

Fig. 4-40 Modified Isochronal Test

[Note that frequently in well testing we 'flow the well until stable', although in reality the flowing bottomhole pressure can never stabilize, except in very special circumstances. If it did, the semi-log slope 'm'

would become zero, which would correspond to an infinite *kh*. The pressure must always be coming down, but the well is 'stable' when the pressure is dropping very slowly ...]

From this data the following plot is constructed, based upon the empirical relationship that D(p2) vs q, on a log-log scale, will give a straight line, as long as the pwf values are recorded after the same time in each drawdown. Moreover, the '2-hour', '4-hour', '6-hour' lines, etc., will all be parallel, converging to the 'stabilized deliverability curve' for all of the stabilized points, obtained if the well had been flowed long enough for each drawdown to stabilize:

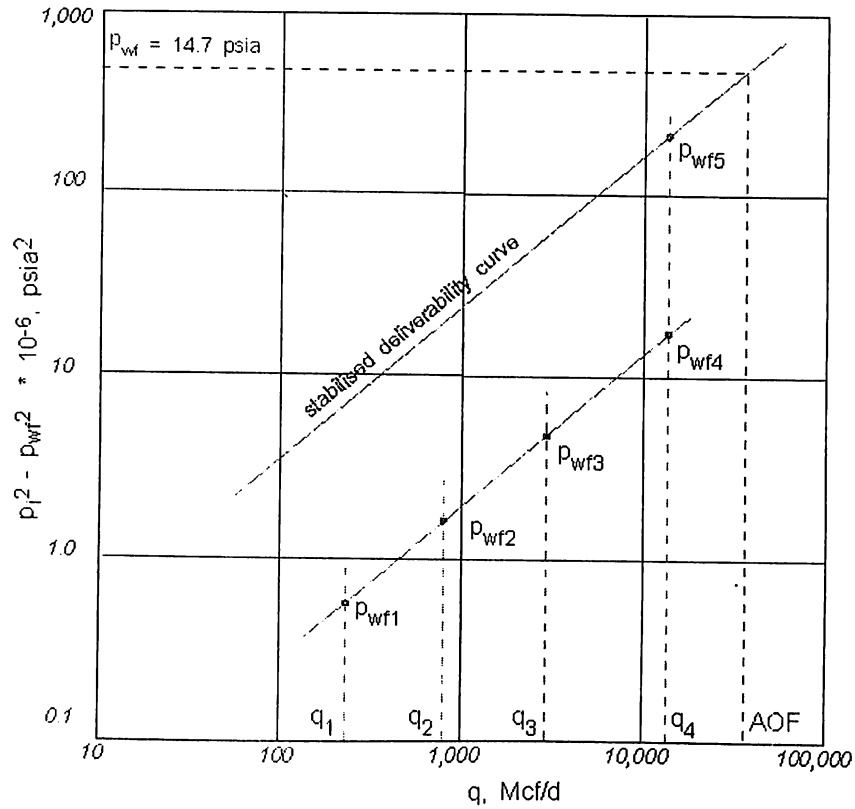

Fig. 4-41 Absolute Open Flow

In a typical test, as shown above, there will be only one stabilized point, and a line is drawn through this point and parallel to the un-stabilized line. By extrapolating the stabilized deliverability curve to a D(p2) value corresponding to a flowing bottomhole pressure of 14.7 psi, the AOF is obtained.

4.5 Curve Shapes

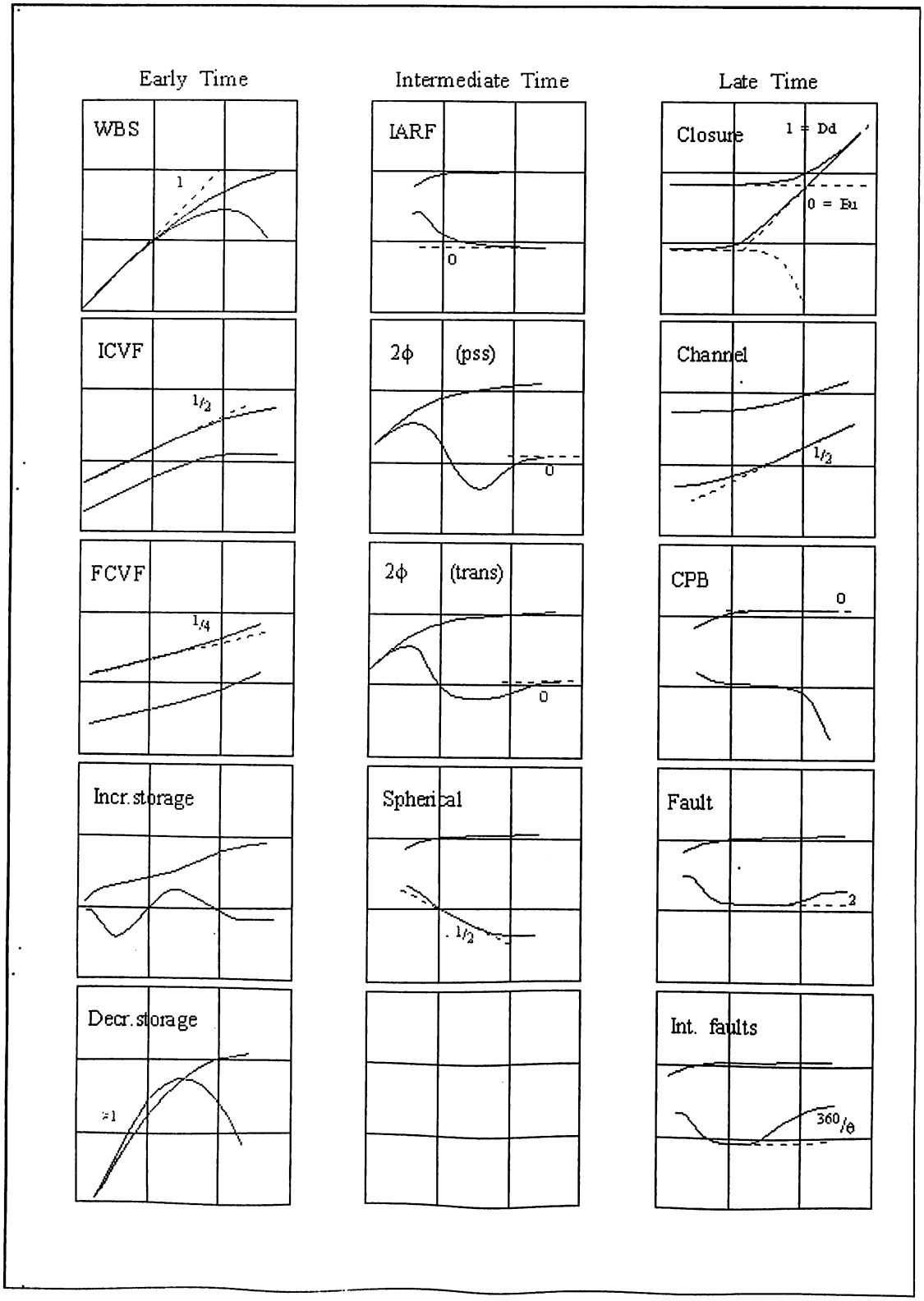

Fig. 4-42 Log-Log Responses

Chapter 5

Well Test Data Interpretation Using PTA Software Like Saphir and Manual Interpretation.

5.1 Well Test Interpretation

The various methods employed for well test interpretation are:

1. Semi Log Approach: (Classical method)
    - Miller-Dyes-Hutchinson or MDH method
    - Horner's Plot method
2. Log-Log Approach (Type Curves)
    - Dimensionless variables and Type Curves
3. Pressure Derivative Method (The diagnostic plot method)
    - Use of Pressure derivative plot with the log-log plot

5.2 Procedure for well test interpretation

Mathematical models are used to simulate the reservoir's response to production rate changes. The observed and simulated reservoir response can then be compared during well test interpretation to verify the accuracy of the model. By altering model parameters such as permeability or the distance from the well to a fault, a good match can be reached between the real and modeled data. The model parameters are then regarded as a good representation of those of the actual reservoir. Today's computer generated models provide much greater flexibility and improve the accuracy of the match between real and simulated data. It is now possible to compare an almost unlimited number of reservoir models with the observed data.

The following steps were performed for the purpose of interpretation of well test data from well xyz:

1. Well test data viz. pressure and time was fed in Sapphire.
2. Gas flow rates and duration of the transient tests viz. consecutive drawdown and final build up was also fed.
3. Log-Log (both pressure and derivative) and Semi-Log plots for the final build up was obtained using the software.
4. A model was fit for the above plots.

Using sensitivity analysis and non linear regression features of the software, the above model was corrected to match the plot

Two DST's was done in that well, one in the oil zone and other in the gas zone.

5.3 DST 1

Following data were used as input:

Fluid Type	Oil
Rate Type	Surface Rates
Rw	200 mm
Net Pay	4 m
Phi	0.16
API gravity	37 ^{0}API
Ref. Date and Time	June 29, 2007, 07:33:00

Table 5.1

PVT Parameters

B	1.23
μg	2.60 mPa*s
C_t	3.6 x 10^{-5}/kPa

Table 5.2

Selected Models

A)

Model Option	External Model, Pseudo-Time
Wel	Vertical
Reservoir	Radial composite model
Boundary	Infinite

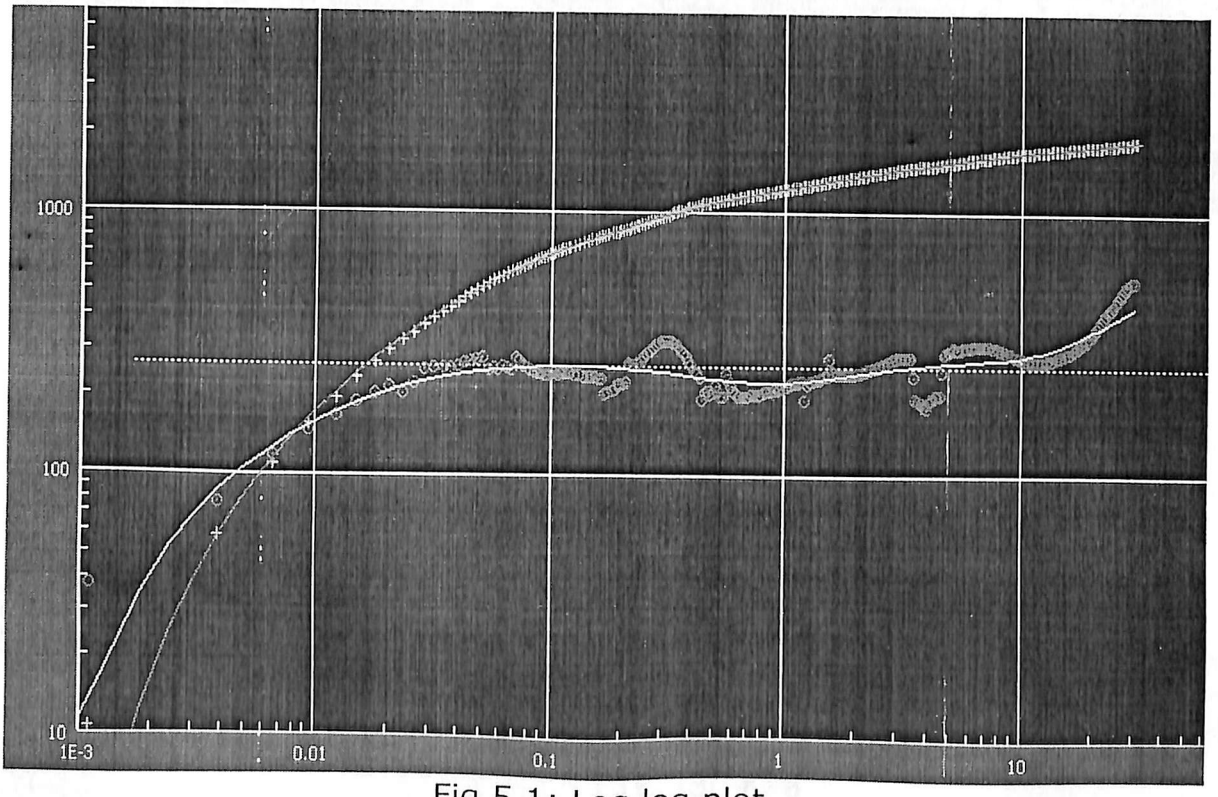

Fig 5.1: Log log plot

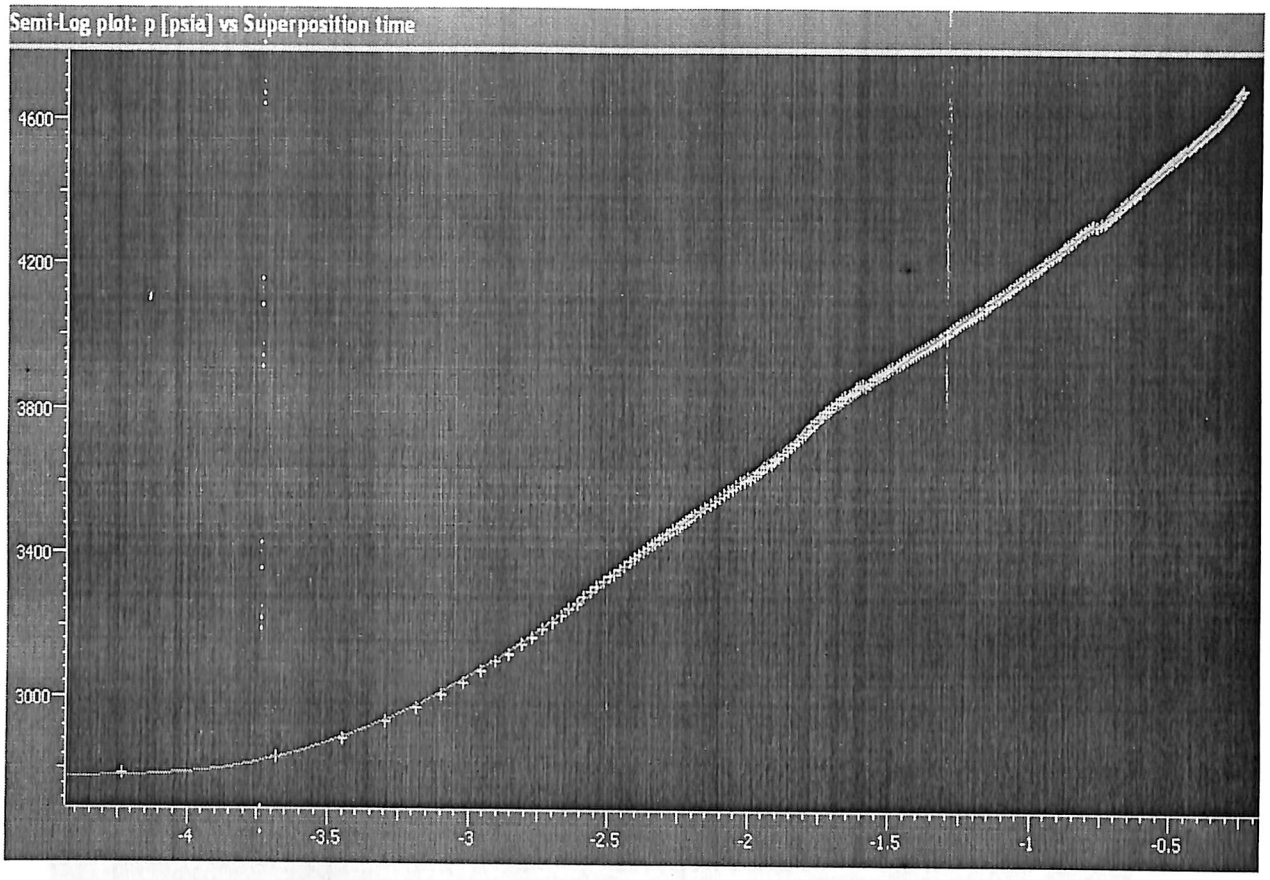

Fig 5.2 : Semilog plot

Results:

Well & Wellbore parameters (Tested well)

Skin	19.3

Table 5.3

Reservoir & Boundary parameters

Pi	16,380 KPa
$Ko.H_{total}$	237 mD.m
K_o	65 md
R_{inv}	8 m

Table 5.4

B)

Model Option	External Model, Pseudo-time
Well	Vertical
Reservoir	Homogeneous
Boundary	Rectangular

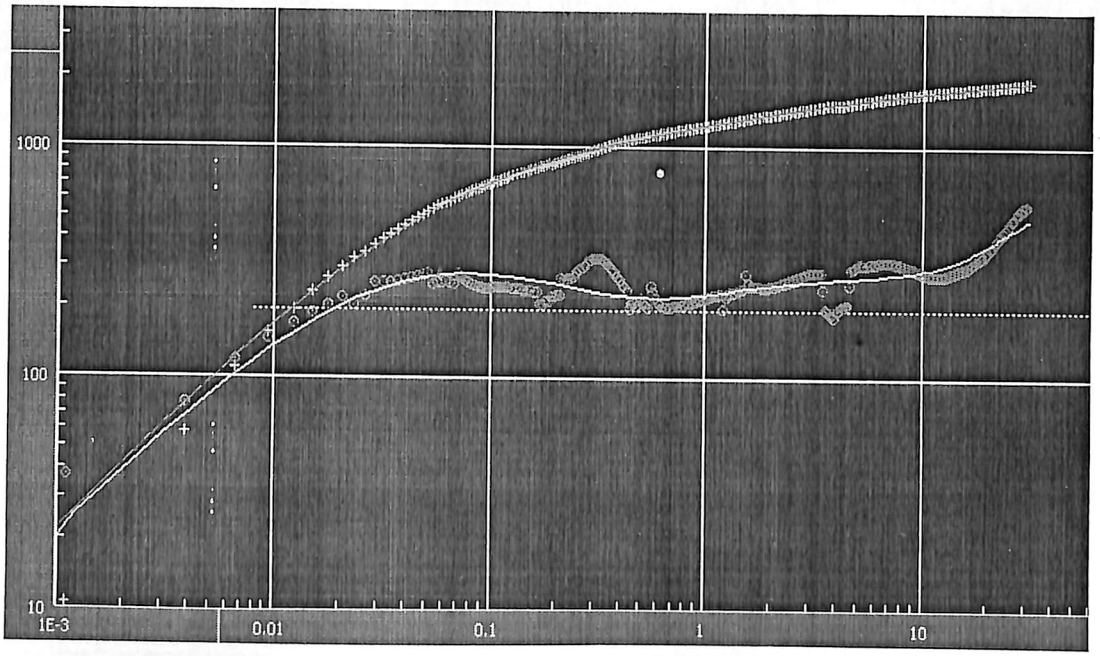

Fig 5.3 : Log log plot

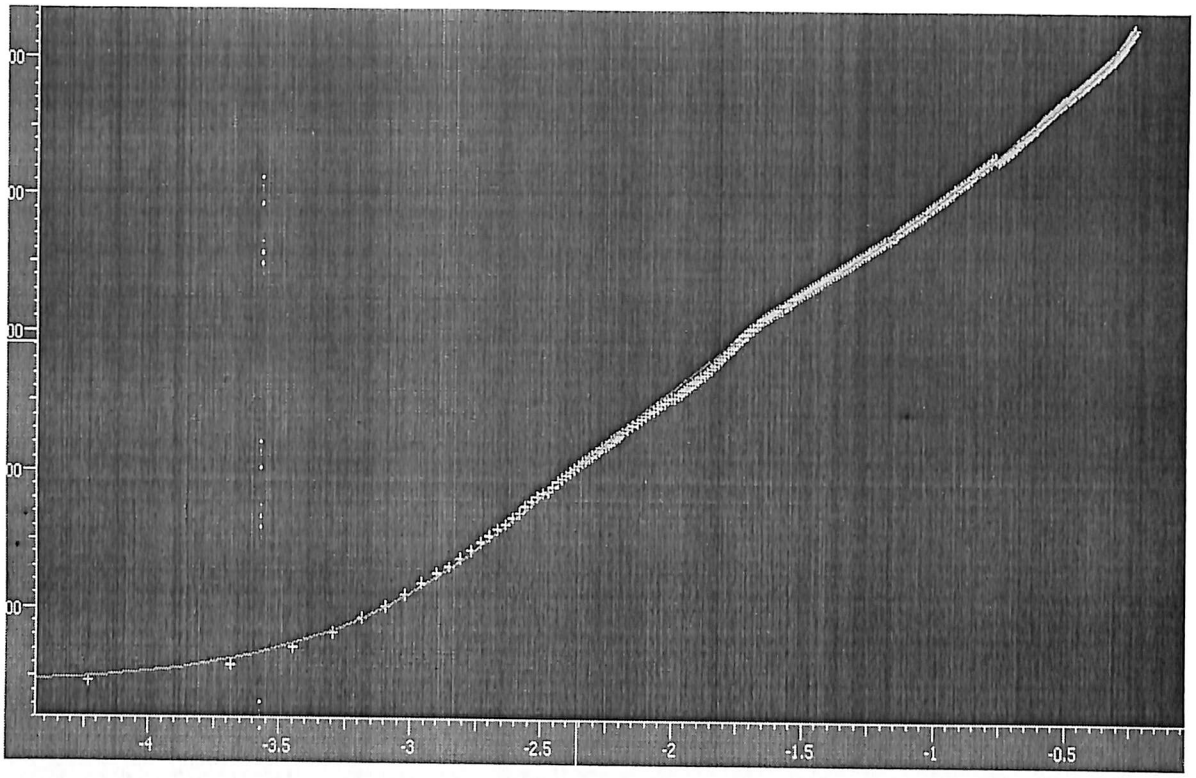

Fig 5.4 : Semilog plot

Other models attempted

Model Option	External Model
Well	Vertical
Reservoir	Triple Porosity Model
Boundary	Infinite

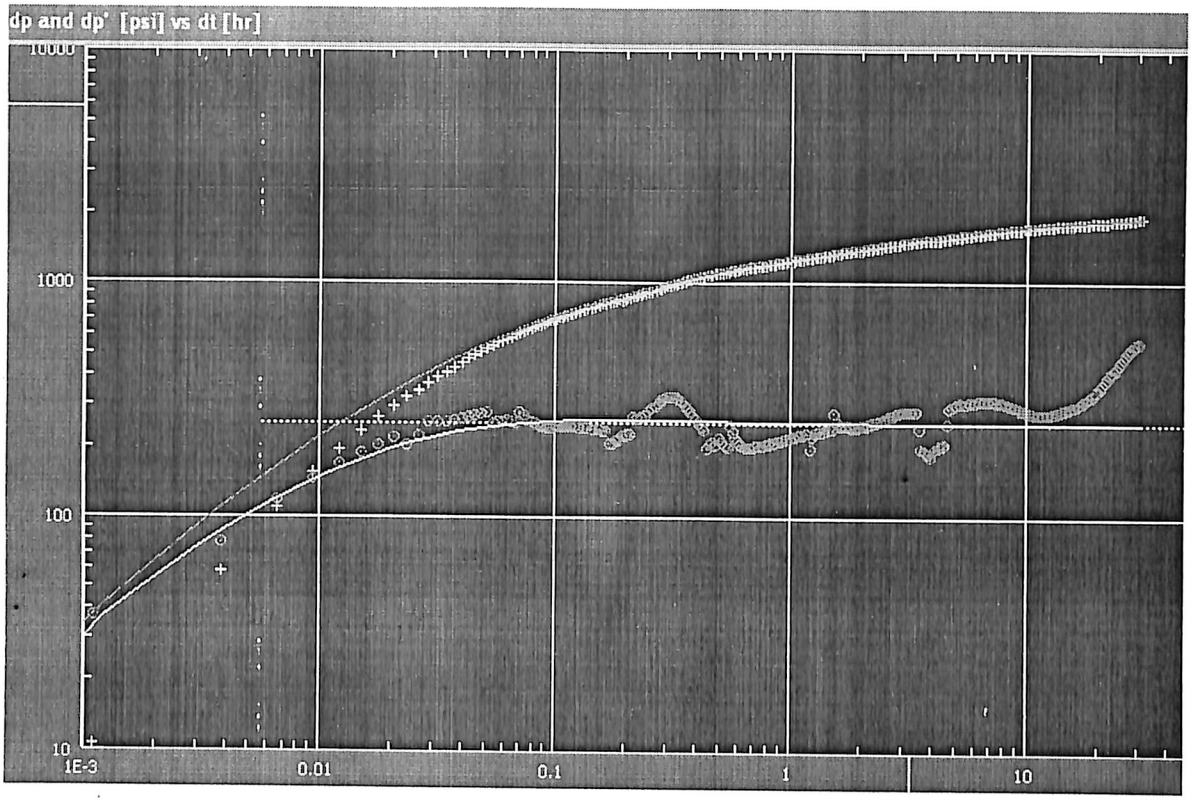

Fig 5.5 : Log log plot

Conclusions(I)

1. Three different radial zones in the derivative curve might show the presence of three different porosity zones but the model didn't match.
2. Different slopes in the derivative curve prove that radial composite model can be the solution.
3. Increase in the slope from the first zero slope line may show that one of the no flow boundaries might have been encountered whereas further increase in slope shows that all the boundaries might have reached.

Manual Interpretation

Case Study 1

Given the following information for a typical drillstem test, calculate:

- the average production rate during the test
- initial reservoir pressure
- transmissibility
- capacity
- effective permeability
- skin factor
- radius of investigation

GIVEN DATA:

General Data:

Well Name == Case Study NO.1

Ground Elevation = 800 m

DST Number = 1

Interval = 1550.0 m - 1560.0 m KB

Total Depth = 1607.0 m KB

Drill Collars = 150.5 m

Collar Capacity = 0.0042 m^3/m

Drillpipe Capacity = 0.0074 m^3/m

Hole Size = 200 mm

Gas Measurements:

Too small to measure.

Liquid Recovery:

200 meters of oil

30 meters of water and drilling mud

Test Times:

First flow = 10 minutes

First shut-in = 60 minutes

Second flow = 60 minutes

Second shut-in = 90 minutes

Key Pressure Points:

1. Initial hydrostatic 18,814 kPa
2. Start of first flow 444 kPa
3. End of first flow 444 kPa
4. End of first shut-in 16,297 kPa
5. Start of second flow 564 kPa
6. End of second flow 1728 kPa
7. End of second shut-in 16,067 kPa

14. Final hydrostatic 18,814 kPa

Reservoir Rock and Fluid Properties:

Reservoir temperature = 329°K

Net pay = 4.00 m

Oil filled porosity = 16%

API gravity = 37 ^{0}API

Viscosity = 2.60 mPa*s

Formation volume factor = 1.23

Compressibility = 3.6 x 10^{-5}/kPa

Pressure Increments - First Shut-in:

Recorder Number = 008892

Recorder Depth = 1552.0 m

Total Flow Time = 10 minutes.

Time (minutes)	tp+Δt/Δt	Pressure (kPa)
0	-	444
2	6	3264
4	3.5	8025
6	2.67	11608
8	2.25	13794
10	2	14720
15	1.67	15650
20	1.50	15907
25	1.4	16031
30	1.33	16120
35	1.29	16173
40	1.25	16209
50	1.2	16253
60	1.17	16297

Pressure Increments-Second Shut-in:

Recorder Number=008892

Recorder Depth=1552 m

Total Flow Time = 70.0 minutes (this is tp)

Initial reservoir pressure is obtained by extrapolating the straight line of the Horner plot to $(tp + \Delta t)/\Delta t = 1$.

This gives Pi= 16,200 kPa.

Time(min)	tp+Δt/Δt	Pressure(kPa)	Log{(tp+Δt)/Δt}
0	-	1728	-
5	15	9522	1.176
10	8	14259	.903
15	5.67	15154	.754
20	4.5	15446	.653
25	3.8	15615	.580
30	3.33	15708	.522
35	3	15801	.477
40	2.75	15854	.439
45	2.55	15890	.407
50	2.4	15916	.380
55	2.27	15943	.356
60	2.17	15960	.336
65	2.08	15978	.318

70	2	15992	.301
75	1.93	16005	.286
80	1.88	16012	.274
85	1.82	16018	.260
90	1.78	16021	.250

Solution:

AVERAGE PRODUCTION RATE DURING THE TEST

A total of 230 meters of liquid were recovered during the two flow periods of this test. The volumetric capacity of the 150.5 meters of drill collars is 0.63 cubic meters. The remaining 79.5 meters of recovery was in the drillpipe. The volumetric capacity of this length of drillpipe is 0.59 cubic meters. Therefore a total of 1.22 cubic meters was recovered. The total flow time for the two flow periods was 70 minutes. The average production rate during the test, then, was:

qa = (1.22 x 60 x 24)/70 = 25.1 m3/day

The initial shut-in pressure of 16,420 kPa is found by extrapolating the straight line to a value on the horizontal axis of 1.0.

TRANSMISSIBILITY

The extrapolated value of the second shut-in pressure is 16,200 kPa. The slope of the Horner

plot is 680 kPa/cycie. The transmissibility is calculated as:

Ko h/μ = (2121*q*B)/m

= (2121*25.1*1.23)/680

= 96.3mD.m/mPa.s

FLOW CAPACITY

$(Ko\ h/\mu o)*\mu o = 96.3*2.6$

$= 250.4\ mD.m$

EFFECTIVE PERMEABILITY

$Ko = Ko\ h/h$

$= 250.4/4$

$= 62.6\ mD$

SKIN FACTOR

$S = 1.151\{P1hr - P1/m - \log[Ko/\Phi\mu ct.Rw^2] + \log[(tp + tp2)/tp2] + 5.10\}$

$= 20$

RADIUS OF INVESTIGATION

$R_{inv} = (Ko\ t/7.036 * 10^4\ \Phi\mu oc_t)^{0.5}$

$= [62.6 * (70/60)/(7.036*10^4)(.16)(2.6)(3.6 * 10^{-5})]$

$= 8.3\ m$

Parameter	Software	Manual
Skin	19.30	20
Pi	16380 KPa	16420 KPa
K.H	237 mD.m	250.40 mD.m
K_o	65 mD	62.6 mD
R_{inv}	8 m	8.3 m

Table 5.5 RESULTS COMPARISON

5.4 DST2

Following data were used as input

Fluid Type	Gas
Rate Type	Surface Rates
Rw	200 mm
Net Pay	1.5 m
Phi	.18
Ref Date and Time	July 7, 2007, 01:02:00

Table 5.6

PVT Parameters:

Gas Gravity	0.60
Hydrogen Sulphide	0
Carbon dioxide	0.2
Nitrogen	0.534
Z	0.90
μg	0.010 mPa*s
C_t	3.6x 10^{-5}/kPa
Temperature	329 ^{o}K

Table 5.7

Selected Models

A)

Model Option	External Model,Pseudo-Time
Well	Vertical
Reservoir	Radial Composite Model
Boundary	Infinite

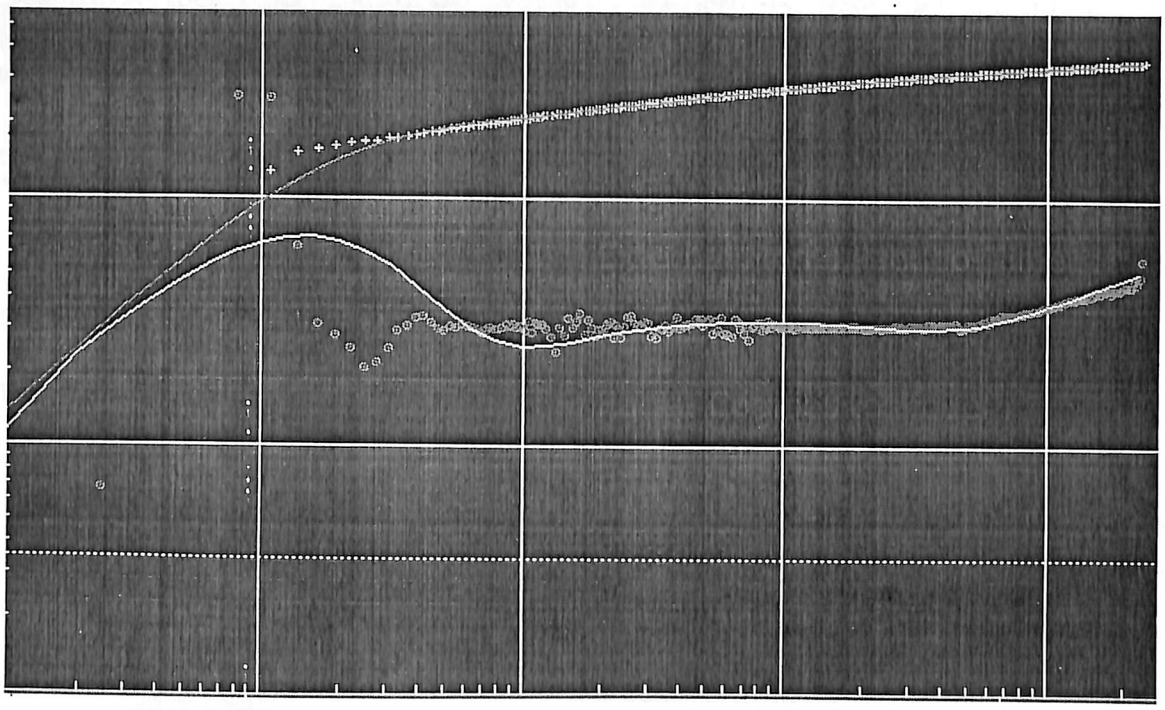

Fig 5.6 : Log log Plot

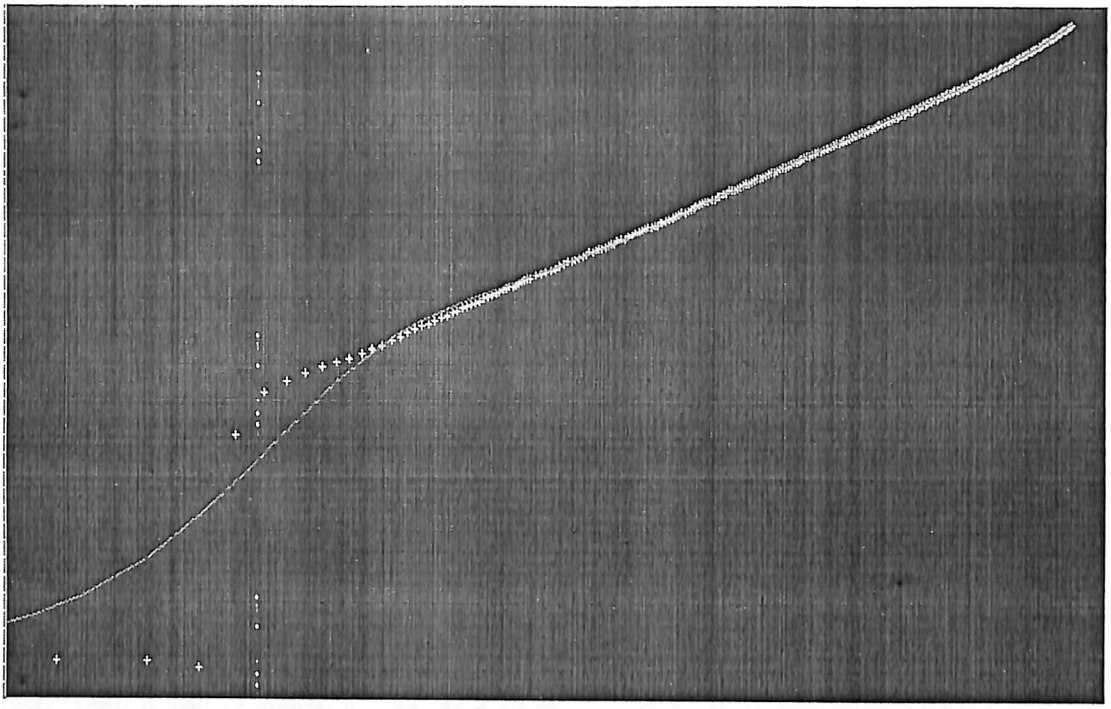

Fig 5.7 : Semilog plot

Results

Well & Wellbore parameters (Tested well)

Skin	8.10

Table 5.8

Reservoir & Boundary parameters

Pi	5200 kPa.
$K.H_{total}$	300 mD.m
K_g	198 mD
R_{inv}	102 m

Table 5.9

B)

Model Option	Standard Model, Pseudo -Time
Well	Vertical
Reservoir	Homogeneous
Boundary	Single Fault

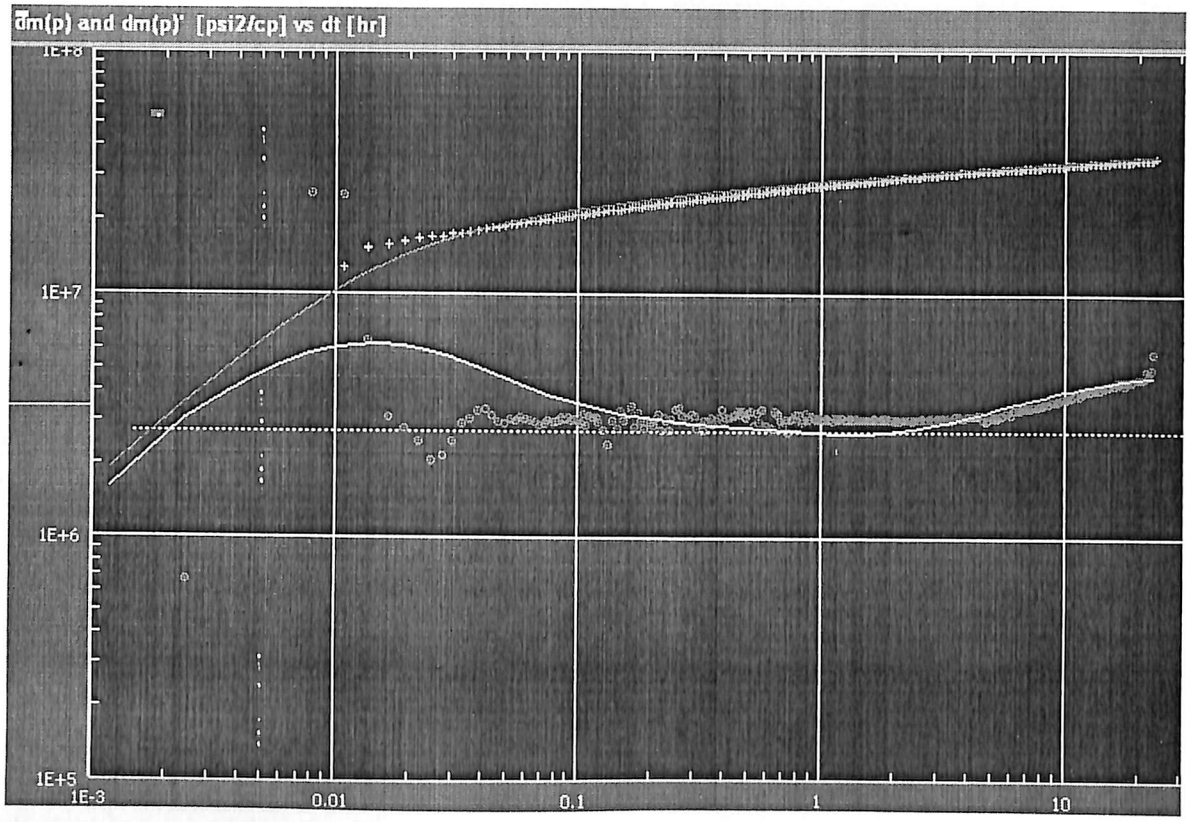

Fig 5.8 : Log log plot

Other models attempted

Model Option	External Model,Pseudo Time
Well	Vertical
Reservoir	Homogeneous
Boundary	Intersecting Faults

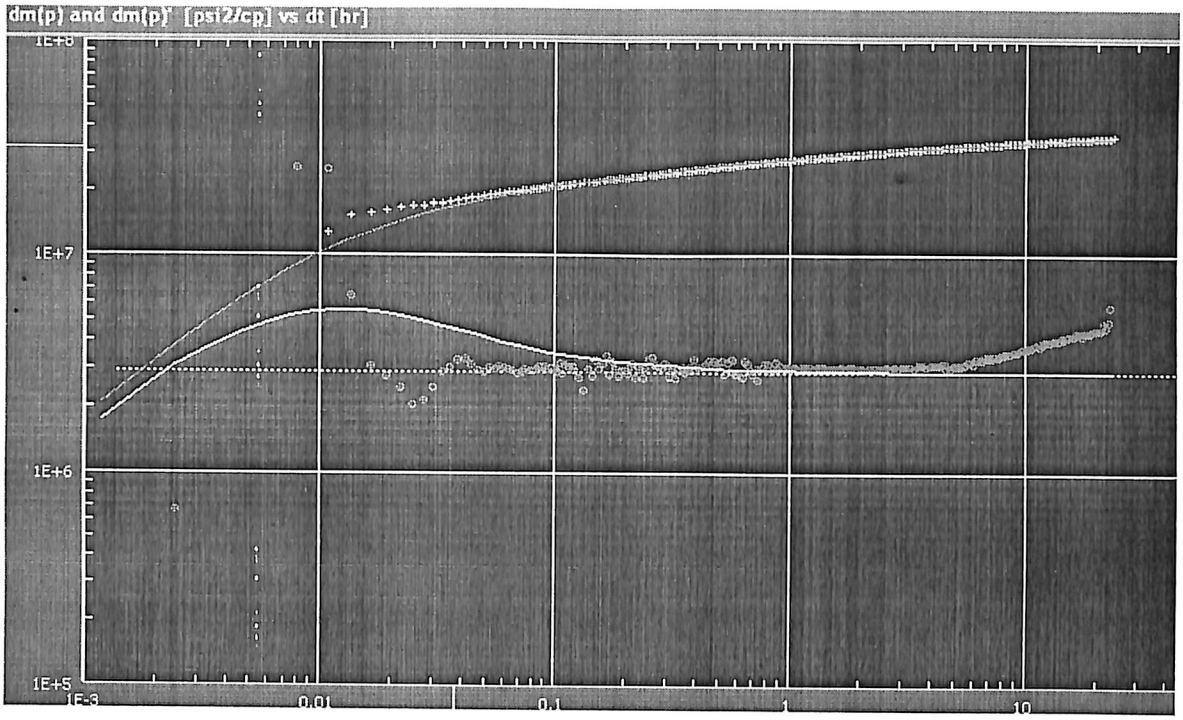

Fig 5.9 : Log log plot

Conclusions(II)

1. Permeability as pointed in DST1 comes out to be very low but higher in case of DST2.
2. Increase in the zero slope line in the derivative curve indicates that transient has reached lower mobility zone.
3. After that existence of half slope lines are evident which shows that either the transient has reached the single fault boundary or entering the yet another permeability zone.
4. The match of radial composite and single fault model clearly testifies the above facts.

Manual Interpretation

Case Study 2

- initial reservoir pressure
- transmissibility
- capacity
- effective permeability
- apparent skin factor
- radius of investigation

GIVEN DATA:

General Data:

Well Name = Case Study NO.2

Ground Elevation = 670 m

DST Number = 2

Interval = 750 m to 754 m KB

Total Depth = 800 m KB

Drill Collars = 102.4 m

CQllar Capacity = 0.0042 m3jm

Drillpipe Capacity = 0.0074 m3jm

Hole Size = 0.200 m diameter

Gas Measurement:

Measured with Critical Flow Prover

Final Flow Period

Flow Time(min)	Pressure (kPa)	FlowRate (m^3/d)
10	606	61475
20	689	69364
30	689	69364
40	689	69364
50	689	69364
60	689	69364

Liquid Recovery:

5 meters of muddy water

Test Times:

First flow = 5 minutes

First shut-in = 60 minutes

Second flow = 60 minutes

Second shut-in = 90 minutes

Key Pressure Points:

1. Initial hydrostatic 8523 kPa
2. Start of first flow 2220 kPa
3. End of first flow 3500 kPa
4. End of first shut-in 5276 kPa
5. Start of second flow 2638 kPa
6. End of second flow 3999 kPa

7. End of second shut-in 5241 kPa

8. Final hydrostatic 8523 kPa

Reservoir Rock and Fluid Properties:

Reservoir temperature = 301 °K

Net pay = 1.5 m

Gas filled porosity = 18%

Specific gravity = 0.60

Average viscosity = 0.010 mPa*s

Average compressibility = 1.9 x 10-4/kPa

Average z Factor = 0.90

Pressure Increments - First Shut-in:

Recorder Number = 008193

Recorder Depth = 752 m KB

Total Flow Time = 5 minutes

Time (min)	$(t_p + \Delta t)/\Delta t$	Pressure (KPa)	PressureSquared ($KPa^2 \times 10^{-4}$)
0.0	-	3500	12.25
2.0	3.50	5107	26.08
4.0	2.25	5146	26.48
6.0	1.83	5186	26.89
8.0	1.62	5235	27.40
10.0	1.50	5239	27.45
12.0	1.42	5250	27.56

14.0	1.36	5255	27.62
16.0	1.31	5259	27.66
20.0	1.25	5265	27.72
25.0	1.20	5268	27.75
30.0	1.17	5271	27.78
40.0	1.13	5274	27.81
50.0	1.10	5275	27.83
60.0	1.08	5276	27.84

Pressure Increments - Second Shut-in:

Recorder Number = 008892

Recorder Depth = 1552.0 m

Total Flow Time = 70.0 minutes

Time (min)	$(t_p + \Delta t)/\Delta t$	Pressure (KPa)	PressureSquared ($KPa^2 \times 10^{-4}$)
0	-	3999	15.99
2	33.50	5089	25.90
4	17.25	5105	26.06
6	11.83	5138	26.40
8	9.13	5165	26.68
10	7.50	5182	26.85
12	6.42	5200	27.04
14	5.64	5209	27.13

16	5.06	5217	27.22
18	4.61	5223	27.28
20	4.25	5229	27.33
25	3.60	5236	27.42
30	3.17	5242	27.48
35	2.86	5246	27.52
40	2.63	5249	27.55
45	2.44	5252	27.58
50	2.30	5254	27.60
60	2.08	5257	27.64
70	1.93	5261	27.68
80	1.81	5263	27.70
90	1.72	5265	27.72

SOLUTION

INITIAL RESERVOIR PRESSURE

The plot extrapolates to 27,925 * 10^6 kPa^2 at (tp + Δt)/Δt = 1. therefore the initial reservoir pressure of this zone is 5284 kPa.

The plot extrapolates to 27.925 x 10^6 kPa^2 (the same as the initial). Therefore, the initial reservoir pressure is 5284 kPa.

TRANSMISSIBILITY

Reservoir parameter calculations are done using data from the final buildup period. The slope of the Horner plot for the final buildup is:

mg = 0.9 x 106 kPa^2/cycle

The gas flow rate prior to the second shut-in was 69,364 m^3/d. Therefore:

$Kg.h/\mu g = 1491*q*Z*T/ m$

$Kg.h /\mu g = 1491 * 301 * 0.90 * 69,364/ 0.9 * 10^6$

$= 31,129$ mD.m / mP.s

FLOW CAPACITY:

$k_g h = kh = 31,129 \times 0.010 = 311.29$ mD·m.

EFFECTIVE PERMEABILITY:

$Kg = K = 311.29/15 = 207.5$ mD

APPARENT SKIN FACTOR:

P_{1hr} is obtained as 5276 kPa:

$S' = 1.151\{(P1hr)^2-(P1)^2/m-\log[Ko/\Phi\mu ct.Rw^2]+\log[tp + tp2/tp2]+ 5.10\}$

$= 8.94$

RADIUS OF INVESTIGATION

$R_{inv} = (Ko\ t/7.036 * 10^4\ \Phi\mu oc_t)^{0.5}$

$= [207.5 * (65/60)/(7.036*10^4)(.18)(0.010)(1.9 * 10^{-4})]^{0.5}$

$= 97$ m

Parameter	Software	Manual
Skin	8.10	8.94
Pi	5200 KPa	5284 KPa
K.H	300 mD.m	311.29 mD.m
Kg	198 mD	207.5 mD
R_{inv}	102 m	97 m

Table 5.10 Results Comparison

Nomenclature

k - Permeability of formation, milliDarcy

h - Thickness of formation, ft(m)

q - Flow rate of fluid, m3/s

p -Pressure of reservoir fluid, psi

t - Time, hrs

p - Density of fluid, kg/m^3

Φ-Porosity of formation

r - Radius of investigation, ft[m]

c - Compressibility of fluid, psi

μ - viscosity of fluid, cp

r_D-dimensionless radius

P_D- dimensionless pressure

t_D- dimensionless time

Pi- intial reservoir pressure, psi

Q_{sf}- sandface flow rate, m^3/sec

r_w- radius of well bore, firm]

r_{wa}- apparent radius of wellbore, ft[m]

Ei - exponential integral

S - skin factor

k_s - Permeability of invaded zone, milliDarcy

r_s – Radius of invaded zone,ft(m)

p_s - pressure due to skin, psi

pwf - flowing bottom hole pressure, psi

m - slope of log-log & Homer's plot

sup. - Superposition

IARF - Infinite acting radial flow

P_{BU}- Buildup pressure, psi

P_{DD}- Drawdown pressure, psi

t_p - production time, hrs

M - shut-in time, hrs

T_N - multi rate time, hrs

T_{pe} - equivalent production time

C - performance coefficient

n - inertial effect exponent

AOFP -Absolute open flow potential

h_w- perforated interval

ω - storativity ratio

A - interporosity flow coefficient

C_t - total compressibility offormation, psi-1

MMSCFD - * 10^6 standard cubic feet per day

Bibliography

1. Home, Roland N.: Modern Well Test Analysis, Petroway, Inc,United States of America (2003).

2. "Introduction to computer-aided analysis ",KAPPA Consultancies http://www.kappa.com/contents/saphir/info.htm.April 2009

3. John Lee, W.: Well Testing Society of Petroleum Engineers of AIME,Dallas (1982).

4. Olivier Houze, Didier Viturat, Ole S. Fjaere: Dynamic Flow Analysis © Kappa 1998-2007 v4.02 - February 2007.

5. Peter Ramsay: DST Manual 403-537-3469 (2004).

6. Schlumberger Wireline and Testing: Introduction to Testing Services, Texas (2000).

7. Schlumberger Wireline and Testing: Introduction to Well Testing, Phi Solutions, Bath, England (March 1998).

8. Schlumberger Wireline and Testing: Well Test Interpretation (2002).